⑫

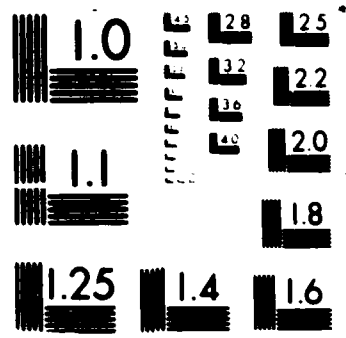# THE DEVELOPMENT OF NEW PROCEDURES FOR RATING THE IGNITION QUALITY OF FUELS FOR DIESEL ENGINES

INTERIM REPORT
BFLRF No. 223

By

T.W. Ryan, III
Belvoir Fuels and Lubricants Research Facility (SwRI)
Southwest Research Institute
San Antonio, Texas

Prepared for

**U.S. Army Belvoir Research, Development
and Engineering Center
Materials, Fuels and Lubricants Laboratory
Fort Belvoir, Virginia**
and

**U.S. Department of Energy
Alternative Fuels Utilization Branch
Washington, D.C. 20585**

AD-A181 617

DTIC
ELECTE
JUN 1 9 1987
D

Under

Contract No. DAAK70-85-C-0007

December 1986

87

REPORT DOCUMENTATION PAGE

1a. REPORT SECURITY CLASSIFICATION	1b. RESTRICTIVE MARKINGS
Unclassified	None

2a. SECURITY CLASSIFICATION AUTHORITY	3. DISTRIBUTION/AVAILABILITY OF REPORT
N/A	Approved for public release;
2b. DECLASSIFICATION/DOWNGRADING SCHEDULE	distribution unlimited
N/A	

4. PERFORMING ORGANIZATION REPORT NUMBER(S)	5. MONITORING ORGANIZATION REPORT NUMBER(S)
Interim Report BFLRF No. 223	

6a. NAME OF PERFORMING ORGANIZATION	6b. OFFICE SYMBOL (If applicable)	7a. NAME OF MONITORING ORGANIZATION
Belvoir Fuels and Lubricants Research Facility (SwRI)		

6c. ADDRESS (City, State, and ZIP Code)	7b. ADDRESS (City, State, and ZIP Code)
Southwest Research Institute 6220 Culebra Road San Antonio, TX 78251	

8a. NAME OF FUNDING/SPONSORING ORGANIZATION	8b. OFFICE SYMBOL (If applicable)	9. PROCUREMENT INSTRUMENT IDENTIFICATION NUMBER
Belvoir Research, Development and Engineering Center	STRBE-VF	DAAK70-85-C-0007; WD 8, 27

8c. ADDRESS (City, State, and ZIP Code)	10. SOURCE OF FUNDING NUMBERS			
Fort Belvoir, VA 22060-5606	PROGRAM ELEMENT NO.	PROJECT NO.	TASK NO.	WORK UNIT ACCESSION NO.
	62733	1L762733AH20	VM	

11. TITLE (Include Security Classification)
The Development of New Procedures for Rating the Ignition Quality of Fuels for Diesel Engines (U)

12. PERSONAL AUTHOR(S)
Ryan, III, T.W.

13a. TYPE OF REPORT	13b. TIME COVERED	14. DATE OF REPORT (Year, Month, Day)	15. PAGE COUNT
Interim	FROM Oct 84 TO Oct 86	1986 December	120

16. SUPPLEMENTARY NOTATION

17. COSATI CODES			18. SUBJECT TERMS (Continue on reverse if necessary and identify by block number)
FIELD	GROUP	SUB-GROUP	Cetane, Combustion, Bomb, fuels
			Variable Compression Ratio, Ignition

19. ABSTRACT (Continue on reverse if necessary and identify by block number)

The ignition delay times of 42 different fuels were measured in a constant volume combustion bomb. The measurements were performed at three different initial air temperatures using fuels ranging from the primary reference fuels for cetane rating to complex mixtures of coal-derived liquids. A single-cylinder, variable compression-ratio, direct-injection diesel engine was designed and constructed to study the ignition quality of 17 of the 42 fuels.

The total ignition delay times in the bomb were studied in the context of providing a means for rating the ignition quality of the fuels. Fuel ignition quality rating schemes are discussed, including one based on the current cetane number scale as well as one based on a new scale which includes a measure of the sensitivity of the various fuels to the air temperature.

The ignition delay times in the engine have been measured as functions of the engine speed, load, and compression rato. As in the standard cetane rating technique, injection timing was adjusted

20. DISTRIBUTION/AVAILABILITY OF ABSTRACT	21. ABSTRACT SECURITY CLASSIFICATION
☒ UNCLASSIFIED/UNLIMITED ☐ SAME AS RPT. ☐ DTIC USERS	Unclassified

22a. NAME OF RESPONSIBLE INDIVIDUAL	22b. TELEPHONE (Include Area Code)	22c. OFFICE SYMBOL
Mr. F.W. Schaekel	(707) 664-3576	STRBE-VF

DD FORM 1473, 84 MAR
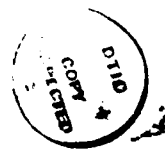83 APR edition may be used until exhausted.
All other editions are obsolete.

19. ABSTRACT (Cont'd)

so that combustion started at top dead center. This was accomplished by adjusting the injection timing as the speed, load, and compression ratio were varied. The resulting data are plotted as the ignition delay times versus compression ratio at the various speed-load conditions. For one of the test fuels, a very narrow-cut middle distillate, excursions in compression ratio were performed at the various speed-load-injection timing settings. The resulting data indicated that the compression ratio is the dominant factor in controlling the ignition delay times.

The current cetane rating scale is discussed in terms of the extremely nonlinear nature of the scale and the inability of the ASTM technique to either distinguish the good ignition quality fuels or even rate the poor ignition quality fuels. The bomb technique does provide a measure of the current cetane scale. The engine data are discussed in terms of comparisons between the standard CFR engine rating technique and a proposed new technique based on the variable-compression, direct-injection engine.

FOREWORD

Accesion For	
NTIS CRA&I	☑
DTIC TAB	[]
Unannounced	[]
Justification	
By	
Distribution /	
Availability Codes	
Dist	Avail and/or Special
A-1	

iii

ACKNOWLEDGEMENTS

TABLE OF CONTENTS

LIST OF ILLUSTRATIONS

LIST OF TABLES

I. INTRODUCTION

Historically, fuels have been made to meet the requirements of specific engine types. This tailoring of the fuels has been accomplished in recent time by what may be considered extreme processing steps, at the cost of increased energy consumption at the refinery. The mechanism for defining the fuels has evolved through the efforts of organizations such as Coordinating Research Council (CRC), American Petroleum Institute (API), Society of Automotive Engineers (SAE), American Society of Mechanical Engineers (ASME), and American Society for Testing and Materials (ASTM). The basic mechanism consists of the definition of standard fuel rating test procedures and the compilation of fuel specifications which define the allowable limits of the variety of fuel properties controlled by the specification. The development of specifications has been based on a wealth of empirical data and usually in response to specific problems.

The specifications of the fuels for the various types of heat engines (spark ignition, compression ignition, and gas turbine) can generally be considered in terms of those properties which affect, or reflect, the fuel stability, contamination, and combustion characteristics. The emphasis of the work described in this report has been the examination of the potentials of two new techniques for rating the combustion characteristics of fuels for compression ignition engines. The need for this work has been demonstrated on several occasions when the current standard cetane rating procedure has clearly failed to provide accurate indication of ignition quality.

The specific shortcomings of the currently used cetane rating procedure (ASTM D 613) were extensively discussed during the CRC-hosted workshop on Diesel Fuel Combustion Performance held in Atlanta, GA in 1984. It appears that the basic problem with the cetane procedure is that neither the engine nor the test conditions are representative of current engine design or typical operating condition. The current procedure involves the use of a Waukesha CFR engine equipped with a cylindrical prechamber. The prechamber has a movable end plate which is used to change the volume of the prechamber and, thus, the compression ratio. The specified operating conditions of the test are equivalent to a high-speed idle test, with the speed set at 900 rpm and fuel flow set at 13 mL/min (equivalent to an air/fuel ratio of approximately 30).

A. Summary

As indicated previously, the work reported in this document has involved the preliminary development of two new techniques for rating the ignition quality of fuels for diesel engines. In one approach, a specially designed high-temperature, high-pressure Constant Volume Combustion Bomb (CVCB) was used to determine the ignition delay times of a variety of different types of fuels as a function of initial temperatures. The results for the test fuels were compared to the corresponding results obtained using blends of the primary reference fuels. In a similar fashion, a specially designed variable compression-ratio, direct-injection diesel engine was used to determine the ignition delay times of the same fuels (as used in the CVCB experiments) as functions of the engine speed, load, and compression ratio.

The work performed over the course of the project is described in this document. A comprehensive literature review was performed, and a summary of this review is presented in the following section. The experimental apparatus, procedures, and results are presented separately for the two different types of experiments. The results of the two different types of experiments are compared and discussed in detail in the Results Section. The final section of the report summarizes the conclusions as well as recommendations for additional work.

B. Background

The combustion of any fuel can be divided into three main phases: (1) formation of the fuel/air mixture; (2) ignition; and (3) completion of combustion. Combustion in a diesel engine occurs when fuel is injected into a chamber of air at high pressure and temperature. The droplets of fuel vaporize and then mix with the air in the chamber. The mixture then autoignites and, if mixing is adequate, burns to completion.

In a diesel engine, the fuel does not ignite instantaneously as it is injected. The time elapsed from injection to ignition is known as the ignition delay time. The ignition delay time develops because a certain amount of time is required for the fuel to vaporize and ignite. The time necessary for the fuel to vaporize is known as the physical delay, while the chemical delay is the time required for the chemical reactions leading to ignition to take place.

2

In 1932, Boerlage and Broeze (1)* proposed that the quality of a fuel be based on a comparison of its ignition delay time in a diesel engine to that of a blend of two reference fuels. They developed the "cetene scale" in which a fuel was assigned a "cetene number." The reference fuels used were cetene, $C_{16}H_{32}$, and mesitylene, C_9H_{12}, with cetene numbers of 100 and 0, respectively. These particular fuels were chosen because cetene burned readily in a normal engine, while mesitylene did not burn at all. In 1935 the ASTM adopted this form of diesel rating system using cetane, $C_{16}H_{34}$, and alpha-methylnaphthalene, $C_{11}H_{10}$, as the reference fuels. The former was assigned a cetane number of 100, while the latter was given a cetane number of 0.(2) In 1962 the ASTM added heptamethylnonane, $C_{16}H_{34}$, to the cetane scale as an intermediate, low-ignition-quality fuel with a cetane number of 15.(3)

The standard apparatus for determining and comparing ignition delay times is a CFR diesel engine developed by the Waukesha Motor Company. It is a one-cylinder, four-cycle engine with swirl-type combustion chamber and a compression ratio capability ranging from 6:1 to 28:1. Unfortunately, a number of problems are associated with using the CFR engine for evaluating ignition delay time and thus cetane number. Researchers have reported problems with the expense and time involved (4), with the repeatability and reproducibility of the test (4-6), with finding the proper cetane number for alternate fuels and fuels with ignition improvers added (7),and with fuels at the lower end of the cetane scale.(5,8) Many researchers are even questioning the validity of the cetane scale as an indicator of ignition quality.(3,5,7,9-11) These problems are discussed in greater detail in this report, along with a general discussion of the work that has been done in the area of ignition quality evaluation.

A major criticism of the CFR engine test for measuring the cetane number of a fuel sample has been the poor repeatability and reproducibility of the results. LeBreton (5) conducted tests on the repeatability of the CFR engine results and found the standard deviation for the data to be 0.8 cetane numbers. However, the sample only contained fuels with cetane numbers between 45 and 50. It is likely that the repeatability would not be as good for lower cetane number fuels. Glavinceveski, et al. (6), reported repeatability results for a set of 48 fuels as being 1.57 cetane numbers. The reproducibility for these same fuels performed on a number of engines differed by as

---

* Underscored numbers in parentheses refer to the list of reference at the end of this report.

much as ± 4 cetane numbers. Once again, the majority of the fuels had cetane ratings between 40 and 50, and none had a cetane number less than 37.

Much of the research into ignition quality has centered on how the ignition delay time and cetane number relate to the conditions under which the tests are conducted. Uyehara, et al. (12), in experiments performed in a specially designed research engine, conducted duplicate tests in which there was combustion in one cycle but not in the following cycle. They found that the peak of the difference in the pressure traces of the fired and unfired tests increased with decreasing ignition delay time. Tsao, et al. (13) found that delay times increased with decreasing air temperature and engine speed. Hardenberg and Hase (14) reported that delay times decreased with increasing compression pressure and air temperature. Finally, both Parker, et al. (15) and Walsh and Cheng (16) showed that ignition delay time can be decreased by increasing the fuel temperature at injection.

Other studies of the ignition delay time have focused on either the physical delay time or the chemical delay time. Elliott (17) noticed that ignition delay time decreased with lower fuel/air ratio. In a more comprehensive study of physical delay time, Wakil, et al. (18) drew the same conclusion and showed that it was caused by the relative spacing of the fuel droplets. They also found that physical delay times increased with droplet size and fuel boiling point due to vaporization characteristics. Rao and Lefebvre (19) also determined that the physical delay time is always a significant part of ignition delay. In a study of chemical delay times, Chiang, et al. (20) found that the rate of reaction of high-cetane-number fuels increases faster after ignition than that of low-cetane-number fuels. Cox and Cole (21) studied the chemical kinetics involved in chemical delay time and demonstrated a large increase in delay time with decreasing oxygen concentration of the air/fuel mixture.

There have been a number of studies concerning the effects on cetane number caused by blending alternate fuels with DF-2. Saeed and Henein (22) found that the addition of 10 vol% ethanol with DF-2 caused only a slight decrease in cetane number. However, they noted a drastic decrease in cetane number as the amount of ethanol in the blend increased from 20 to 70 percent. Henein and Fragoulis (3) studied the effects of blending a number of alternate fuels with DF-2. They found that blends containing indolene, unleaded gasoline, and No. 6 fuel oil each produced a drastic drop

4

in cetane number. Blends of DF-2 with medium naphtha and Jet A fuel produced very small decreases in cetane number, while a blend with No. 4 fuel oil caused the cetane number to increase slightly. Dabovisek and Savery (23) concluded that the ignition delay and therefore cetane number of a blend of two fuels is controlled by the component with the greatest autoignition resistance. Needham and Doyle (7) determined cetane numbers for synthetic and alternative fuels. They conducted studies of the cetane number of blends containing naphtha, sunflower oil, sunflower oil ester, shale oil, SRC-II, methanol, and tar sands. They found that ignition delay was not accurately predicted by ASTM D 613 for the vegetable oil and the blends of naphtha and methanol with DF-2. Finally, Siebers (11) conducted CVCB tests on blends of naphtha and coal-derived liquid fuel with DF-2, and on a degummed sunflower oil, a sunflower oil monoester, and methanol to determine how the delay times varied with temperature in the CVCB. All fuels behaved similarly to reference fuels with the exception of methanol, for which the delay time increased dramatically as the temperature decreased.

A substantial amount of work has been done with ignition quality improvers. Hardenberg and Ehnert (24) studied a number of ignition quality improvers and their effects on ethanol fuel blends. They found significant improvements in cetane number by using triethylene glycol dinitrate, diethylene glycol dinitrate, cyclohexyl nitrate, and isoamyl nitrate. They also found that adding 17.5 vol% of hexyl nitrate could decrease the delay time of ethanol and methanol to such an extent that the indicated cetane number approached extremely high values. Bowden and Frame (25) determined that disulfides and polysulfides increased cetane number. Olree and Lenane (26) reported that engine response to chemically induced cetane numbers is the same as engine response to natural cetane numbers. Collins and Unzelman (27) suggested that the best use of ignition quality improvers at this time would be increasing the volume of diesel fuel stocks by blending with light cycle oils and then adding improvers to bring the cetane number up to the acceptable range. They also stated the need in the future for a cetane improver that could increase the ignition quality of a light cycle oil from 35 cetane numbers to 50. Unzelman (28) also conducted a study of the economics of cetane improvement with different levels of DII-3 improver.

Due to the time and expense required to conduct ignition quality tests on the CFR engine, attempts have been made to obtain the same results using CVCBs.

5

CVCBs are advantageous because they require much less fuel than an engine. Therefore, tests can be conducted when only a small amount of fuel is available.(2) The early CVCBs recorded ignition delay times on the order of tenths of a second, as opposed to delay times of several milliseconds in CFR engines. This discrepancy was partially resolved in the 1930's through the use of high pressure and turbulence in the CVCB.(2) However, the CVCB still yielded a delay time longer than that of an engine by a factor of two (18), although Tsao, et al. (13) determined that cetane numbers follow the same trend in both engines and CVCBs. Another problem with CVCBs was that they had to be placed in a heater to achieve the necessary temperature to simulate a diesel engine. Oren, et al. (29) solved this problem by developing a modified CVCB for which heating was unnecessary. Simulation of the compression stroke was achieved by burning a lean precharge composed of acetylene, oxygen, and nitrogen. Siebers (11) used a similar approach of spark igniting a premixed $C_2H_4/H_2/O_2$ charge.

Also motivated by the time and expense required to conduct cetane rating tests on the CFR engine, many attempts have been made to develop correlations using fuel properties and test conditions to predict cetane number. Hardenberg and Hase (16) tried activation energy as an indicator of cetane number, and Collins and Unzelman (30) used API gravity and mid-boiling point temperature. Klopfenstein (31) correlated density and mid-boiling point temperature with cetane number, while Murphy (32) included percent hydrogen with density and mid-boiling point temperature. Glavincev-ski, et al. (6) tried to use aromatics to predict cetane number, and Steere (33) developed a correlation between cetane number, aniline point, viscosity, density, and D 86 distillation. All of the above correlations provided good, but not exceptional, agreement with known values of cetane number. However, the one variable which has been used to predict cetane number effectively is nuclear magnetic resonance (NMR).(4,25,34) Bailey, et al. (34), in using NMR data, obtained cetane numbers for nonaromatics as a function of the relative quantities of methine hydrogen and methylene hydrogen. They also developed a model for aromatic hydrocarbon fuels which included the relative quantity of alpha hydrogen and relative squared sum of alkyl hydrogen along with the two parameters listed above. The R-squared curve fits for these two correlations were 0.999 and 0.997, respectively. The resulting deviations were not any resulting deviations were not any greater than that caused by the repeatability of the cetane rating as obtained in CFR engine tests.

The results of Bailey, et al. (34) provide an accurate and less expensive means of predicting cetane number. However, there remains an undesirable characteristic of this and some of the other more accurate cetane number predictors -- the complexity of the necessary instrumentation. As Henein and Fragoulis (3) pointed out, the majority of the correlations for cetane number are in terms of physical properties that cannot be measured by sensors. There is still no existing correlation for cetane numbers based on the most easily determined fuel characteristics. One possible exception is the Viscosity-Gravity number, although it was developed to predict cetane numbers for more viscous fuels than the alternate fuels that are now being proposed for diesels.(3) At present, there is also no good cetane number predictor for alternate fuel blends or fuels with ignition improvers.

The main question concerning the cetane number rating scale seems to be whether the cetane number is an accurate measure of the ignition quality of a given fuel. Taracha and Cliffe (10) noted that cetane number is simply a measure of ignition delay, not ignition quality. Also, Needham and Doyle (7) found that ignition delay is not the controlling factor in determining overall fuel performance. They have stated that a new rating method is necessary. Siebers' (11) results showed that cetane number does not provide an accurate measure of ignition quality of fuels whose ignition delay dependence on temperature (i.e., compression ratio) and type of ignition process (single-stage or two-stage) differ from the reference fuels. LeBreton (5) noticed a reduction in repeatability of cetane numbers for low-quality fuels, while Henein and Fragoulis (3) reported difficulty in achieving the necessary compression ratio in the CFR engine to get fuels below 15 cetane numbers to ignite. To sum up the dissatisfaction with the cetane number scale, Hardenberg and Ehnert (24) stated, "the cetane number is just as unrepresentative of the ignition characteristics of a fuel in the practical diesel engine as the measurement range of the cetane rating method is of the operating range of diesel engines."

In summary, the basic problems associated with the current ASTM cetane rating procedure are that neither the engine nor the test conditions are representative of modern practice. In addition to the basic problem, there are several, more practical problems with the current system. These can be summarized as follows:

1. Cetane number does not correlate directly with engine startability in modern engine designs;(24)

2. The standard deviation of the measurement is high (0.7 CN) in a given laboratory (5) and laboratory-to-laboratory variations can be as high as 4 to 6 CN;(4)

3. The cetane number does not provide an accurate measure of ignition quality of fuels in which the ignition delay dependence on temperature and type of ignition (single-stage or two-stage) differ from the reference fuels; (11) i.e., the procedure is realistically limited to petroleum diesel fuels.

4. The time and cost factors associated with the current procedure (ASTM D 613) are prohibitive.(4)

New approaches to rating ignition quality should address the underlying problems of adequate representation of modern practice, in addition to the other problems listed above. CVCB techniques offer several advantages over engine-based procedures. Preliminary examination of the CVCB approach indicated that the technique could be useful in defining differences in the temperature sensitivity (and, therefore, the fuel compositional/ignition-kinetics interactions) of various fuels. Added advantages of a CVCB-based procedure include:

- It requires very little fuel;

- It is quick and inexpensive;

- It can be used to provide a cetane number during the transition to a new rating scale;

- It can be performed in an inexpensive apparatus;

- The apparatus can be portable or can be used for quality control during processing.

If engine-based techniques are required for some reason, the new rating techniques must be performed in an engine configuration and at test conditions representative of current practice. It is envisioned that the test engine should be direct-injection and

8

capable of speeds up to 2500 rpm to be representative of the current design of heavy-duty engines. Design features deemed to be important in the performance of the evaluation are variable compression ratio, accurate control of inlet air and coolant temperatures, and accurate control of fuel flow rates.

It was felt at the beginning of this project that both the CVCB- and the engine-based techniques should be pursued. The logic was that if the CVCB technique was successful, the engine technique would not be necessary. However, the engine data would enhance the CVCB data through correlation. If, on the other hand, the CVCB procedure did not meet expectations, a new engine-based technique would be available as a replacement for the current ASTM procedure.

As a measure of the ignition quality of a diesel fuel, it may not be reasonable to expect current procedure or future procedures to produce a result which correlates universally with other engine parameters such as power, efficiency, or emissions. If a procedure results in a true indication of ignition quality, this same parameter would not indicate efficiency, which depends on the complete combustion process, or emissions, which depend on both the combustion chemistry as well as the engine/injection system geometry.

C.   Objectives

The overall objective of this project was to investigate the possibility of developing new techniques for rating the ignition quality of fuels for diesel engines. The first specific objective included the development of a Constant Volume Combustion Bomb apparatus and technique which, in addition to being acceptable as a standard technique, could be developed into a mobile or laboratory-based system for use by the U.S. Army. The second specific objective involved the development of the apparatus, consisting of a direct-injection, variable compression-ratio diesel engine, and the technique for a new engine-based ignition quality rating procedure.

9

II. EXPERIMENTAL

The two different experimental apparatus used in this project are described separately in this section. The development of each apparatus and the associated operating procedures are described in terms of the preliminary experiments which were performed in each. The refinements made to both systems over the course of the project are described. The test fuels used in this project are described at the end of this section.

A. Ignition/Combustion Apparatus

The experimental apparatus used in the CVCB experiments consist of the CVCB pressure vessel, the fuel injection system, and the data acquistion and reduction system. Fig. 1 is a schematic showing the various components of the experimental apparatus.

1. Constant Volume Combustion Bomb

The heart of the apparatus is a high-pressure, high-temperature combustion apparatus. Fig. 2 is a cross-sectional simplified sketch of the CVCB. The apparatus consists of a stainless-steel cylinder machined internally to prevent fuel impingement on the metal surfaces when using a pintle nozzle. The internal volume is 52.3 cm^3 with a diameter of 2.5 cm and an approximate length of 10 cm.

The CVCB can be charged with any gaseous oxidizer or inert gas, but the design limits were based on an initial pressure and temperature of 4.1 MPa (600 psia) and 538°C (1000°F), respectively, with a stoichiometric mixture of diesel fuel and air. The theoretical peak pressure corresponding to the design condition is approximately 34.9 MPa (5000 psia). The CVCB is equipped with electrical resistance heaters that are used to heat the vessel walls as well as the contents of the combustion chamber. An automatic controller is used to control the surface temperature of the CVCB. Surface thermocouples and thermocouple probes are used to determine the temperature of the CVCB walls and contents, respectively. A water-cooled piezoelectric pressure transducer is installed for measurement of the pressure-time relationship, while a charge amplifier is used to condition the transducer signal.
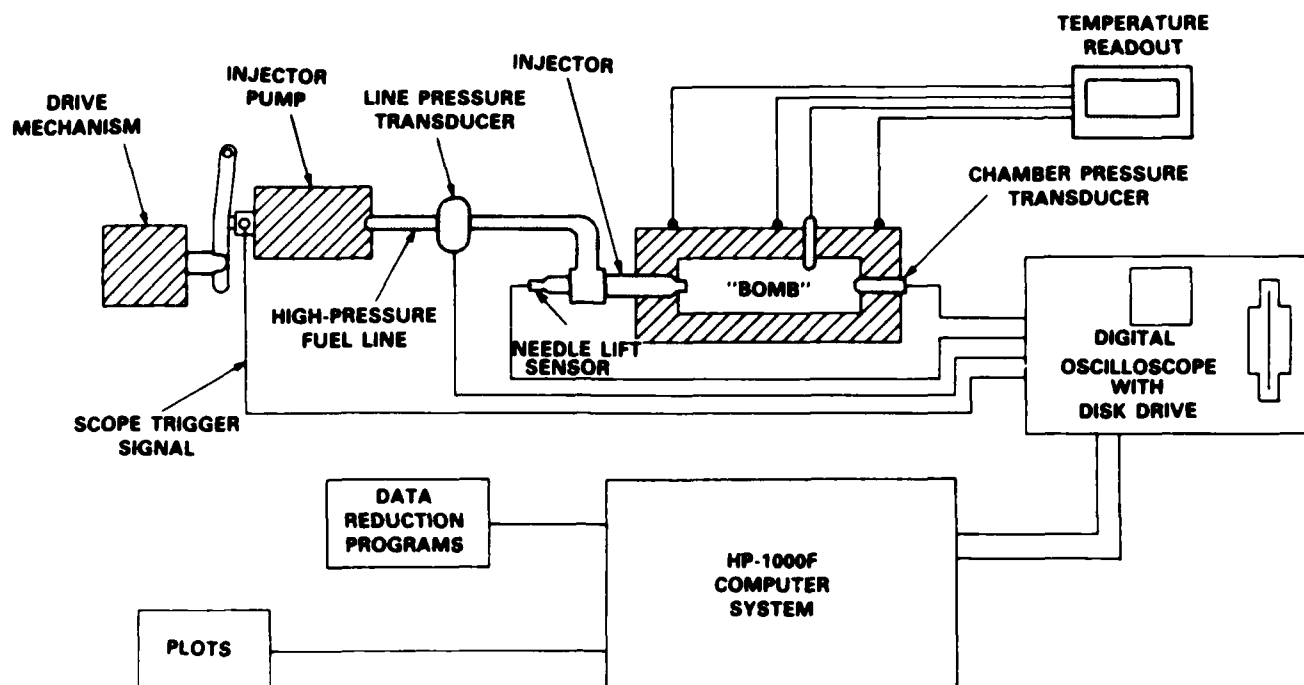
Figure 1. Schematic of the ignition/combustion apparatus
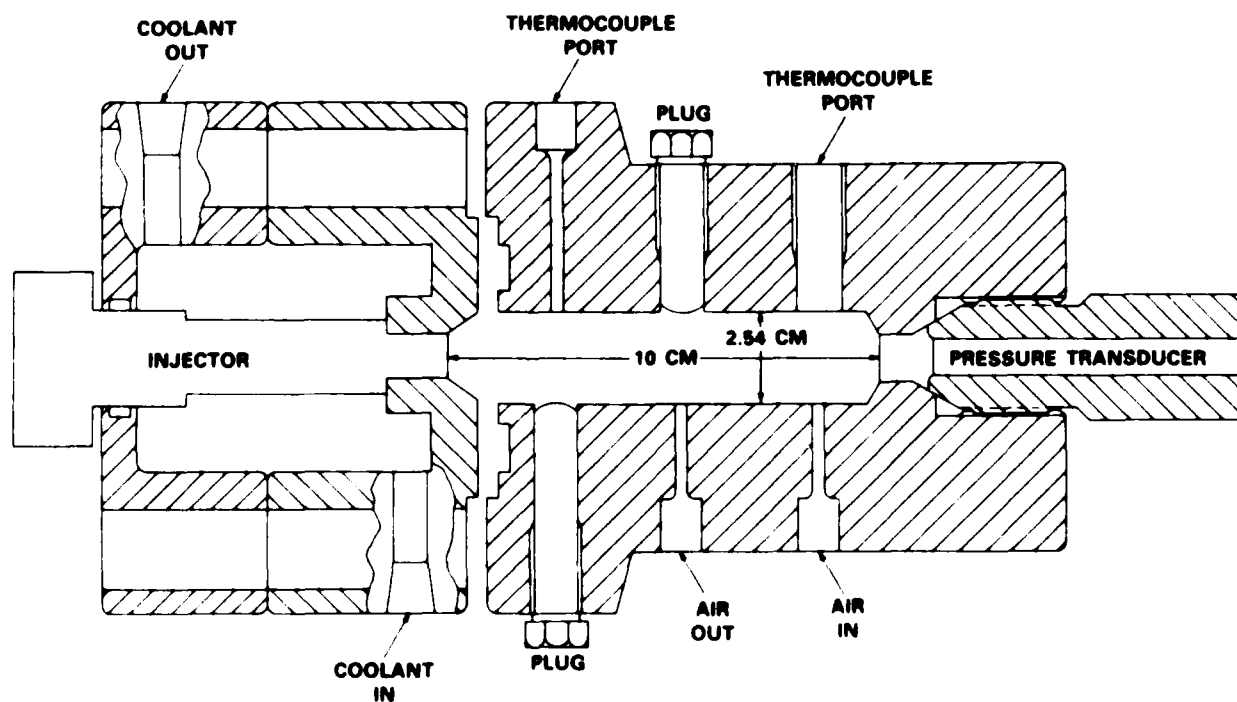
Figure 2. Cross-sectional schematic of the ignition/combustion apparatus

2. Fuel Injection System

The injection nozzle selected for use in this project is an inward-opening, throttling-pintle nozzle. The spray characteristics of this type of nozzle have been well-documented in previous SwRI projects on a variety of fuels (35,36), ranging from coal/DF-2 slurries to selected mixtures of lube oil blending stocks. This characterization of the injection nozzle included cone angle and penetration rate data, and drop size determinations, all as functions of the fuel viscosity. The CVCB size and geometry were selected such that fuel impingement on the CVCB walls would not occur when using this nozzle, even with fuels of different viscosities.

As a general observation, the viscosities of most fuels tend to converge as the fuel temperature is increased. In many engines, the normal fuel temperature is within the range at which this effect is observed. In this program, considerable effort was devoted to the design of the injection nozzle to provide for adequate cooling and to allow for measurement of the nozzle temperature. The nozzle was provided with internal cooling in addition to the external cooling jacket. Fuel temperatures were monitored by measuring the temperature of the nozzle close to the tip. It was hoped that these measures would allow for observation of fuel viscosity effects by maintaining the fuel temperatures at less than 38°C.

As indicated by Hurn, et al. (8), the ignition delay times are greatly affected by the rate of fuel injection. Considerable effort was therefore devoted to the development of the injection system. The primary concern was the repeatability of the injection event not only when using fuels with similar physical properties (viscosity, gravity, and surface tension) but also with fuels of broadly varying physical properties. Although several parameters can be chosen for defining the repeatability of the injection rate, the mass flow rate, based on line pressure and needle lift, was selected because of the impact of the fuel mass flow rate on the cooling of the air charge in the CVCB.

The injection nozzle is equipped with a line pressure transducer installed at the nozzle and a needle-lift sensor. The fuel injection system, specially designed for single-shot injection, has been designed to develop injection-system dynamics and characteristics similar to those observed on systems installed on engines. The injection system

12

consists of a 9-mm barrel-and-plunger assembly mounted in a pneumatically actuated drive system.

On a given fuel, the repeatability of the injection process is excellent as demonstrated in Fig. 3 and 4. The figures are plots of the line pressure (Fig. 3) and needle lift (Fig. 4) of four injections of hexadecane. The plots have been shifted slightly to permit examination of each trace. As can be seen, the traces are virtually identical. A similar comparison indicated that the fuel-to-fuel results were also repeatable. This is demonstrated in Fig. 5 where the line pressure traces for a high-viscosity (20.28 cSt) blend is compared to that of a 50/50 blend of hexadecane and heptamethylnonane (3.05 cSt). Although some variation is evident, it was felt that these results were acceptable for the comparative studies discussed in this report.

3. Experimental Procedures

The technique used in the experiments consists basically of the development and application of a technique suggested by Hurn, et al. [8] and Yu, et al. [12]. As adapted and applied to the CVCB described previously, the technique consists of measuring the pressure change that occurs in the CVCB during the injection process. These measurements are made under identical thermodynamic conditions, using the same spray characteristics with fuel being injected first into air and then into nitrogen. In a typical experiment, two pressure traces are obtained, one with the fuel injected into air with subsequent combustion, and one with the fuel injected into nitrogen. An example of the data obtained from the CVCB is plotted in Fig. 6. The pressure time records are shown for the injection of 50 percent (V/V) blend of hexadecane and heptamethylnonane into both nitrogen and air.

Comparing the pressure traces, it can be seen that, in both cases, the pressure decreases during the early part of the injection event. In the case with air, the pressure ultimately rises due to the onset of self-sustaining combustion. In nitrogen, the pressure remains below the baseline. In both cases, the pressure drop is due to the vaporization of the fuel. The physical delay (τ_p) has in the past [12,20] been defined as the time measured from the start of injection to the point at which the nitrogen and air cases diverge. The chemical delay (τ_c) is then defined as the time elapsed from the divergence point to the point where the air case crosses the baseline. These
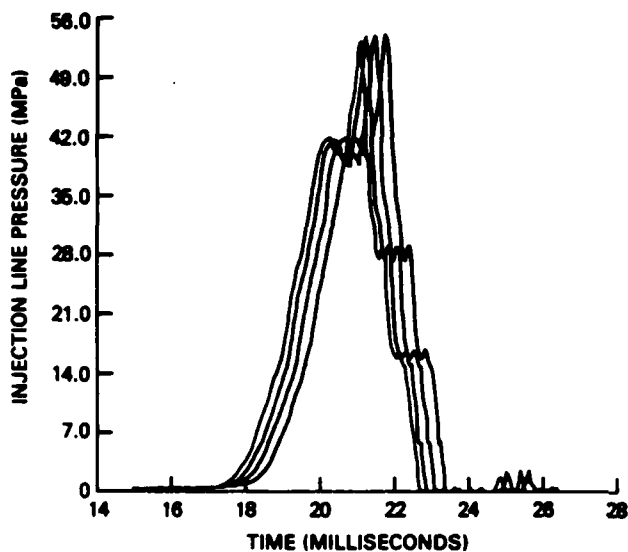
Figure 3. Injection line pressure traces for hexadecane
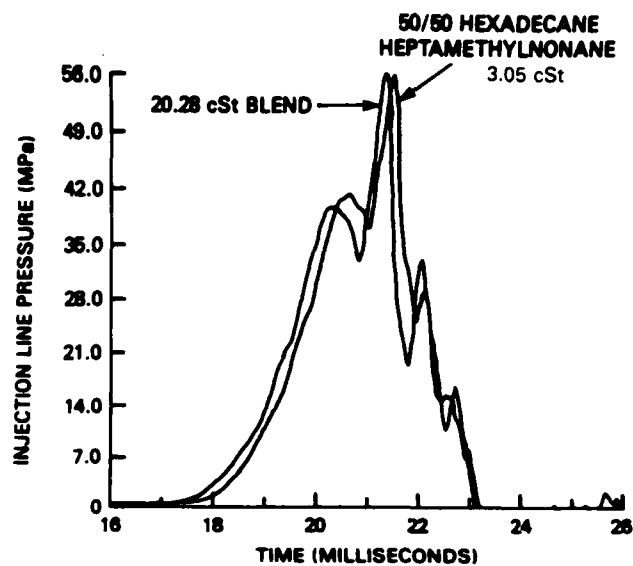
Figure 5. Injection line pressure traces for the 50/50 blend of hexadecane and heptamethylnonane and the 20.28 cSt blend
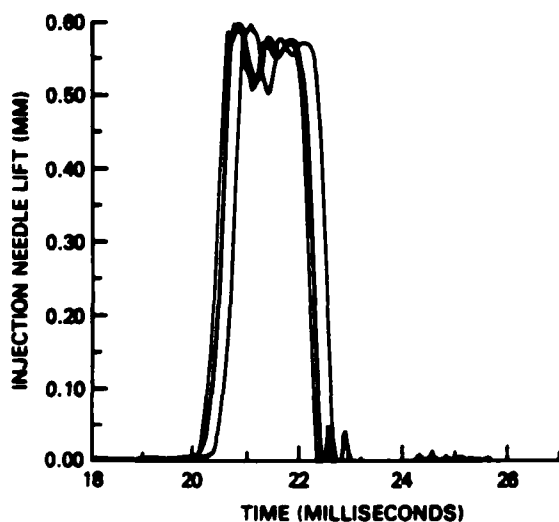
Figure 4. Injection needle lift traces for hexadecane
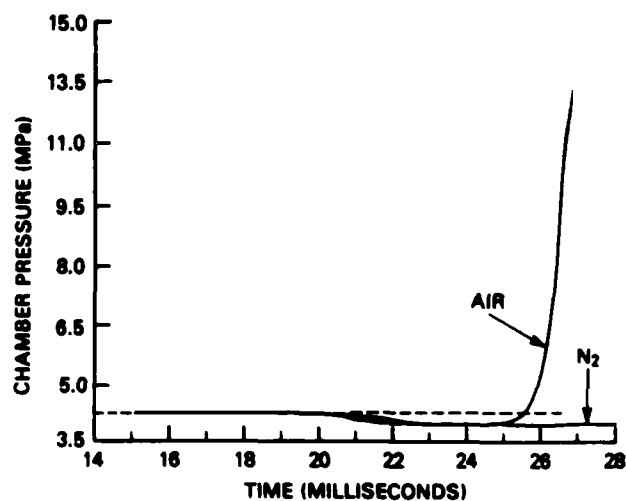
Figure 6. Pressure–time records, 50/50 blend of hexadecane and heptamethylnonane in both air and nitrogen

14

definitions are somewhat arbitrary in that chemical reactions could occur during the defined physical-delay period, while the definition of chemical delay implies that the reactions become self-sustaining only after the cooling effect of fuel vaporization is overcome.

A better definition of the physical delay time is based on the realization that the fuel vaporization and mixing are coupled, and affect the chamber pressure during the same time interval. The improved definition for the physical delay, therefore, is measured in terms of the elapsed time from the start of injection (needle lift rise) to the minimum of the chamber pressure trace. The definitions of the various points on the scope trace are shown in Fig. 7.
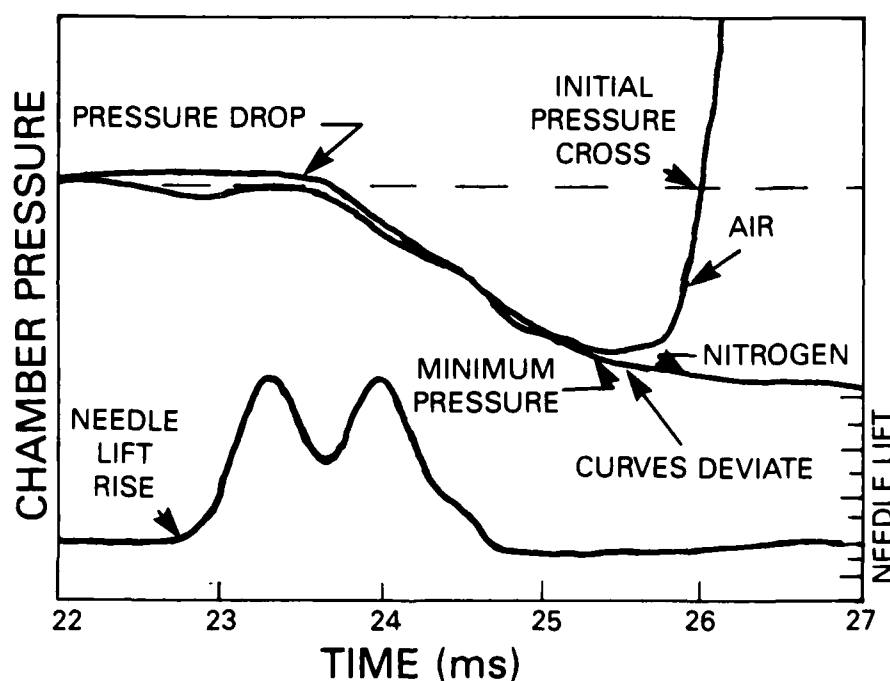
Figure 7. Pressure-time records and injection-nozzle needle-lift trace with identification of the various points of interest

The question of defining the ignition delay time usually results from the difficulty of identifying the start of combustion. Several possibilities include the start of pressure rise, the start of heat release, or the occurrence of a luminous flame. In this work, the total ignition delay time (τ_d) is defined as the time from the start of injection, as

15

indicated by needle lift, to the initial pressure cross-point (see Fig. 7). It was felt that this definition was acceptable for these comparisons because of the similarity in the shapes of the combustion pressure traces. The chemical delay time is defined as the difference between the total delay and the physical delay times.

The repeatability of the overall combustion event, including the ignition as well as later burning, is demonstrated in Fig. 7 for a 75/25 blend of hexadecane and heptamethynonane. As noted in the following paragraphs, the standard deviations of the ignition delay times were generally small. From a purely visual observation of the results with several fuels, some differences were observed in the later stages of combustion. These differences were generally evident in the slopes of the later stages of the pressure traces, indicative of differences in the global reaction rate. Since the ignition process was apparently not affected, the differences were not examined in this study.

4. Data Acquisition and Analysis

The chamber pressure data and the line-pressure and needle-lift data are displayed, digitized, and stored on floppy disc using a high-resolution digital oscilloscope. An interface installed between the digital oscilloscope and a Hewlett-Packard 1000F computer is used to transfer data from the scope to the computer for computations and permanent storage. Data reduction and analysis, including the determination of the various delay times, are performed using computer programs specifically developed for use on this project. These procedures are described in Appendix A.

5. Experimental Test Matrix

Most of the experiments in this study were performed at an initial pressure of 4.1 MPa (600 psia) and at initial temperatures of 371°C (700°F), 427°C (800°F), and 482°C (900°F). Forty-two test fuels were evaluated at these conditions. The experiments for each fuel, at each test condition, were repeated a minimum of four times.

Several preliminary experiments were performed to identify the effects of various test conditions and operating parameters on the ignition delay times. The test conditions examined in the preliminary experiments included the initial temperature and pressure

in the CVCB. The operating parameters examined included fuel supply pressure to the injection system, fuel temperature, and total mass of fuel injected.

During the experiments, it was found that the ignition delay time is affected by both the pressure and the temperature of the air in the CVCB at the time of fuel injected. These thermodynamic properties both affect the air density, but in opposite directions. From the preliminary experiments, it was found that the ignition delay time increased as pressure decreased and also as the temperature decreased. The pintle-type nozzle used in these experiments has been found in previous work (35,36) to perform similar to a pressure atomizer in response to variations of the air density, i.e., as the density is decreased, the penetration rate and cone angle both increase. As the CVCB pressure decreases at constant temperature, the air density also decreases, possibly resulting in better atomization (increases penetration and cone angle) which would be expected to result in a decrease in the ignition delay time. The lower density most definitely results in a decrease in the molar concentration of oxygen molecules which would be expected to increase the ignition delay times. Since the ignition delay times increased with decreased pressure, the molar oxygen concentration was obviously the dominant factor. The effects of the atomization process were minimized in these experiments as indicated by the fact that the CVCB density did not affect the ignition delay time in the expected manner if atomization were the dominant factor. This is also verified by the fact that the physical ignition delay time was not observed to be a function of fuel viscosity or test condition. This observation is discussed in more detail in another section.

An increase in the CVCB temperature, at constant pressure, results in a decrease in the air density. This factor, coupled with the improvement in atomization and the Arrhenius temperature effects on ignition, are expected to result in a decrease in the ignition delay as the temperature is increased. This is indeed the case as observed throughout these experiments and as reported by others.(8,11)

The operating conditions of fuel supply pressure at the injection pump (not the injection pressure) and the fuel temperature did not affect the observed ignition delay times. These experiments were performed over a range of fuel temperatures from 31° to 59°C and supply pressures ranging from 0.17 to 0.69 MPa. The operating conditions could be easily controlled within these ranges, and these experiments were performed

17

to verify that the results would not be affected by minor variations in these parameters.

The total mass of fuel injected was varied from full rack, approximately 70 cm^3/1000 strokes, to approximately 15 cm^3/1000 strokes. Within this range, the ignition delay time was not affected by variations in the total delivery. The overall combustion event was obviously affected in terms of the rate of combustion pressure rise and the total pressure, but these parameters were not observed to have an effect on the ignition delay times. In an engine this would not happen because increases in fuel delivery (increases in load) result in higher combustion chamber temperatures and, in turn, shorten ignition delay times.

B.   Variable Compression-Ratio Engine

The test engine used in this program was specially designed and fabricated by SwRI for use on this program. The engine is located in a dedicated test cell equipped with a motoring eddy-current dynamometer, high- and low-speed data acquisition links to a central computer, and a dedicated data acquisition system for storage and monitoring of selected data for rapid analysis.

1.   Test Engine

The test engine incorporates several design features which make it unique. The engine was designed around the crankcase of a standard Laboratory Equipment Company CLR engine. The major standard components incorporated in the CLR design included the crankcase, the crankshaft, the counter balance case and flywheel, the connecting rod and piston assembly, the cylinder liner, and the cam shaft. The SwRI engine incorporates a new head assembly design which includes a chain-driven overhead cam, liner carriers for wet liners, and a continually variable head elevating system. The compression ratio of the engine is varied by moving (raising or lowering) the head assembly relative to the crankshaft. This movement is accomplished using a hand crank which activates the head elevating mechanism through a chain drive. A simplified cross-sectional view of the head assembly is presented in Fig. 8. As seen in the drawing, the overhead cam and the cylinder liner carrier and the liner all move with the head. Although variations in valve timing are easily accomplished in this

18
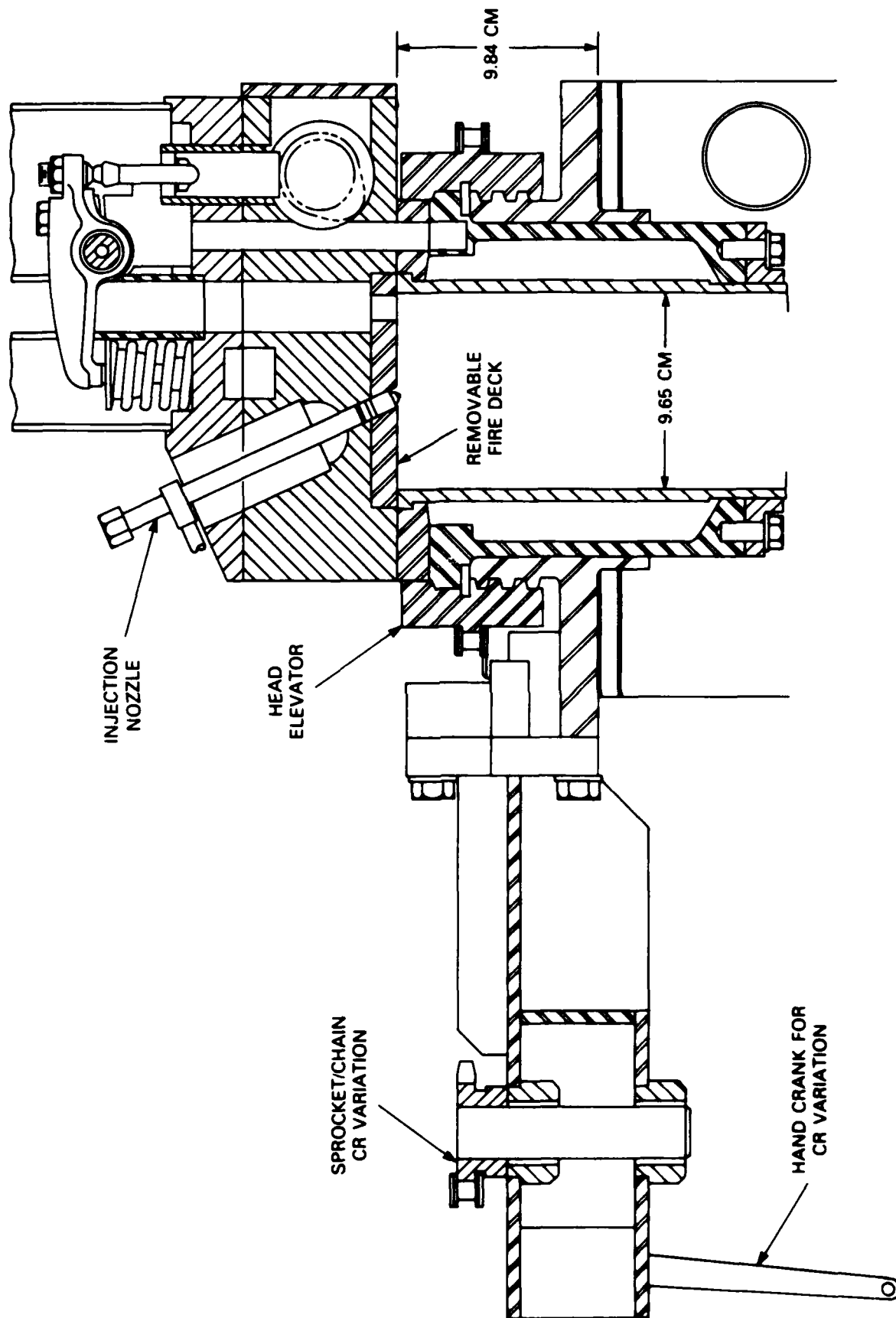
Figure 8. Variable compression-ratio test engine

design, a special chain drive mechanism was designed to maintain constant valve timing during changes in the compression ratio. The compression ratio can be varied while the engine is running.

The engine configuration used in this program consisted of direct-injection system using a four-hole injection nozzle located centrally over a deep "Mexican Hat" combustion chamber in the piston. As seen in Fig. 8, the injection nozzle is mounted through a large hole incorporated in the head. The location and geometry of this hole are such that the engine can be converted to either a prechamber or a swirl chamber indirect-injection configuration.

The fire deck of the engine consists of a removable steel plate which contains the valve seats, a port for a water-cooled pressure transducer, and two ports for the light source and an optical probe of an in-cylinder high-speed movie system. While not important in this program, the removable fire deck was incorporated in the design so that material changes could be easily made. This feature would be desirable in studies involving high-temperature ceramic coating or monolithic ceramic parts.

The engine design specifications, while variable in most instances, were held constant for this project. The important specifications are listed in TABLE 1. The maximum

TABLE 1. Test Engine Specifications

Bore	9.65 cm
Stroke	9.53 cm
Compression Ratio	9.2 - 18.5
Value Timing:	
Intake Opening	15° BTDC
Intake Closing	40° ABDC
Exhaust Opening	60° BBDC
Exhaust Closing	20° ATDC
Combustion Chamber Configuration	"Mexican Hat"
Combustion Chamber Volume	37 cm^3
Combustion Chamber Diameter	5.5 cm 5.5 cm

operating speed of the engine is 3000 rpm. The experiments in this project were performed at 1000 and 2000 rpm. The test matrix and test procedures are described in another section.

The intake air system for the engine consists of a large mixing tank and an in-line electric heater located upstream of the engine. The air is supplied at pressures up to 100 psi using a compressed air system. Air flow rate to the engine is monitored using a precision rotameter. The intake pressure is monitored using a manometer, and is controlled using a two-stage pressure regulator.

The engine is started, motored, and controlled using an eddy-current dynamometer directly coupled to the crankshaft. The dynamometer controller is designed to maintain the speed within $\pm$ 5 rpm at any of the test conditions. The torque transmitted to the cradled dynamometer is measured using a strain gauge load cell.

The engine injection system consists of an American Bosch, type AKF-1005 injection nozzle with a four-hole nozzle tip that has a spray angle of 140°. The nozzle is equipped with a needle lift indicator to provide an accurate measurement of injection timing. The nozzle opening pressure was set at 20.7 MPa (3000 psi). A line pressure transducer was installed in the injection line as close to the nozzle as possible. The injection pump is a three-cylinder CAV Simms attached to the same drive mechanism as the camshaft. The middle pump location is equipped with an 8.5-mm barrel and plunger assembly, and the two end locations are sealed. Fuel flow rate is adjusted using a micrometer barrel attached directly (no governor) to the pump rack. The pump is flange mounted on the engine using slotted bolt holes. Injection timing is adjusted by simply rotating the fuel injection pump.

The fuel flow rate is determined gravimetrically using a load cell digitizer in conjunction with an electronic weighing platform. The supply and return lines for the injection system were run to a common container on the weighing platform. The digitizer provided digital readout of the change in the weight of the container as a function of time. These readings were integrated over a precisely determined time increment to give the net rate of fuel flow to the engine.

21

2. Data Acquisition and Analysis

The primary experimental data developed in the engine studies consisted of the ignition delay time as a function of the other experimental variables. The definition of ignition delay time used in the engine experiments was analogous to that used in the CVCB experiments. The ignition delay time, in milliseconds, was determined using the first motion of the nozzle valve, as sensed by the needle lift indicator, as the start of injection. The start of combustion was defined in terms of the start of combustion pressure rise as determined using a water-cooled piezoelectric pressure transducer installed in the combustion chamber. The outputs from the pressure transducer amplifier, the needle lift indicator, and a TDC marker were monitored using a digital oscilloscope. The scope data from each test was stored on floppy disc using a disc drive unit associated with the oscilloscope. Numerical reduction of the data, in terms of the ignition delay time, was obtained using a digitizing option on the oscilloscope.

3. Engine Test Procedures

A baseline diesel fuel and eighteen different test fuels were examined using the same procedure. In this procedure, the test fuel is flushed through the fuel system and the engine is run on the test fuel for several minutes prior to the start of testing. The air flow rate is fixed for the given speed, and the load is varied by changing the fuel flow rate. At the given test condition, the fuel flow rate is adjusted to give the desired air/fuel ratio, and the injection timing is set such that combustion starts at top dead center (TDC). Once at the desired condition, the data are recorded, and the ignition delay time is determined using the procedure described previously. Data were obtained for each fuel at three compression ratios (11:1, 14:1, 17:1), at three air/fuel ratios, 20:1, 30:1, and 40:1 (corresponding approximately to full, 75- and 50-percent loads), and at two different speeds (1000, 2000 rpm). These factors resulted in a test matrix of 18 different test conditions for each fuel.

In the standard cetane rating procedure (ASTM D 613), the injection timing is fixed at 13° BTDC, and the compression ratio is adjusted to get the start of combustion at TDC. This results, effectively, in a test at constant ignition delay time, and which serves as a measure of the autoignition temperature (indirectly through the compression ratio) of the test fuel. This procedure provides a direct measurement of the

22

ignition delay time as a function of temperature (compression ratio) and the engine speed (turbulence) and load (air/fuel ratio).

Preliminary experiments were performed using the baseline fuel and a modified test procedure. In these experiments, the injection timing was adjusted so that the start of combustion occurred at TDC for the given speed, load, and compression ratio. Holding all other parameters constant, the compression ratio was then varied over the largest possible range at the given test condition. For example, if the test condition were 1000 rpm, 20:1 air/fuel ratio, and 14.1 compression ratio, the injection timing was fixed to give the start of combustion at TDC. The ignition delay time was recorded at this point and also at the 11:1 and 17:1 compression ratio settings. Injection timing was not adjusted from the original setting for the other two compression ratios.

As expected, the injection timing had to be retarded as the compression ratio was increased in order to set the start of combustion at TDC. The excursions in compression ratio at fixed injection timing resulted in conditions in which ignition occurred either before or after TDC, depending upon the particular test condition. A general trend which became obvious during the analysis of the data was an increase in the ignition delay time (at fixed compression ratio) as the injection timing is advanced. The observed effect is a manifestation of two factors. The major factor is simply the longer residence time before reaching the autoignition temperature, which for a given fuel, speed, and compression ratio is fixed, within limits, by the piston location. The secondary factor, while related to the residence time, involves the fuel and air mixing and the resulting air/fuel ratio and temperature distributions throughout the combustion chamber. As an example, the highest temperature locations could incorporate the leanest regions and the longest ignition delay times. In this regard, the data trends indicate that ignition delay time increases as the overall air/fuel ratio increases. In the limit, this would be expected, at least for a homogeneous system, since the ignition delay time is infinitely long at conditions beyond the lean limits of combustion.

The trends were repeated at the other speed/load test conditions for the baseline fuel. Since these data appeared to add little to the understanding of the ignition delay time and since it involved a very large test matrix, these experiments were not repeated for the other test fuel.

23

C.   Test Fuel Description

As indicated previously, 42 test fuels were evaluated in the CVCB experiments.
Seventeen of these test fuels and a special baseline fuel were tested in the variable
compression ratio, direct-injection engine.   The gravity, viscosity, boiling points (50
percent point for mixtures), cetane number, and the fuel descriptions are listed in
TABLE 2. The test fuels used in the engine experiments are designated by an asterisk.
The test fuels can be considered in terms of three general groups: pure hydrocarbons
or blends of pure hydrocarbons (Fuels 1 through 17); special blends, including several
alternative fuels (Fuels 18 through 37); and military specification jet and diesel fuels
(Fuels 38 through 42).

Although all the fuel properties are of interest, those properties which affect
atomization, vaporization, and ignition were of prime interest in this project. The
atomization process is generally modeled in terms of the fuel viscosity and specific
gravity.   The boiling point distribution, or the boiling point for pure compounds,
provides a direct indication of fuel volatility and thus the vaporization characteristics.
The ignition quality has been historically defined in terms of the cetane number.

As can be seen in TABLE 2, the range of property value is fairly large for each of the
three groups. For the pure compounds, the specific gravity ranges from 0.34 to 0.885,
viscosity ranges from 0.41 to 3.09 cSt; boiling points range from 64° to 287°C, and
cetane numbers range from 15 to 100. For the special blends, the range of specific
gravity is 0.8484 to 0.992, viscosity varies from 2.09 to 33.93 cSt, boiling points (50
percent point) range from 239° to 588C, and cetane numbers vary from 31.5 to 59.9.
The property ranges for the jet and diesel fuels are 0.7632 to 0.9048 for specific
gravity, 0.76 to 6.99 cSt viscosity, 166° to 314°C for 50 percent boiling point, and 27.8
to 43.3 cetane number.

The pure compounds include paraffins, olefins, cycloparaffins, and aromatics. Included
in the list are the primary reference fuels for cetane rating (hexadecane and
heptamethylnonane) and also for octane rating (isooctane and normal hexane). The
special blends include blends of light lube oil blending stocks, selected specifically for
variations in viscosity (Fuels 18, 19, 20, 25, 26), fuels selected as representative of
future or alternative fuels (Fuels 21 through 24), including fuels which have already

TABLE 2. List of Test Fuels With Selected Fuel Properties

Fuel No.	Fuel Description	Specific Gravity	Viscosity, cSt at 40°C	Boiling Point or or 50% Point, °C	Cetane No.
1	100% Isooctane	0.6962	0.65	99	17.5
2	75% Isooctane 25% Tetradecane	--	--	—	36.9
3	50% Isooctane 50% Tetradecane	--	--	—	56.3
4	25% Isooctane 75% Tetradecane	--	--	—	75.7
5	100% Tetradecane	0.7667	1.83	252	95.0
6*	100% Hexadecane	0.773	3.00	287	100.0
7*	100% Heptamethylnonane	0.793	3.09	240	15.0
8*	75% Hexadecane 25% Heptamethylnonane	--	--	—	78.8
9*	50% Hexadecane 50% Heptamethylnonane	--	--	—	57.5
10*	25% Hexadecane 75% Heptamethylnonane	--	--	—	36.3
11*	100% N-Octane	0.7068	0.65	125	64.4
12	100% 1-Hexene	0.34	0.68	64	27.3
13*	100% N-Hexane	0.6640	0.41	69	44.8
14	100% 1-Tetradecene 93%	0.7752	1.92	251	80.5
15*	100% Cyclohexane Ultrapure	0.7834	0.95	81	16.9
16	100% 2 Xylene	0.8848	0.74	144	8.3
17	100% Benzene	0.8844	0.59	79	14.3
18*	19-cSt Hydrocarbon Blend	0.8702	19.47	351	53.8
19*	12-cSt Hydrocarbon Blend	0.8571	12.84	368	55.8
20*	5-cSt Hydrocarbon Blend	0.8607	4.96	316	48.5
21	FL-0403-F SRC-11/DF-2 Blend	0.889	2.47	259	35.6
22*	FL-0442-F Sunflower Oil	9.220	33.93	588	35.8
23*	FL-0433-F Sunflower Ethylester	0.8870	4.96	368	59.9
24	FL-0413-F Tar Sand/DF-2 Blend	0.8810	2.82	267	35.2
25	14.4-cSt Hydrocarbon Blend	0.8756	14.39	347	48.5
26	20.3-cSt Hydrocarbon Blend	0.8581	20.28	378	57.5
27	FL-0744-F Wisconsin Hi Vol., Hi CN Blend	0.8314	2.01	239	48.7
28	FL-0745-F Wisconsin Hi Vol., Lo CN Blend	0.8934	2.25	264	31.5
29	FL-0746-F Wisconsin Lo Vol., Lo CN Blend	0.9147	3.48	284	32.7
30	FL-0747-F Wisconsin Lo Vol., Hi CN Blend	0.8488	2.84	262	49.3
31	AL-13279-F DF-2 Blend A	0.8484	2.75	273	48.7
32	AL-13639-F DF-2 Blend B	0.8545	2.53	266	45.2
33	AL-13664-F DF-2 Blend C	0.8565	2.44	262	44.3
34	AL-13694-F DF-2 Blend D	0.8597	2.75	274	44.9
35	AL-13992-F DF-2 Blend E	0.8644	2.76	274	43.5
36	AL-13736-F DF-2 Blend F	0.8519	2.28	264	43.8
37	AL-13850-F DF-2 Blend G	0.8524	2.09	258	41.8
38*	AL-10583-F JP-4	0.7632	0.79	148	35.0
39*	AL-14216-F JP-8	0.8232	1.28	200	41.4
40	AL-14948-F DF-2 Referee	0.8692	2.94	274	43.3
41*	AL-10999-F Type I Referee DF-2	0.7869	0.76	166	27.8
42*	AL-14751-F Type II Referee DF-2	0.9048	6.99	314	40.2

* Fuels tested in the variable compression-ratio engine.

demonstrated problems related to the current cetane rating procedures, and several blends of petroleum-derived distillates designed to be representative of current and future petroleum-derived diesel fuels (Fuels 27 through 37). The jet and diesel fuels (Fuels 38 through 42) represent the extremes of what might be available in the future for use by the military.

While the test fuels were selected to provide the largest possible variation in the various properties, all fuels were selected from the inventory of fuels available at SwRI. The pure hydrocarbon blends were the only fuels prepared especially for this project. In addition to the near infinite number of blends which could be prepared, it is estimated that there are at least 100 more fuels available at SwRI which could be evaluated in the CVCB. As discussed in the following sections, the future success of the two rating techniques developed in this project depends upon the development of a data base with the maximum number of test fuels. In this respect, the work performed in this project represents only the initial effort.

III. RESULTS AND DISCUSSION

The experimental results for the two different experiments are presented separately in this section. The data are discussed in detail in this section. When appropriate, comparisons will be made between the CVCB and the engine experiments. A considerable amount of data was developed for this project. The complete data sets for both experiments are presented in this report.

A. CVCB Experiments

The primary dependent variable of the CVCB experiments is the total ignition delay time. In the experiments performed during this project, ignition delay data were obtained for 42 different fuels, at three different initial gas temperatures. In addition, the total ignition delay time was examined in terms of the contributions of the physical and chemical delay times. The ignition delay times for all of the test fuels are presented in TABLES 3, 4, and 5 for the 371°, the 427°, and the 482°C test conditions, respectively. Included in these tables are the same fuel property data as was presented in TABLE 2, in addition to the total, the physical and the chemical

26

TABLE 3. Ignition Delay Data at 371°C (700°F) and Fuel Property Data

Fuel No.	Fuel Description	Specific Gravity	Viscosity, cSt at 40°C	Boiling Point or 50% Point, °C	Cetane No.	τ_d	τ_c	τ_p
1	100% Isooctane	0.6962	0.65	99	17.5	28.70	26.32	2.38
2	75% Isooctane 25% Tetradecane	--	--	--	36.9	19.88	16.56	3.32
3	50% Isooctane 50% Tetradecane	--	--	--	56.3	7.42	5.11	2.31
4	25% Isooctane 75% Tetradecane	--	--	--	75.7	5.79	2.73	3.06
5	100% Tetradecane	0.7667	1.83	252	95.0	5.88	2.66	2.22
6*	100% Hexadecane	0.773	3.00	287	100.0	6.63	3.06	3.57
7*	100% Heptamethylnonane	0.793	3.09	240	15.0	17.99	15.40	2.59
8*	75% Hexadecane 25% Heptamethylnonane	--	--	--	78.8	7.28	4.14	3.14
9*	50% Hexadecane 50% Heptamethylnonane	--	--	--	57.5	7.62	4.69	2.93
10*	25% Hexadecane 75% Heptamethylnonane	--	--	--	36.3	8.41	4.93	3.48
11	100% N-Octane	0.7068	0.65	125	64.4	9.98	8.48	1.50
12	100% 1-Hexene	0.34	0.68	64	27.3	37.50	35.58	1.92
13*	100% N-Hexane	0.6640	0.41	69	44.8	21.52	19.26	2.26
14	100% 1-Tetradecene 93%	0.7752	1.92	251	80.5	8.19	5.60	2.59
15*	100% Cyclohexane Ultrapure	0.7834	0.95	81	16.9	26.16	23.03	3.13
16	100% 2 Xylene	0.8848	0.74	144	8.3	30.37	27.13	3.24
17	100% Benzene	0.8844	0.59	79	14.3	--	--	--
18*	19-cSt Hydrocarbon Blend	0.8702	19.47	351	53.8	9.36	6.43	2.93
19*	12-cSt Hydrocarbon Blend	0.8571	12.84	368	55.8	8.16	5.59	2.57
20*	5-cSt Hydrocarbon Blend	0.8607	4.96	316	48.5	9.39	6.76	2.63
21	FL-0403-F SRC-11/DF-2 Blend	0.889	2.47	259	35.6	23.19	20.72	2.47
22*	FL-0442-F Sunflower Oil	0.220	33.93	588	35.8	11.02	7.51	3.51
23*	FL-0433-F Sunflower Ethylester	0.8870	4.96	368	59.9	5.70	2.61	3.09
24	FL-0413-F Tar Sand/DF-2 Blend	0.8810	2.82	267	35.2	8.69	5.60	3.09
25	14.4-cSt Hydrocarbon Blend	0.8756	14.39	347	48.5	6.03	2.89	3.14
26	20.3-cSt Hydrocarbon Blend	0.8581	20.28	378	57.5	5.17	2.04	3.13
27	FL-0744-F Wisconsin Hi Vol., Hi CN Blend	0.8314	2.01	239	48.7	7.75	4.53	3.22
28	FL-0745-F Wisconsin Hi Vol., Lo CN Blend	0.8934	2.25	264	31.5	9.69	6.49	3.20
29	FL-0746-F Wisconsin Lo Vol., Lo CN Blend	0.9147	3.48	284	32.7	9.45	6.23	3.22
30	FL-0747-F Wisconsin Lo Vol., Hi CN Blend	0.8488	2.84	262	49.3	6.82	3.64	3.18
31	AL-13279-F DF-2 Blend A	0.8484	2.75	273	48.7	8.22	4.30	3.92
32	AL-13639-F DF-2 Blend B	0.8545	2.53	266	45.2	8.46	4.60	3.96
33	AL-13664-F DF-2 Blend C	0.8565	2.44	262	44.3	8.03	4.29	3.74
34	AL-13694-F DF-2 Blend D	0.8597	2.75	274	44.9	8.11	4.46	3.65
35	AL-13992-F DF-2 Blend E	0.8644	2.76	274	43.5	8.55	4.86	3.69
36	AL-13736-F DF-2 Blend F	0.8519	2.28	264	43.8	7.85	4.33	3.52
37	AL-13850-F DF-2 Blend G	0.8524	2.09	258	41.8	7.53	4.40	3.13
38*	AL-10583-F JP-4	0.7632	0.79	148	35.0	7.72	4.07	3.65
39*	AL-14216-F JP-8	0.8232	1.28	200	41.4	11.12	7.39	3.73
40	AL-14948-F DF-2 Referee	0.8692	2.94	274	43.3	7.94	3.85	4.49
41*	AL-10999-F Type I Referee DF-2	0.7869	0.76	166	27.8	15.07	11.43	3.64
42*	AL-14751-F Type II Referee DF-2	0.9048	6.99	314	40.2	10.35	4.16	6.19

* Fuels tested in the variable compression ratio engine.

27

TABLE 4. Ignition Delay Data at 427°C (800°F) and Fuel Property Data

Fuel No.	Fuel Description	Specific Gravity	Viscosity, cSt at 40°C	Boiling Point or 50% Point, °C	Cetane No.	τ_d	τ_c	τ_p
1	100% Isooctane	0.6962	0.65	99	17.5	13.22	10.60	2.62
2	75% Isooctane 25% Tetradecane	--	--	--	36.9	7.43	5.43	2.00
3	50% Isooctane 50% Tetradecane	--	--	--	56.3	4.92	2.65	2.27
4	25% Isooctane 75% Tetradecane	--	--	--	75.7	4.11	1.01	3.10
5	100% Tetradecane	0.7667	1.83	252	95.0	3.76	0.58	3.18
6*	100% Hexadecane	0.773	3.00	287	100.0	3.94	0.80	3.14
7*	100% Heptamethylnonane	0.793	3.09	240	15.0	11.93	9.13	2.80
8*	75% Hexadecane 25% Heptamethylnonane	--	--	--	78.8	4.88	2.41	2.47
9*	50% Hexadecane 50% Heptamethylnonane	--	--	--	57.5	5.97	3.48	2.49
10*	25% Hexadecane 75% Heptamethylnonane	--	--	--	36.3	8.54	5.94	2.60
11	100% N-Octane	0.7068	0.65	125	64.4	5.44	3.25	2.19
12	100% 1-Hexene	0.34	0.68	64	27.3	16.09	14.35	1.74
13*	100% N-Hexane	0.6640	0.41	69	44.8	8.99	6.64	2.35
14	100% 1-Tetradecene 93%	0.7752	1.92	251	80.5	4.84	1.69	3.15
15*	100% Cyclohexane Ultrapure	0.7834	0.95	81	16.9	10.50	7.47	3.03
16	100% 2 Xylene	0.8848	0.74	144	8.3	36.90	33.65	3.25
17	100% Benzene	0.8844	0.59	79	14.3	--	--	--
18*	19-cSt Hydrocarbon Blend	0.8702	19.47	351	53.8	6.13	3.08	3.05
19*	12-cSt Hydrocarbon Blend	0.8571	12.84	368	55.8	5.37	2.57	2.80
20*	5-cSt Hydrocarbon Blend	0.8607	4.96	316	48.5	5.91	3.09	2.82
21	FL-0403-F SRC-II/DF-2 Blend	0.889	2.47	259	35.6	8.43	5.27	3.16
22*	FL-0442-F Sunflower Oil	9.220	33.93	588	35.8	8.95	5.52	3.43
23*	FL-0433-F Sunflower Ethylester	0.8870	4.96	368	59.9	4.00	0.89	3.11
24	FL-0413-F Tar Sand/DF-2 Blend	0.8810	2.82	267	35.2	5.84	2.61	3.23
25	14.4-cSt Hydrocarbon Blend	0.8756	14.39	347	48.5	4.14	1.08	3.06
26	20.3-cSt Hydrocarbon Blend	0.8581	20.28	378	57.5	3.57	0.63	2.94
27	FL-0744-F Wisconsin Hi Vol., Hi CN Blend	0.8314	2.01	239	48.7	5.62	2.45	3.17
28	FL-0745-F Wisconsin Hi Vol., Lo CN Blend	0.8934	2.25	264	31.5	6.23	3.00	3.23
29	FL-0746-F Wisconsin Lo Vol., Lo CN Blend	0.9147	3.48	284	32.7	6.25	2.99	3.26
30	FL-0747-F Wisconsin Lo Vol., Hi CN Blend	0.8488	2.84	262	49.3	5.33	2.12	3.21
31	AL-13279-F DF-2 Blend A	0.8484	2.75	273	48.7	5.65	2.08	3.57
32	AL-13639-F DF-2 Blend B	0.8545	2.53	266	45.2	5.62	2.00	3.62
33	AL-13664-F DF-2 Blend C	0.8565	2.44	262	44.3	5.92	2.22	3.70
34	AL-13694-F DF-2 Blend D	0.8597	2.75	274	44.9	5.88	2.34	3.54
35	AL-13992-F DF-2 Blend E	0.8644	2.76	274	43.5	5.77	2.05	3.72
36	AL-13736-F DF-2 Blend F	0.8519	2.28	264	43.8	6.12	2.76	3.36
37	AL-13850-F DF-2 Blend G	0.8524	2.09	258	41.8	5.94	2.13	3.81
38*	AL-10583-F JP-4	0.7632	0.79	148	35.0	5.26	1.58	3.66
39*	AL-14216-F JP-8	0.8232	1.28	200	41.4	6.99	3.28	3.71
40	AL-14948-F DF-2 Referee	0.8692	2.94	274	43.3	5.92	1.83	4.09
41*	AL-10999-F Type I Referee DF-2	0.7869	0.76	166	27.8	9.45	5.32	4.13
42*	AL-14751-F Type II Referee DF-2	0.9048	6.99	314	40.2	6.20	1.96	4.24

* Fuels tested in the variable compression ratio engine.

28

TABLE 5. Ignition Delay Data at 482°C (900°F) and Fuel Property Data

Fuel No.	Fuel Description	Specific Gravity	Viscosity, cSt at 40°C	Boiling Point or 50% Point, °C	Cetane No.	T_d	T_c	T_p
1	100% Isooctane	0.6962	0.65	99	17.5	7.02	4.07	2.95
2	75% Isooctane 25% Tetradecane	--	--	--	36.9	4.09	2.07	1.92
3	50% Isooctane 50% Tetradecane	--	--	--	56.3	3.13	0.89	2.24
4	25% Isooctane 75% Tetradecane	--	--	--	75.7	2.82	0.52	2.30
5	100% Tetradecane	0.7667	1.83	252	95.0	2.74	0.41	2.33
6*	100% Hexadecane	0.773	3.00	287	100.0	2.58	0.40	2.18
7*	100% Heptamethylnonane	0.793	3.09	240	15.0	7.99	5.06	2.93
8*	75% Hexadecane 25% Heptamethylnonane	--	--	--	78.8	2.69	0.44	2.25
9*	50% Hexadecane 50% Heptamethylnonane	--	--	--	57.5	3.04	0.54	2.50
10*	25% Hexadecane 75% Heptamethylnonane	--	--	--	36.3	3.86	0.99	2.87
11	100% N-Octane	0.7068	0.65	125	64.4	3.34	1.13	2.21
12	100% 1-Hexene	0.34	0.68	64	27.3	6.74	4.70	2.04
13*	100% N-Hexane	0.6640	0.41	69	44.8	4.27	2.13	2.14
14	100% 1-Tetradecene 93%	0.7752	1.92	251	80.5	2.83	0.40	2.43
15*	100% Cyclohexane Ultrapure	0.7834	0.95	81	16.9	7.90	5.09	2.81
16	100% 2 Xylene	0.8848	0.74	144	8.3	23.35	19.21	4.14
17	100% Benzene	0.8844	0.59	79	14.3	--	--	--
18*	19-cSt Hydrocarbon Blend	0.8702	19.47	351	53.8	3.70	0.85	2.85
19*	12-cSt Hydrocarbon Blend	0.8571	12.84	368	55.8	3.36	0.67	2.69
20*	5-cSt Hydrocarbon Blend	0.8607	4.96	316	48.5	3.28	0.70	2.58
21	FL-0403-F SRC-II/DF-2 Blend	0.889	2.47	259	35.6	5.55	2.20	3.35
22*	FL-0442-F Sunflower Oil	9.220	33.93	588	35.8	3.80	0.79	3.01
23*	FL-0433-F Sunflower Ethylester	0.8870	4.96	368	59.9	2.57	0.34	2.23
24	FL-0413-F Tar Sand/DF-2 Blend	0.8810	2.82	267	35.2	4.37	1.31	3.06
25	14.4-cSt Hydrocarbon Blend	0.8756	14.39	347	48.5	3.01	0.46	2.55
26	20.3-cSt Hydrocarbon Blend	0.8581	20.28	378	57.5	2.75	0.40	2.35
27	FL-0744-F Wisconsin Hi Vol., Hi CN Blend	0.8314	2.01	239	48.7	3.90	0.81	3.09
28	FL-0745-F Wisconsin Hi Vol., Lo CN Blend	0.8934	2.25	264	31.5	5.76	2.44	3.32
29	FL-0746-F Wisconsin Lo Vol., Lo CN Blend	0.9147	3.48	284	32.7	5.43	1.59	3.84
30	FL-0747-F Wisconsin Lo Vol., Hi CN Blend	0.8488	2.84	262	49.3	3.50	0.72	2.78
31	AL-13279-F DF-2 Blend A	0.8484	2.75	273	48.7	3.78	0.72	3.06
32	AL-13639-F DF-2 Blend B	0.8545	2.53	266	45.2	3.82	0.53	3.29
33	AL-13664-F DF-2 Blend C	0.8565	2.44	262	44.3	3.72	0.57	3.15
34	AL-13694-F DF-2 Blend D	0.8597	2.75	274	44.9	4.13	0.55	3.58
35	AL-13992-F DF-2 Blend E	0.8644	2.76	274	43.5	3.78	0.51	3.27
36	AL-13736-F DF-2 Blend F	0.8519	2.28	264	43.8	3.87	0.57	3.30
37	AL-13850-F DF-2 Blend G	0.8524	2.09	258	41.8	3.99	0.62	3.37
38*	AL-10583-F JP-4	0.7632	0.79	148	35.0	3.72	0.57	3.15
39*	AL-14216-F JP-8	0.8232	1.28	200	41.4	4.35	0.91	3.44
40	AL-14948-F DF-2 Referee	0.8692	2.94	274	43.3	4.41	0.69	3.72
41*	AL-10999-F Type I Referee DF-2	0.7869	0.76	166	27.8	6.86	2.55	4.31
42*	AL-14751-F Type II Referee DF-2	0.9048	6.99	314	40.2	6.79	0.55	6.24

* Fuels tested in the variable compression ratio engine.

ignition delay times. As can be seen, a considerable amount of data was obtained from the CVCB experiments.

It should be realized that the data presented in TABLES 3 through 5 are the averages of at least four repeats at each test condition. The repeatability of the experiment depended upon the ignition quality of the test fuel and the test condition. In general, the standard error, or coefficient of variation, of the measurements was on the order of 0.01 to 0.06. Larger values of the coefficient of variation were generally observed for the measurements involving the shorter delay times, independent of whether the short delay time resulted from a high test temperature or the use of a good ignition quality fuel. The errors associated with the shorter ignition delay times were not viewed as a problem in this technique. As the delay times decrease, due either to the fuel or to the test temperature, all the data tend to coverge to a single value, which may represent the absolute physical delay time of the system. Based on this observation, however, it was realized early in the project that the test conditions should be adjusted to give the longest possible ignition delay times. This approach is limited, however, in that delay times beyond approximately 30 ms appear to be more indicative of surface ignition (ignition at the wall) than autoignition in the hot gas.

The data listed in TABLES 3 through 5 can be presented in many different ways. In the short term, the CVCB technique is of interest in terms of replacing ASTM D 613 in providing a cetane number. Under these conditions, it is most enlightening to present the data as functions of cetane number and to compare the results, in terms of cetane number, to those obtained for the primary reference fuels (hexadecane and hepta-methylnonane). In the longer term, the technique offers some potential in not only replacing ASTM D 613, but also in eliminating, or at least improving, the cetane number concept. In this regard, the data may be most conveniently discussed in terms of direct comparisons of the ignition delay times and in the development of a new ignition quality index. Successful attainment of this longer term goal depends upon the inclusion of engine ignition data, such as that developed in the variable compression-ratio test engine. Fuel-to-fuel comparisons as well as comparisons to the primary reference fuels are presented in this section. Comparisons of the CVCB and engine data are presented in the next section.

30

The 371°C data are presented in Fig. 9 through 11 for the total, the chemical, and the physical delays, respectively, for all fuels. Fig. 12 through 14 are plots of the 427°C data, and the 482°C data are presented in Fig. 15 through 17. Some general observations can be made by simply scanning the figures.

Examination of the plots of the physical delay times (Fig. 10, 14, and 17) reveals that the physical delay times are independent of both the cetane number and the test temperature. This indicates that, at least for the apparatus used in these experiments, the experimental procedure provides a measure of the chemical effects on ignition. It should be realized, however, that the cetane rating procedure does not provide an indication of the effects of the fuel's physical properties on ignition. In both the engine and the CVCB, it could be hypothesized that the viscosity would affect the atomization, which in turn would affect the vaporization and thus the physical delay time. The fuel volatility, or boiling point, could be expected to have a similar effect on vaporization and ignition. For the fuels tested in this project, the cetane number was not a function of either viscosity or boiling point. This is demonstrated in Fig. 18 for viscosity.

In the CVCB, it is felt that the quality of the injection process is such that the atomization was not sufficiently affected by the variation in viscosity and boiling point (even over the larger ranges tested in this project) to have an effect on the ignition process. Similar observations have been made in engine experiments where the physical delay is independent of physical properties of the fuel or of changes made in the engine.(37) It is felt, however, that the fuel physical properties do affect the ignition quality under certain conditions in all engines, such as during cold start. For engines equipped with marginal injection systems, these effects may even extend to warm engine starting and operation. These effects will never be indicated using the ASTM D 613 cetane rating procedure. Although not extensively pursued in this project, the CVCB technique offers at least two opportunities to examine these effects: first, through extended variation in the test temperature; and second, through variation in the injection quality (injection pressure). These possibilities will hopefully be explored in future projects. Based on the fact that the physical ignition delay was observed to be independent of the other parameters, all other discussions in this report involve only the total ignition delay time.
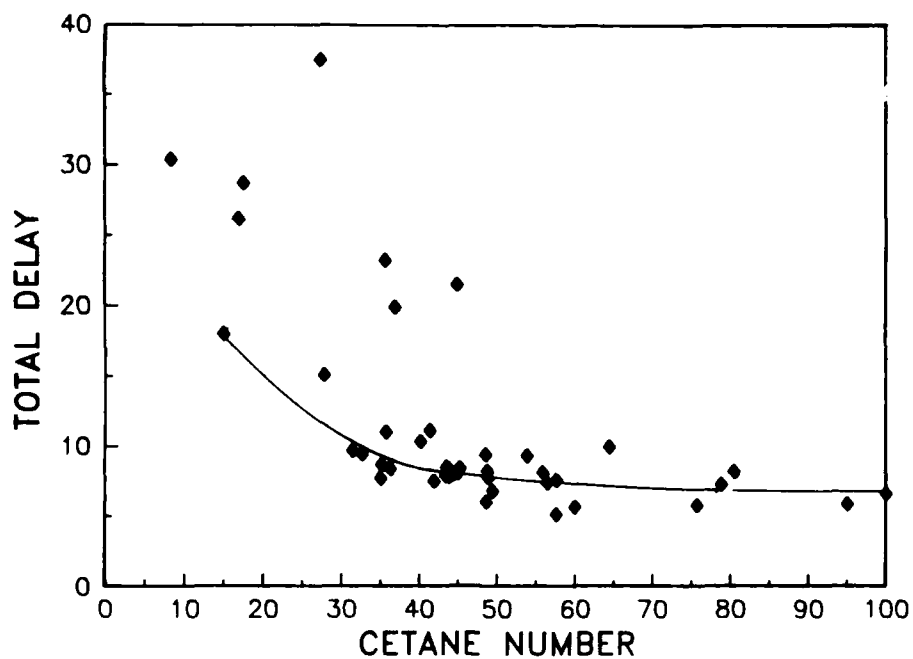
31

Figure 9. Total ignition delay versus cetane number for
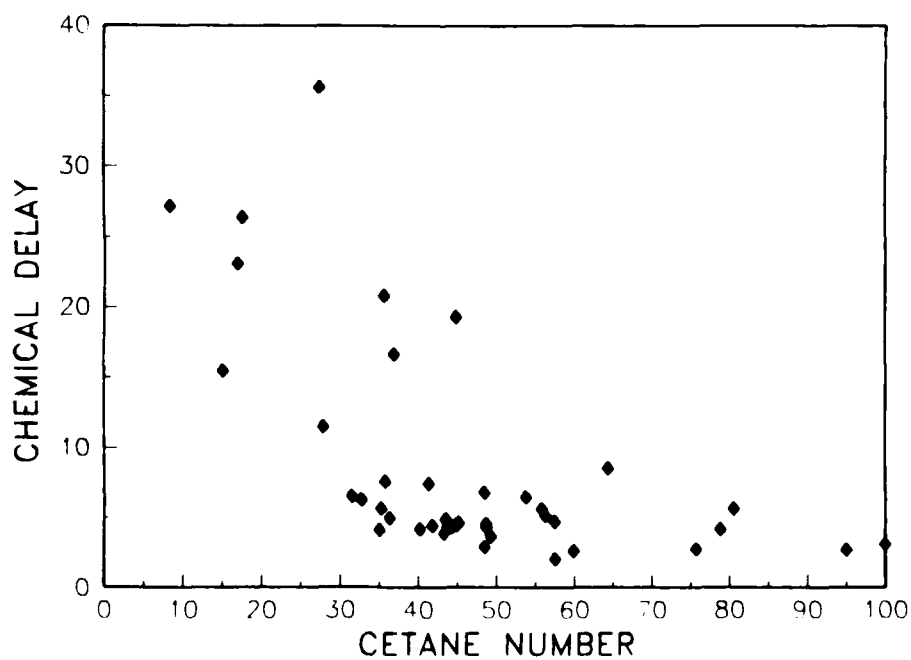all fuels at 371°C

Figure 10. Chemical ignition delay versus cetane number for
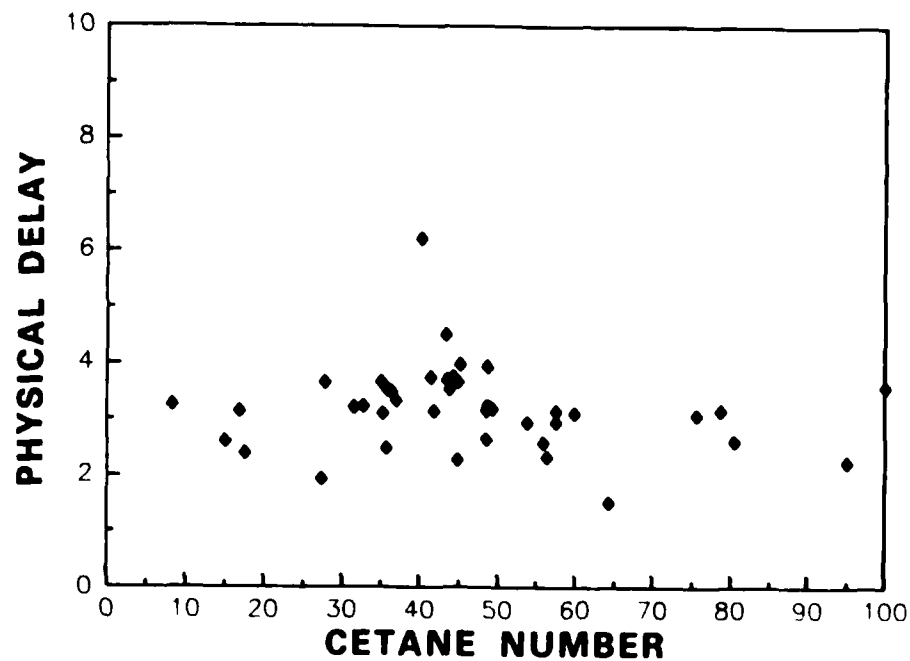all fuels at 371°C

32

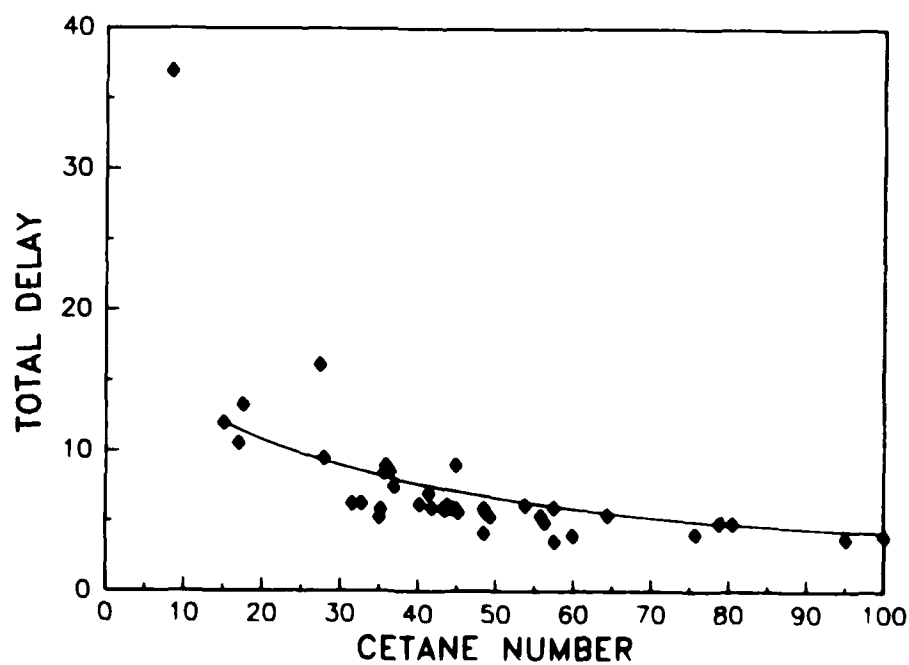Figure 11.   Physical ignition delay versus cetane number for
all fuels at 371°C

Figure 12.   Total ignition delay versus cetane number for
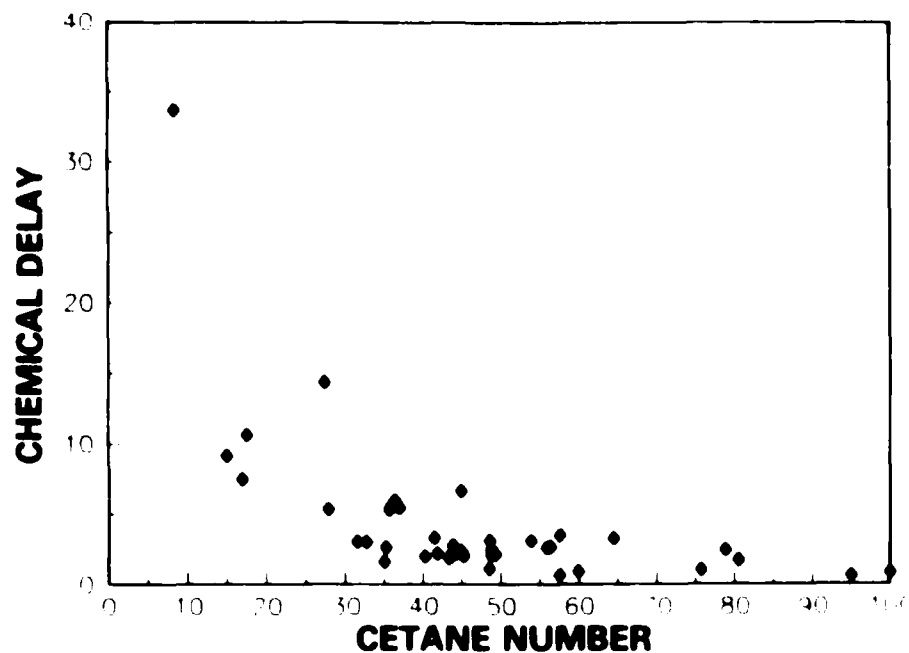all fuels at 427°C

Figure 13. Chemical ignition delay versus cetane number for all fuels at 427°C
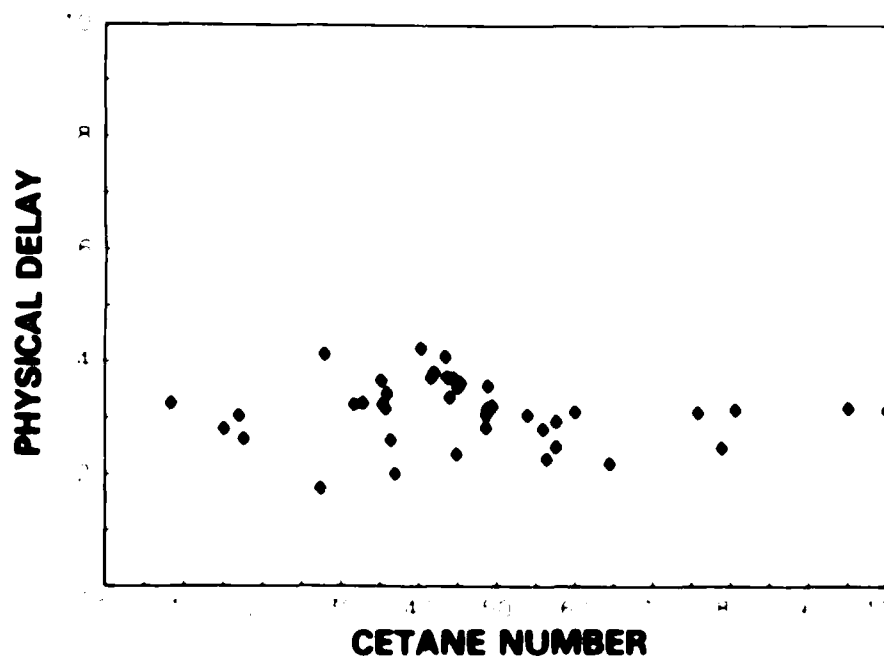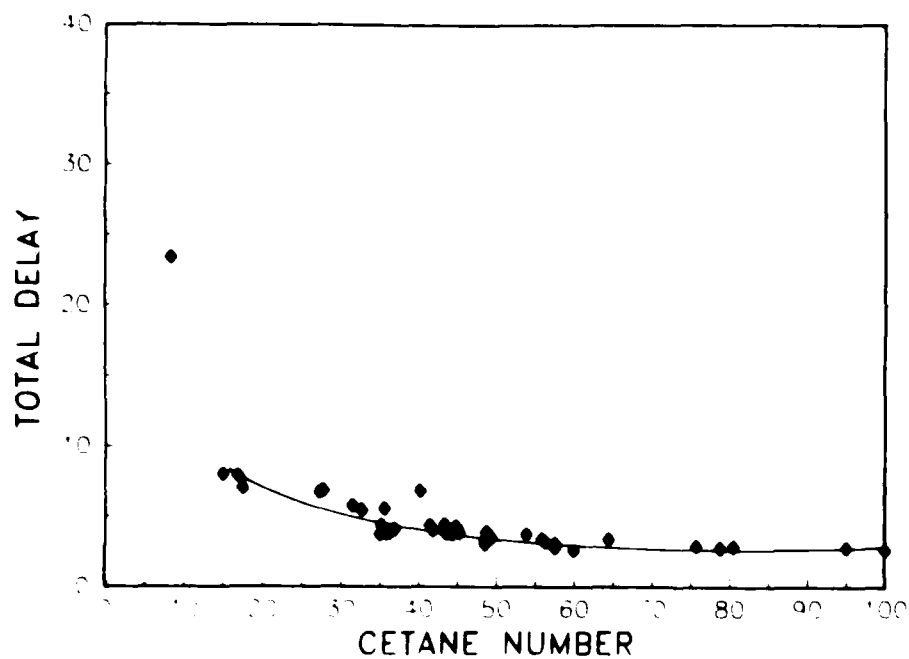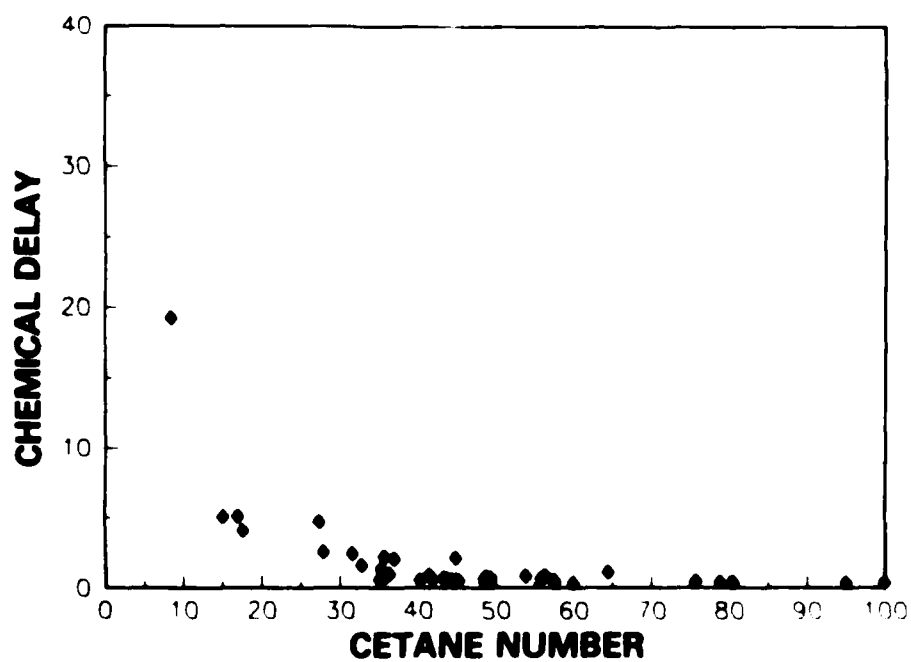

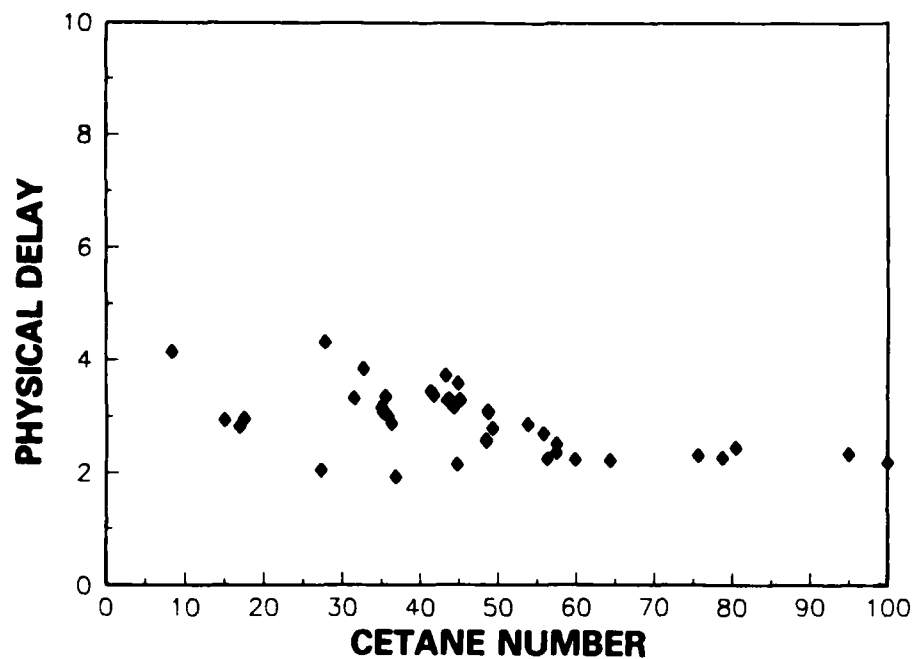Figure 14. Physical ignition delay versus cetane number for all fuels at 427°C

Figure 15. Total ignition delay versus cetane number for all fuels at 482°C

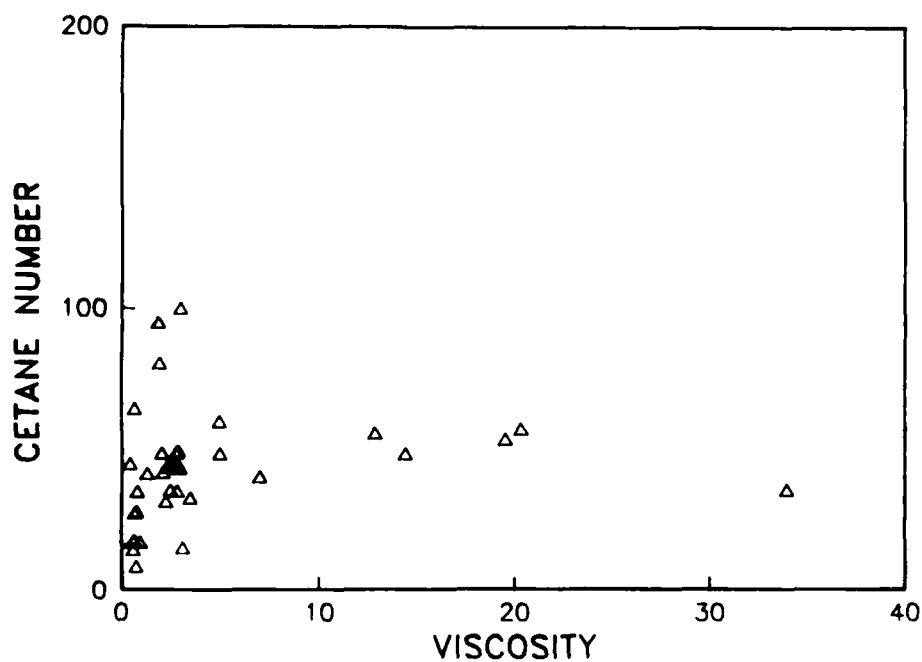**Figure 18. Chemical ignition delay versus cetane number for all fuels at 482°C**

Figure 17. Physical ignition delay versus cetane number for all fuels at 482°C

Figure 18. Cetane number versus viscosity for all test fuels

Plotted on the figures (9, 12, and 15) of the total delay data are curves representing the results for the primary reference fuel blends. These curves, in addition to providing a convenient reference for comparison between CVCB data and ASTM D 613, also demonstrate the temperature dependence (sensitivity) of the CVCB technique. This temperature dependence is expected and is discussed in detail later in this report.

As indicated previously, the repeatability of the individual measurements is from 1 to 6 percent, in terms of the delay times. As can be seen in the figures in which the data are plotted versus cetane number, the variations appear to be larger than the 1 to 6 percent indicated above. These apparent differences result from several factors. First, the cetane rating procedure does not account for variations in test temperature, and thus does not provide an indication of the fuel's sensitivity to temperature. In the CVCB technique, the temperature sensitivity of each fuel can be examined simply by varying the test temperature and observing the change in ignition delay time. The difference between the data for the test fuels and the baseline data (primary reference fuel data) are most pronounced at the lower test temperatures where the temperature dependence is most sensitive, as indicated by the long delay times. It is felt that the CVCB technique reflects these sensitivities and ASTM D 613 does not. The second factor involves the data spread for the lower cetane number fuels. These fuels (cetane numbers of 35 or lower) are extremely difficult to rate using the standard ASTM D 613 procedure. As such, the accuracy or relevance of the existing cetane number measurements is questionable. Thus, the unreliable nature of ASTM D 613, for these fuels, could be contributing to the spread. It is interesting to note that the largest differences between the baseline and the tests fuels, as observed in Fig. 9 and tabulated in TABLE 2, are for fuels which are not normally found as the major components in diesel fuel and are chemically different than the ASTM D 613 reference fuels. These fuels include aromatics (2-Xylene and SRC-II blend), cyclo-compounds (cyclohexane), isomeric paraffins (isooctane) and olefinic compounds (1-hexene). The aromatic fuels generally were difficult to test, first, because of the long ignition times and, second, because of a slow rate of pressure rise at the start of the combustion. This same phenomena of two-stage ignition was reported by Hurn.(8)

1. Cetane Number Predictions

In examining the primary reference fuel data presented in Fig. 9, 12, and 15, it appears that the cetane number is an exponential function of ignition delay. Regression analysis of the primary reference fuel data indicated that the best correlations are obtained using an exponential function of the form

$$CN = A \exp (B \cdot \tau_d) \tag{1}$$

where: CN = Cetane Number

τ_d = Total Ignition Delay (ms)

A, B = Constants.

The regression analysis results are summarized in TABLE 6. The constants A and B were determined at each test temperature. As indicated by the R-square values, the fit is excellent. The expected accuracy, based on the reference fuel data, are also listed in the table as the ranges of the coefficients of variations for respective baseline data.

**TABLE 6. Regression Analysis Results**
$$[CN = A \exp (B \cdot \tau_d)]$$

Temperature, °C	A	B	R^2	Coefficient of Variation
371	189.1	-0.146	0.873	0.015-0.06
427	246.5	-0.234	0.997	0.019-0.06
482	169.2	-0.314	0.903	0.025-0.08

The regression equations are plotted in Fig. 19 through 21 for the 371°, 427°, and the 482°C data, respectively. As can be seen, the data demonstrate a much larger slope at the higher cetane numbers, or shorter delay times. The slope appears to be approaching zero at approximately a cetane number of 10. This could be a limitation of the cetane scale in terms of the applicability of the scale to fuels which have longer ignition delay times than heptamethylnonane (15 CN reference fuel). As a matter of
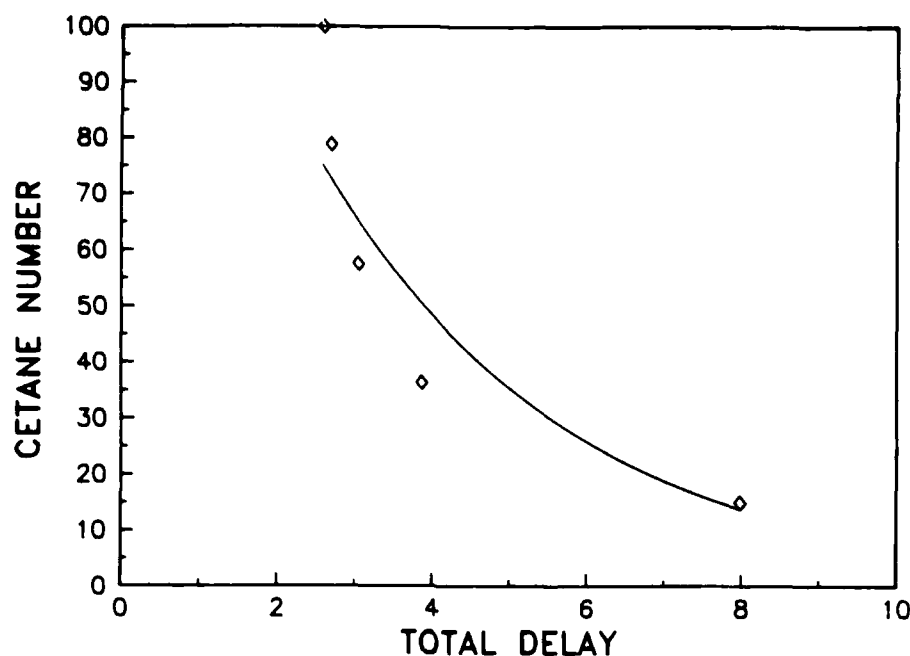
38
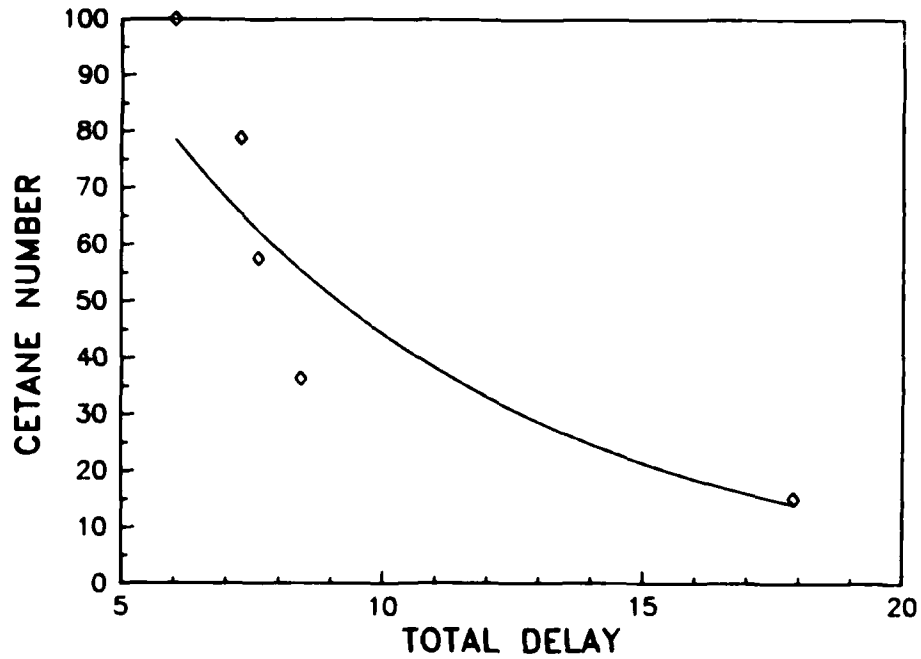
Figure 19. Cetane number versus total delay for the primary reference fuels, temperature of 371°C
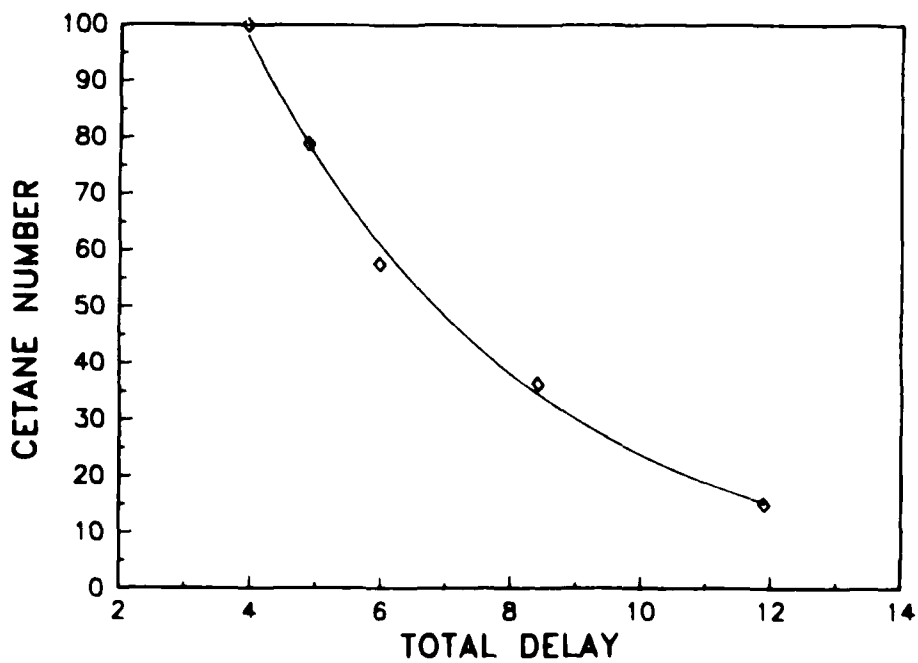
Figure 20. Cetane number versus total delay for the primary reference fuels, temperature of 427°C

Figure 21. Cetane number versus total delay for the primary reference fuels, temperature at 482°C

fact, the asymptotic nature of the slope of the CN versus τ_d plot demonstrates a problem with the cetane number scale in differentiating the lower cetane number fuels. While the data appear to be correct in terms of repeatability, the trends with the base fuel need to be verified using many more blends of the reference fuels with corresponding verification in the cetane engine using ASTM D 613.

As indicated previously, the repeatability of the measurements for each individual test fuel is on the order of 1 to 6 percent for the ignition delay time. In attempting to use this technique as an indicator of cetane number, it should be recalled that this procedure provides a measure of the ignition delay time as a function of temperature. The cetane procedure, on the other hand, provides a measure of the ignition temperature (compression ratio) required to produce a constant ignition delay of 2.4 ms (13 degrees of crankshaft rotation at 900 rpm). Thus, in one technique, the ignition temperature is held constant, and the delay time varies, while in the other, the delay time is constant, and the ignition temperature is varied. Because of these factors, it is not possible to simply use the reference fuel calibration and regression equations, at

a given test condition, to predict the cetane number. It is felt that the most rigorous approach consists of establishing an ignition delay time in the CVCB that is "equivalent" to that used in the cetane engine. Since the CVCB ignition delay data for both the test and the reference fuels are determined as functions of temperature, it would then be a simple matter to establish the ignition temperature, "equivalent" to the engine condition, based on the test fuel data from the CVCB. This temperature, in conjunction with the "equivalent" delay time, would be used to determine the cetane number based on the reference fuel data.

Based upon the work performed in this project, the "equivalent" ignition delay time for the CVCB procedure is not equal to the actual delay time used in the engine procedure, or 2.4 ms. The use of this time results in predicted cetane numbers that are higher than the actual. This would tend to indicate that the turbulence present in the engine experiments results in lower ignition delay time, as compared to the CVCB data. Development of the "equivalent" delay time for use in the rigorous approach requires the development of an extensive data base involving additional test conditions, test data using additional fuel blends, and actual cetane numbers for several blends with cetane numbers below 30 and above 50.

In lieu of the more rigorous approach, a simple averaging technique was used to provide a measure of the ability of the CVCB technique to predict cetane number. In this technique, the ignition delay time at each test temperature, for the given test fuel, is used to predict a cetane number based upon the equivalent reference fuel data. These predictions are then averaged and considered as the predicted cetane number. Linear interpolation of the reference fuel data, between the appropriate test points, was used to calculate the cetane number of the test fuel at each test temperature. The results of these calculations are presented in TABLE 7. The coefficients of the interpolation equations for each test temperature are presented in TABLE 8. At a given test temperature, the regression equations overlap very well for each range of ignition delay time.

The test results summarized in TABLE 7 are for a wide range of materials, including blends and compounds, that are not normally found in middle distillate diesel fuels. The only fuels that could be considered as typical diesel fuels are Fuels 31 through 37. Fuels 18 through 20, 25 through 30, and 41 through 42 are special blends, formulated to

TABLE 7. List of the Test Fuels and Selected Fuel Properties

Fuel No.	Fuel Description	Specific Gravity	Viscosity, cSt at 40°C	Boiling Point or 50% Point, °C	D 613 Cetane No.	Predicted Cetane No.
1	100% Isooctane	0.6962	0.65	99	17.5	5.9
2	75% Isooctane 25% Tetradecane	--	--	—	36.9	29.5
3	50% Isooctane 50% Tetradecane	--	--	—	56.3	67.2
4	25% Isooctane 75% Tetradecane	--	--	—	75.7	90.4
5	100% Tetradecane	0.7667	1.83	252	95.0	94.1
6*	100% Hexadecane	0.773	3.00	287	100.0	97.6
7*	100% Heptamethylnonane	0.793	3.09	240	15.0	15.2
8*	75% Hexadecane 25% Heptamethylnonane	--	--	—	78.8	79.1
9*	50% Hexadecane 50% Heptamethylnonane	--	--	—	57.5	57.5
10*	25% Hexadecane 75% Heptamethylnonane	--	--	—	36.3	35.9
11*	100% N-Octane	0.7068	0.65	125	64.4	42.1
12	100% 1-Hexene	0.34	0.68	64	27.3	0.0**
13*	100% N-Hexane	0.6640	0.41	69	44.8	24.4
14	100% 1-Tetradecene 93%	0.7752	1.92	251	80.5	64.1
15*	100% Cyclohexane Ultrapure	0.7834	0.95	81	16.9	12.0
16	100% 2 Xylene	0.8848	0.74	144	8.3	0.0**
17	100% Benzene	0.8844	0.59	79	14.3	--
18*	19-cSt Hydrocarbon Blend	0.8702	19.47	351	53.8	42.0
19*	12-cSt Hydrocarbon Blend	0.8571	12.84	368	55.8	51.5
20*	5-cSt Hydrocarbon Blend	0.8607	4.96	316	48.5	46.5
21	FL-0403-F SRC-11/DF-2 Blend	0.889	2.47	259	35.6	22.2
22*	FL-0442-F Sunflower Oil	9.220	33.93	588	35.8	33.2
23*	FL-0433-F Sunflower Ethylester	0.8870	4.96	368	59.9	100.0**
24	FL-0413-F Tar Sand/DF-2 Blend	0.8810	2.82	267	35.2	42.9
25	14.4-cSt Hydrocarbon Blend	0.8756	14.39	347	48.5	84.9
26	20.3-cSt Hydrocarbon Blend	0.8581	20.28	378	57.5	99.3
27	FL-0744-F Wisconsin Hi Vol., Hi CN Blend	0.8314	2.01	239	48.7	51.0
28	FL-0745-F Wisconsin Hi Vol., Lo CN Blend	0.8934	2.25	264	31.5	38.2
29	FL-0746-F Wisconsin Lo Vol., Lo CN Blend	0.9147	3.48	284	32.7	38.8
30	FL-0747-F Wisconsin Lo Vol., Hi CN Blend	0.8488	2.84	262	49.3	64.3
31	AL-13279-F DF-2 Blend A	0.8484	2.75	273	48.7	46.8
32	AL-13639-F DF-2 Blend B	0.8545	2.53	266	45.2	45.4
33	AL-13664-F DF-2 Blend C	0.8565	2.44	262	44.3	46.9
34	AL-13694-F DF-2 Blend D	0.8597	2.75	274	44.9	45.7
35	AL-13992-F DF-2 Blend E	0.8644	2.76	274	43.5	44.4
36	AL-13736-F DF-2 Blend F	0.8519	2.28	264	43.8	47.3
37	AL-13850-F DF-2 Blend G	0.8524	2.09	258	41.8	50.0
38*	AL-10583-F JP-4	0.7632	0.79	148	35.0	53.9
39*	AL-14216-F JP-8	0.8232	1.28	200	41.4	37.1
40	AL-14948-F DF-2 Referee	0.8692	2.94	274	43.3	46.6
41*	AL-10999-F Type I Referee DF-2	0.7869	0.76	166	27.8	24.3
42*	AL-14751-F Type II Referee DF-2	0.9048	6.99	314	40.2	36.2

* Fuels tested in the variable compression-ratio engine.
** Predicted below 0 or above 100 cetane number.

42

TABLE 8. Coefficients of the Interpolation Equations for the Reference Fuel Data

$$(CN = A + B \cdot \tau_d)$$

Temperature, °C	A	B	Range of τ_d (ms)
371	56.4	-2.3	8.4-18.0
371	261.9	-26.8	7.6- 8.4
371	534.7	-62.6	7.3- 7.6
371	201.3	-16.8	6.0- 7.3
427	54.5	-3.3	5.5-12
427	269.5	-42.2	5.0- 5.5
427	157.9	20.9	4.5- 5.0
427	188.9	-22.5	4.0- 4.5
482	52.7	-4.71	3.5- 8.0
482	207.4	-49.3	3.0- 3.5
482	242.4	-60.9	2.7- 3.0
482	599.7	-192.7	2.5- 2.7

meet specific values for the physical properties of viscosity, gravity, and volatility. These blends were formulated using a variety of components (including light cycle oils, lube oil blend stocks, and aromatic solvents) that are not normally found in diesel fuel. Fuels 21 through 24 are fuels that were selected as representative of a wide range of alternative fuels that could be available in the future. These same fuels have already been shown to present some problems in rating using ASTM D 613.([7,11]) In general, this crude application of the CVCB technique reveals the quality of the fuel in terms of indicating the unacceptable fuels with cetane numbers below 35 and excellent fuels with cetane number above 50.

Of the fuels tested with cetane numbers in the range from 40 to 50 (the range of prime concern for accuracy), the method was accurate to within 3.5 cetane numbers for 11 of 15 fuels. In this range, the predictions were generally high, with failures also being on the high side. In the range of fuels below 40 cetane numbers, the method was less accurate. It did indicate, however, in all cases but two, those fuels that had cetane numbers which would present problems. Failures in this range were generally on the

low side. indicating a more severe problem than indicated by the cetane number. In the range of cetane numbers above 50. the predictions were the least accurate due to the low value of the slope of the CN versus T_d relationship in this range. In all cases. the failures were either meaningless (predicting 90 CN versus 75) or on the safe side in terms of predicting a lower value.

It should be realized that the data presented in TABLE 7 represent an interim approach to applying the ignition delay data developed in the CVCB. Many of the largest deviations between the listed CN and the predicted are for the pure hydrocarbons. In addition to the fact that they are not normally primary constituents of diesel fuel. the cetane numbers of many of these compounds are questionable. especially at the extremes. since they were generally developed by extrapolation from blend data. This was necessary because with fuels such as isooctane. with a cited cetane number of 17.5. it is physically difficult to make a determination using D 613. For fuels with cetane number above 50 to 55. it is difficult to distinguish differences using D 613. For the other fuels. the aromatics content appears to have an effect on the CVCB predictions. Fuels 21. 24. 28. and 29 all have aromatics contents in excess of 50 percent and all could be considered as outliers.

In examining the data and predictions presented in TABLE 7. the predictions of most concern are those which fail in a direction that could lead to the use of a lower than acceptable ignition quality. This failure occurred for Fuels 24. 28. 29. 37. and 38. In these cases. the predictions of cetane number were higher than measured and were into the region of acceptability. All other deviations of the predicted and the measured were fail safe in terms of predictions lower than the low measured values or higher than the high values.

It is felt that the deviations result from the fact that the two techniques measured different parameters. In the case of the high predictions. the largest contributions to the deviations generally result from high predictions at the lower temperature. This indicates an ignition quality that is better at low temperature than the reference fuels. This. in turn. tends to indicate a better cold start characteristic than is predicted by D 613. In the case of the diesel fuels that were tested. it appears that in most cases the crude application of the technique is good to within 1 to 2 CN with an overall average deviation of 2.6 CN. For the entire data set. the average deviation is

9.3 CN, but this includes the large deviations observed for the high cetane number fuels. Some improvement in the predictive ability of the method is possible using a correction procedure described later.

It is felt that this technique could be improved by inclusion of a larger data set including a variety of diesel fuels and blends simulating diesel fuels. Simultaneous verification using D 613 is also desirable. This would be particularly interesting using blends containing various types and quantities of aromatic compounds. The two-stage ignition process, described previously for the aromatics, would also require additional study. On this same line of thought, the overall accuracy of the cetane predictions and the general quality of the ignition delay times could be improved by defining the ignition delay in terms of the heat release rate as suggested by Ryan (38) and Bair, et al.(37) In this technique, the ignition would be defined in terms of a given rate of heat release (combustion rate) eliminating the uncertainties involved with variations in the slope of the pressure trace at the baseline crossing point (the current technique). Additional improvements could be attained through the inclusion of an "equivalent" delay time, as described previously. Development of this number, or function, also requires the performance of additional CVCB experiments and simultaneous evaluations using D 613.

2.   Ignition Quality Index

While an ignition quality index has not been developed, it is felt that this project has at least indicated a potential for such a development. This is demonstrated in the temperature dependence of the ignition delay times as observed in comparing Fig. 9, 12, and 15. It becomes obvious that a new rating method is necessary when it is realized that the acceptable range of the current scale is from approximately 30 to 50 CN, of a possible range of 0 to 100 CN. In addition, the current cetane scale has not been directly linked to a cold start data base nor to an ignition delay data base for actual engines. The new rating technique, in addition to providing an extensive data base for the CVCB, should incorporate both engine data bases as the foundation of the technique. As a part of that development, the CVCB experiments have been performed at three different temperatures. As discussed in the next section, part of the engine ignition delay data base has also been developed in this project. The CVCB

ignition delay data are discussed in this section in terms of an Arrhenius-type function of temperature. Engine cold start data will hopefully be developed in future projects.

In accordance with accepted chemical kinetics, the ignition delay is generally presented in terms of an Arrhenius function of temperature. Regression analysis was performed on the ignition delay data for each fuel tested in this project. These analyses were performed using a regression equation of the form

$$\tau_d = A \exp\left(\frac{B}{T}\right) \tag{3}$$

$$T = \text{Temperature (K)}$$

The coefficients of this equation for each fuel are presented in TABLE 9. Since the data set for each fuel consists of three data points, it is expected that the R-squared values should be very high. This is indeed the case for the majority of the fuels. It is interesting to note that for some fuels the R-squared values are extremely low, possibly indicating problems with that particular data set or the occurrence of anomalies in the ignition process. In discussing the results for the fuels with R-squared values below 0.90, the low values for the reference fuel blends result from the fact that these data sets are larger and incorporate some data scatter, particularly with the lower ignition quality blends. As indicated previously, the aromatics exhibited what appeared to be a two-stage ignition process. These anomalies appear in the R-squared values for the aromatics and the aromatic blends (Fuels 16, 21, 28, and 29).

The R-squared value for Fuel 42 is the lowest of the entire test matrix and probably reflects a bad data point at one of the test conditions. Examination of the ignition delay data for this fuel reveals that the 482°C data point is probably too high at 6.79 ms. Assuming a value of 3.5, which is more in line with the data for fuels of similar CN, this test condition improves the R-squared to 0.98, and the CN prediction presented in TABLE 7 changes from 36.2 to 40.9 CN as compared to the measured value of 40.2. This suggests a possible method of checking the data set for each fuel to eliminate outliers and thus improve the CN predictions, even using the crude approximation described previously. Using the reference fuel data as the model, it was possible in all cases to improve the R-squared values listed in TABLE 9 (to values in excess of 0.98) by changing only one value in each data set. Application of these

46

TABLE 9. Regression Equation Coefficients for $\tau_d = F(T)$

$$\tau_d = A \exp\left(\frac{B}{T}\right)$$

Fuel No.	Fuel Description	Specific Gravity	Viscosity, cSt at 40°C	Boiling Point or 50% Point, °F	D 616 Cetane No.	A	B	R^2
1	100% Isooctane	0.6962	0.65	99	17.5	0.00198	6168.22	1.000
2	75% Isooctane 25% Tetradecane	--	--	--	36.9	3.917 E-4	6952.50	0.982
3	50% Isooctane 50% Tetradecane	--	--	--	56.3	0.02179	3766.08	0.989
4	25% Isooctane 75% Tetradecane	--	--	--	75.7	0.04489	3138.93	0.989
5	100% Tetradecane	0.7667	1.83	252	95.0	0.03700	3351.08	0.994
6*	100% Hexadecane	0.773	3.00	287	100.0	0.01077	4114.51	1.000
7*	100% Heptamethylnonane	0.793	3.09	240	15.0	0.07363	3546.93	0.997
8*	75% Hexadecane 25% Heptamethylnonane	--	--		78.9	0.00918	4126.86	0.950
9*	50% Hexadecane 50% Heptamethylnonane	--	--		57.5	0.01746	3964.71	0.914
10*	25% Hexadecane 75% Heptamethylnonane	--	--		36.3	0.05504	3317.42	0.465
11	100% N-Octane	0.7068	0.65	125	64.4	0.005797	4795.84	0.999
12	100% 1-Hexene	0.34	0.68	64	27.3	3.394 E-4	7495.23	0.994
13*	100% N-Hexane	0.6640	0.41	69	44.8	3.617 E-4	7080.72	1.000
14	100% 1-Tetradecene 93%	0.7752	1.92	251	80.5	0.006167	4641.16	0.995
15*	100% Cyclohexane Ultrapure	0.7834	0.95	81	15.9	0.00640	5303.66	0.979
16	100% 2 Xylene	0.8848	0.74	144	8.3		Poor Correlation	
17	100% Benzene	0.8843	0.59	79	14.3		No Ignition	
18*	19-cSt Hydrocarbon Blend	0.8702	19.47	351	53.8	0.01794	4045.76	0.981
19*	12-cSt Hydrocarbon Blend	0.8571	12.84	368	55.8	0.02041	3870.57	0.988
20*	5-cSt Hydrocarbon Blend	0.8607	4.96	316	48.3	0.007906	4580.53	0.974
21	FL-0403-F SRC-11/DF-2 Blend	0.889	2.47	259	35.6	0.0011879	6315.65	0.979
22*	FL-0442-F Sunflower Oil	9.220	33.93	588	35.8	0.01017	4576.46	0.719
23*	FL-0433-F Sunflower Ethylester	0.8870	4.96	368	59.9	0.02669	3469.77	0.976
24	FL-0413-F Tar Sand/DF-2 Blend	0.8810	2.92	267	35.7	0.07983	3015.55	0.996
25	14.4-cSt Hydrocarbon Blend	0.8756	14.39	347	44.5	0.05157	3047.96	1.000
26	20.3-cSt Hydrocarbon Blend	0.8581	20.28	374	57.5	0.16741	3770.53	1.394
27	FL-0744-F Wisconsin Hi Vol., Hi CN Blend	0.8314	2.01	139	44.7	0.17577	3995.00	1.986
28	FL-0745-F Wisconsin Hi Vol., Lo CN Blend	0.8914	2.25	264	32.7	0.11730	3093.25	1.947
29	FL-0746-F Wisconsin Lo Vol., Lo CN Blend	0.9147	3.48	284	32.7	0.30764	3453.15	1.495
30	FL-0747-F Wisconsin Lo Vol., Hi CN Blend	0.8488	2.44	252	44.7	0.17494	3434.75	1.475
31	AL-13279-F DF-2 Blend A	0.8484	2.75	272	44.7	0.141.3	3290.77	1.997
32	AL-13639-F DF-2 Blend B	0.8545	2.53	266	45.7	0.03855	3475.74	1.998
33	AL-13664-F DF-2 Blend C	0.8565	3.14	267	44	0.3467	3343.1	1.946
34	AL-13694-F DF-2 Blend D	0.8597	2.75	271	44.9	0.08417	3444.45	1.989
35	AL-13992-F DF-2 Blend E	0.8644	3.76	274	42.7	0.13477	3567.37	1.992
36	AL-13736-F DF-2 Blend F	0.8519	3.78	264	41.4	0.17005	3065.63	1.909
37	AL-13850-F DF-2 Blend G	0.8524	3.09	254	41.4	0.10776	3736.07	1.978
38*	AL-10583-F JP-4	0.7632	0.79	218	77.5	0.35437	3193.89	1.999
39*	AL-14216-F JP-8	0.8232	1.28	409	4.4	3.11419	4044.77	1.495
40	AL-14948-F DF-2 Referee	0.8692	3.94	274	43.7	1.4874	3568.49	1.996
41*	AL-10999-F Type I Referee DF-2	0.7869	0.76	166	77.4	1.36963	3435.7	1.397
42*	AL-14751-F Type II Referee DF-2	0.9048	5.99	313	41.7	1.44774	3.74	1.773

* Fuels tested in the variable compression ratio engine.
** Predicted below 0 or above 100 cetane number.

47

Appendix B. The tabulations include the injection timing in degrees BTDC, the power, the specific fuel consumption, and the ignition delay. All the experiments reported in this section were performed by adjusting the injection timing at each test point so that combustion started at TDC. The start of combustion was defined in terms of the derivative of the combustion chamber pressure data. This is equivalent to an ignition delay based on the rate of heat release, as suggested by Bair (37) and Ryan (38).

As in the CVCB experiments, the engine ignition delay data can be discussed in terms of predictions of cetane number based on the primary reference fuels, or simply in terms of a data base of engine ignition delay times. It should be noted again that ASTM D 613 provides an indirect measure of ignition temperature at a constant ignition delay time of 2.4 ms. In this engine procedure, the ignition delay times are determined at various temperatures (compression ratios) and various speed/load conditions.

1.   Cetane Number Prediction

Blends of the primary reference fuels were evaluated in VCR engines. The results of these experiments are plotted in Fig. 22 through 24 for 1000 rpm tests and in Fig. 25 through 27 for the 2000 rpm tests. In examining this data, it appears that the load or air/fuel ratio has an effect on ignition delay which diminishes, in an absolute sense, as the cetane number increases. The data are somewhat scattered, however, for the 36.3 CN blend (25 percent hexadecane and 75 percent heptamethylnonane), and the effects of air/fuel ratio are not clear for this fuel. An interesting general observation regarding the data presented in Fig. 22 through 27 is the fact that the ignition delay times in milliseconds are apparently independent of engine speed. In terms of crankangle degrees, an ignition delay time of 1.8 ms corresponds to 10.8° at 1000 rpm and 21.6° at 2000 rpm.

The data for primary reference fuels were analyzed using linear regression techniques. In this analysis, the ignition delay time was correlated with compression ratio, cetane number, and air/fuel ratio at each engine speed. The best R-squared value was obtained using an equation of the form:

$$\tau_d = A_1 + A_2 \exp(1/CR) + A_3 \exp(1/CN) + A_4 \, A/F \tag{4}$$
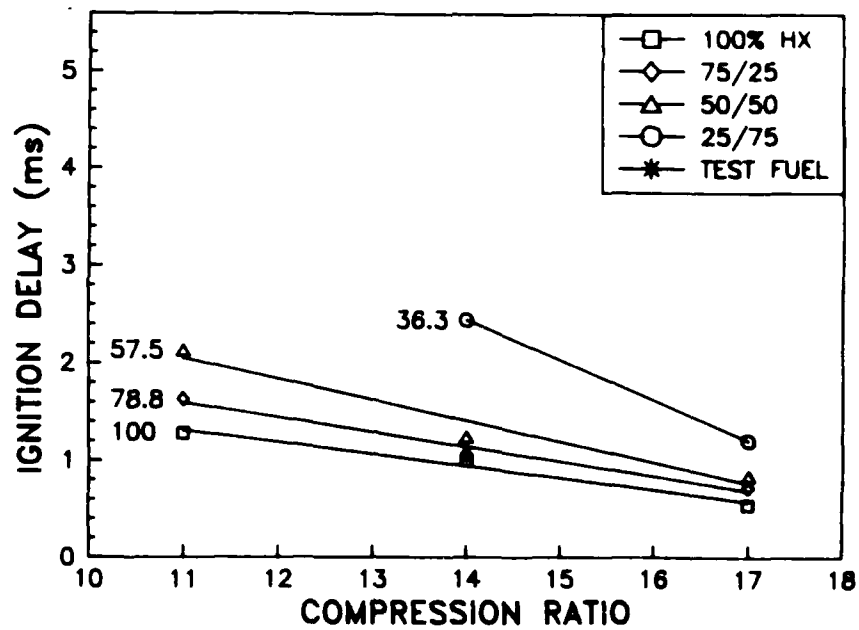
Figure 24. Base fuels at 1000 rpm 40:1 air/fuel
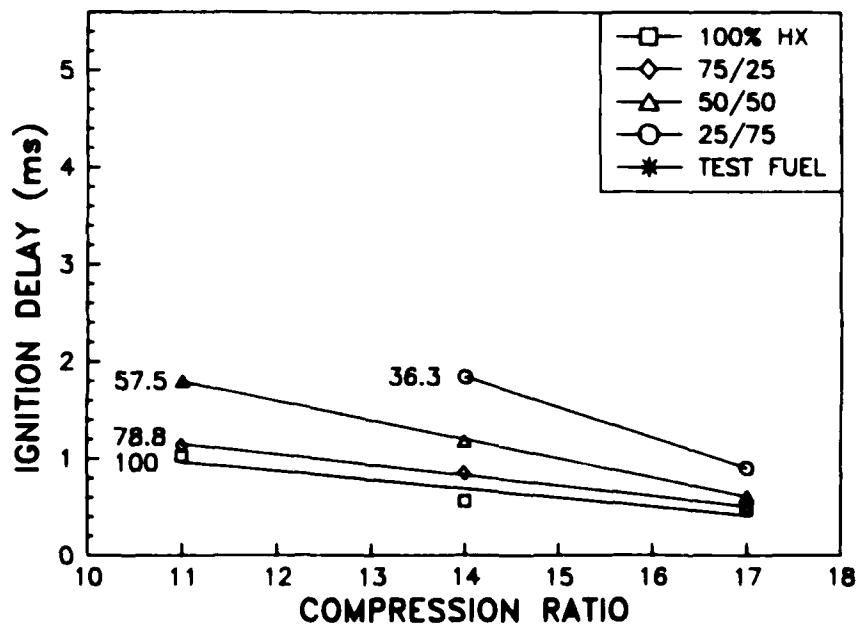
Figure 25. Base fuels at 2000 rpm 20:1 air/fuel

51
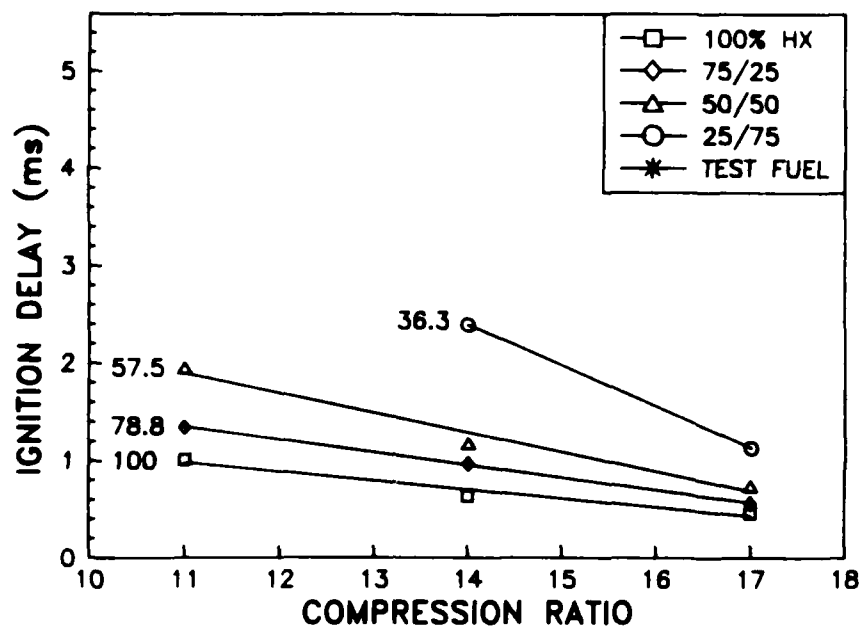
Figure 26. Base fuels at 2000 rpm 30:1 air/fuel
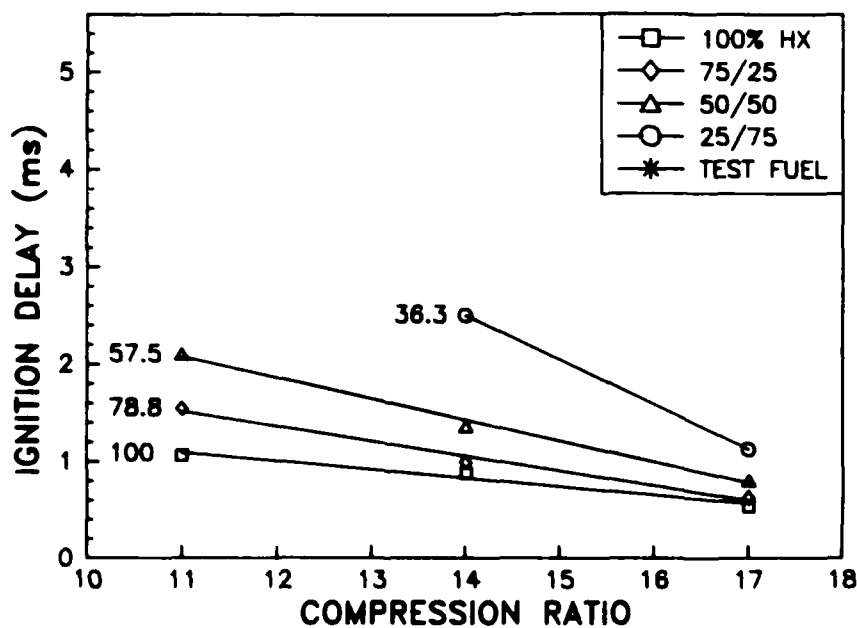
Figure 27. Base Fuels at 2000 rpm 40:1 air/fuel

where: CR = compression ratio

       CN = cetane number

       A/F = air/fuel ratio.

and for 1000 rpm, A_1 = -120.64   and for 2000 rpm, A_1 = -93.81

                  A_2 = 34.65 A_2 = 28.30

                  A_3 = 83.39 A_3 = 63.20

                  A_4 = -0.0021 A_4 = 0.0091

                  R_2 = 0.807 R_2 = 0.808

While the correlations appear to be adequate, use of the correlation equations to predict cetane number for other fuels may not be appropriate. In order to be used as a predictive tool, the regression equations should be based on much more primary reference fuels data, including more blends, more repetitions, and tested over a broader range of air/fuel ratios. In addition, it is felt that the resulting regression equations should have much better R-squared values, resulting from a larger data base or improvement in the form of the regression. These equations should then be verified using several blends of the secondary reference fuels. One of the problems encountered in this program, and which is a major shortcoming of the cetane scale, is the prohibitively high cost of the primary reference fuels.

A simple method of analyzing the engine data consists of graphical comparison of the test fuel data at a given test condition to that of the corresponding reference fuel data. This comparison is presented in Fig. 28 for the sunflower oil and Fig. 29 for the ethylester of the sunflower oil. The same data for all of the other test fuels are presented in Appendix C. In all cases, the test fuel data are plotted using an asterisk and a dashed line. The reference fuel data always consist of the top line representing the 36.3 cetane number blend, going to 57.5, 78.8, and the bottom line is the 100 CN reference fuel data.

For the sunflower oil, it was not possible to attain steady operation at the 11:1 compression ratio (CR) at any test condition. At 20:1 air/fuel ratio, the sunflower oil data cross the 57.5 CN reference fuel data, with a higher indicated CN ($\approx$60) at 14:1 CR and a lower CN ($\approx$45) at the 17:1 CR. At the leaner air/fuel ratios, the apparent CN is in the range of 45 CN. For the 2000 rpm data, the apparent cetane
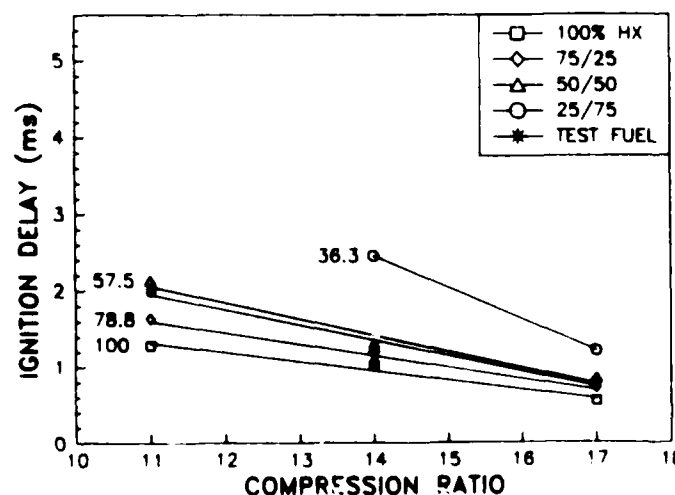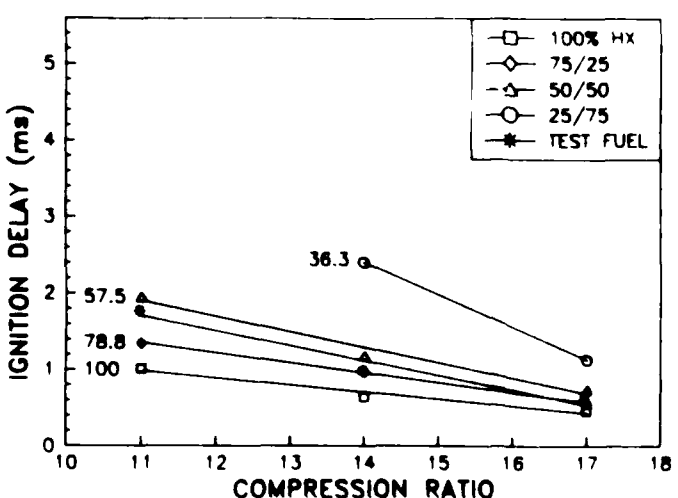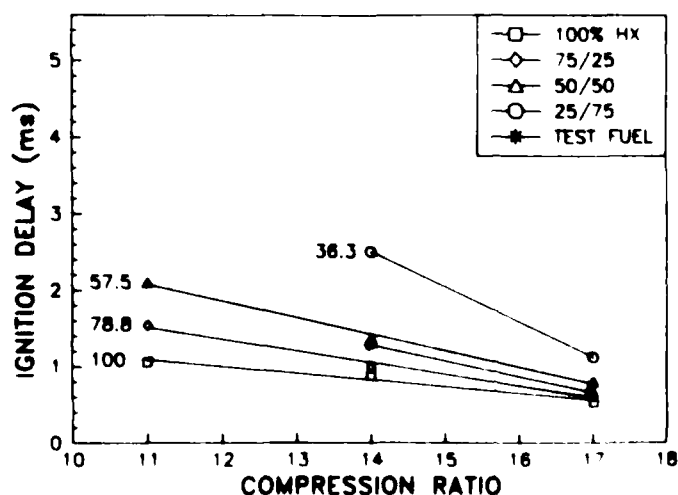
53
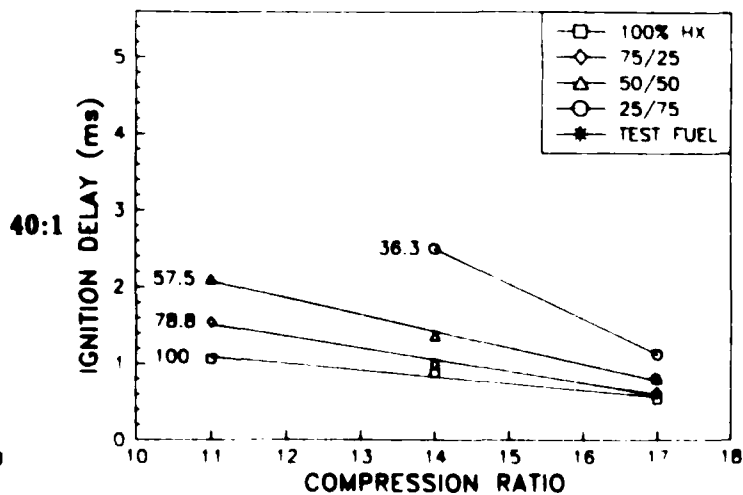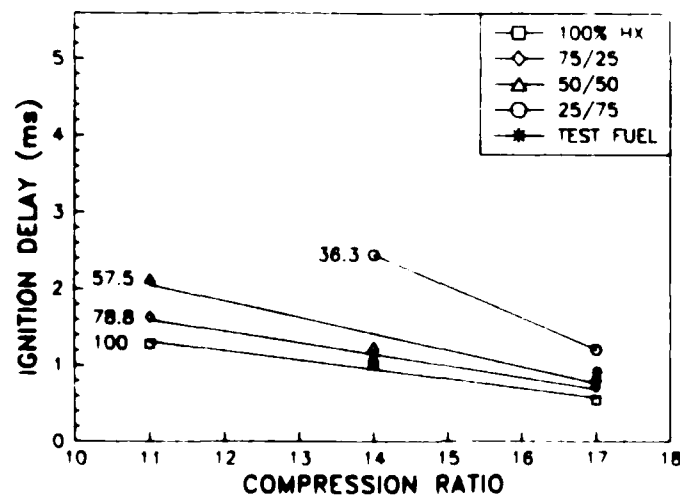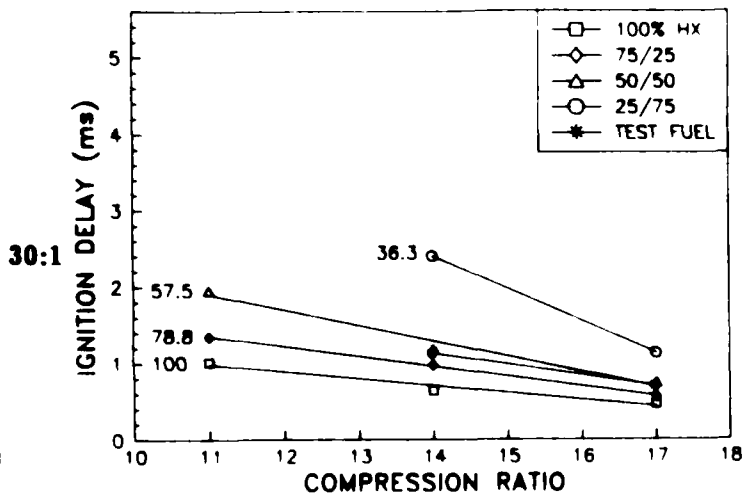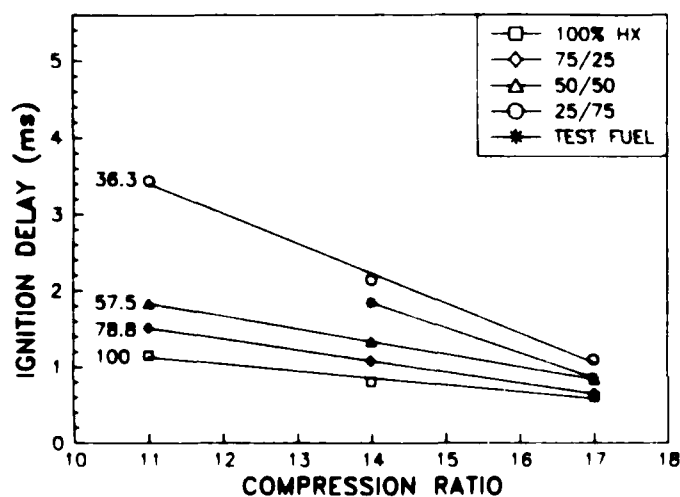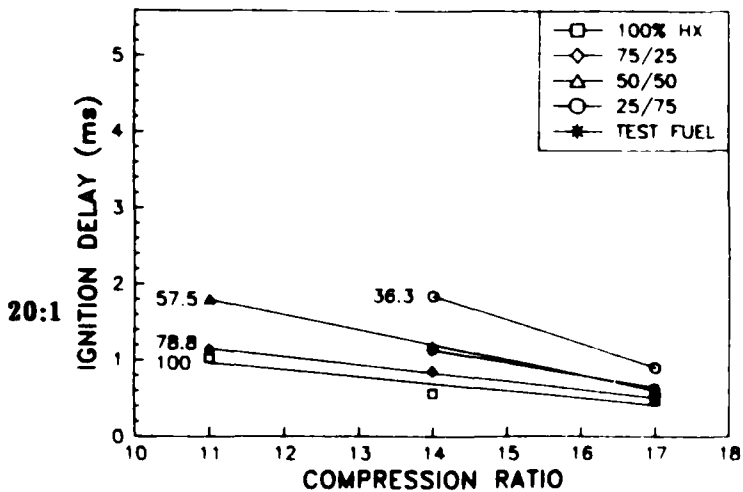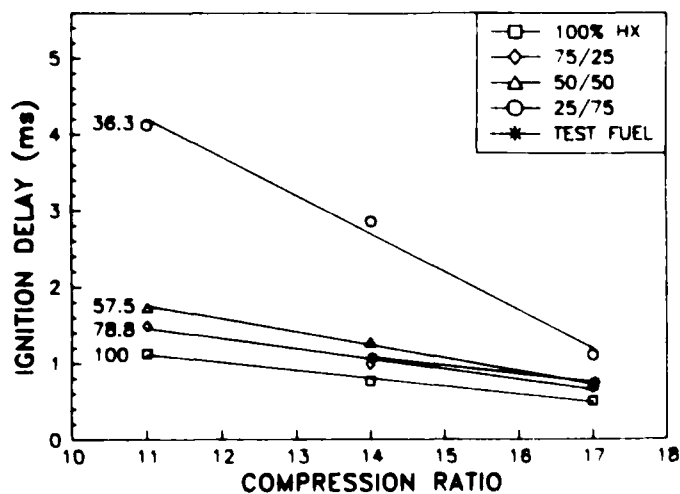
Figure 28. Sunflower oil

54
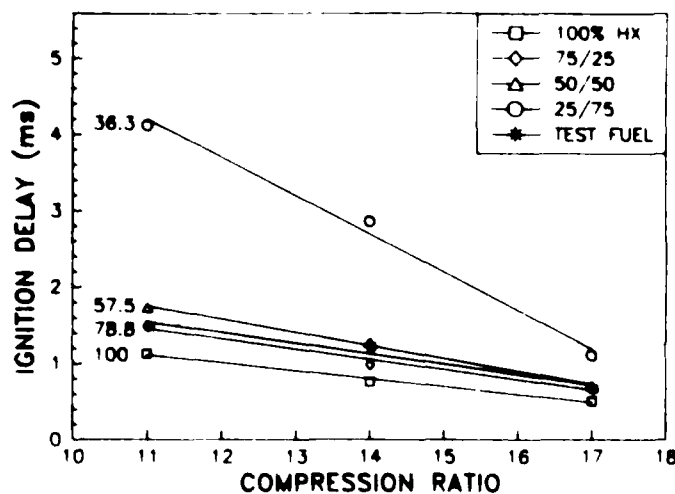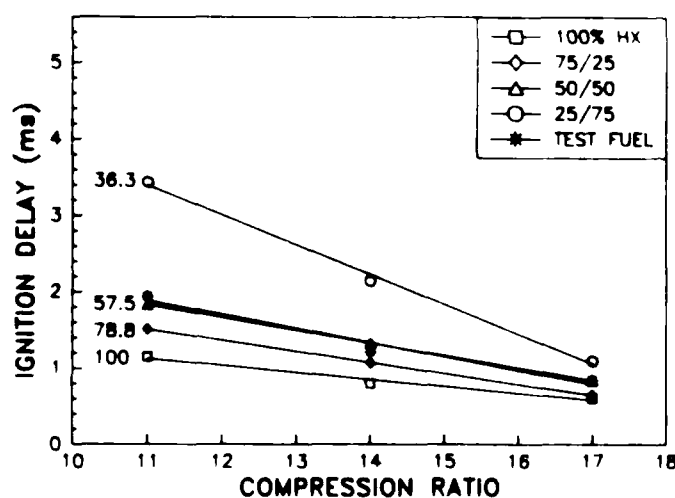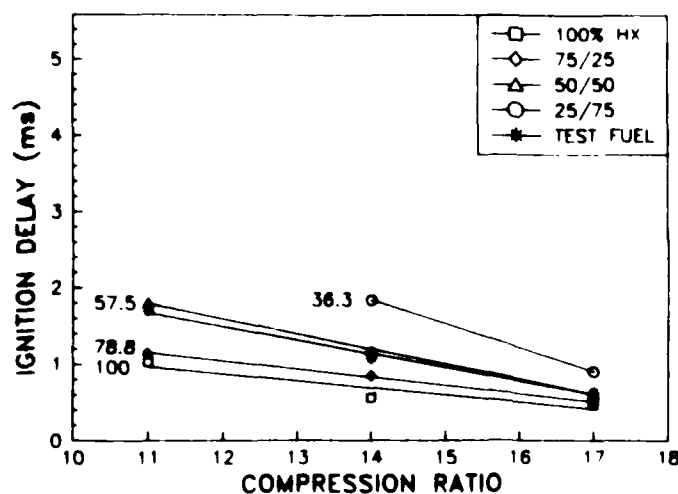
Figure 29. **Sunflower ethylester**

number is consistently in the range of 50 to 57 CN. These results in general indicate a higher apparent cetane number for the sunflower oil than the measured value of 35.8. This would tend to indicate a better cold start characteristic and smoother operation (lower rates of pressure rise) than is predicted by ASTM D 613. This conclusion is in general agreement with the findings of Needham (7), who tested the same fuel in both a direct-injection engine and an indirect injection engine.

The ethylester of sunflower oil has a D 613 cetane number of 59.9. As can be seen in Fig. 29, while there is some indication of a higher apparent CN at the lower compression ratios, the results are in the range of 50 to 60 CN. The higher apparent CN at the lower compression ratios indicates a better cold start characteristic than D 613.

The results of similar analyses performed on the other test fuels (plots presentation in Appendix C) are summarized in TABLE 10. In this table, the range of apparent cetane numbers are presented for each fuel at the various compression ratios and rpms. The ranges presented in the table are those estimated in going from the low compression ratio (11:1) to the high value (17:1). Also presented in the table are the measured D 613 cetane numbers. As can be seen in the table, there is general agreement in that good fuels and bad fuels are separated. In going down the list, it appears that N-octane, N-hexane and the Type I Referee fuel all have lower ignition quality than is indicated by ASTM D 613. JP-4 has a higher ignition quality than is indicated by D 613. The remainder of the fuels appear to perform in general agreement with the indications of D 613.

The 40:1 air/fuel ratio and the 1000 rpm test condition probably provide the best indication of cold start quality. The lighter load (leaner air/fuel ratios and, thus, lower temperatures) and slower speed are more indicative of conditions during cold starting. At this test condition, N-hexane, N-octane, and Type I Referee fuel again demonstrate a potential for worse cold start characteristics and JP-4 better cold start characteristics than are indicated by D 613. The results for all of the other fuels are in agreement with the results of D 613. Verification of this theory requires the actual performance of cold start experiments involving the same fuels. As indicated previously, it is felt that the quality of the predicted apparent CN could be improved through the development of additional reference fuel test data and improvement of

56

TABLE 10. Apparent Cetane Number Ranges Based on Comparisons With Reference Fuel Data

Fuel	D 613	20:1 A/F	30:1 A/F	40:1 A/F	rpm
N-octane	64.4	57-60	50-58	45-48	1000
		60-57	60-57	65-57	2000
N-hexane	44.8	40-37	37-20	~20	1000
		35-20	~37	~20	2000
JP-4	35.0	57-37	50-37	~50	1000
		~57	~55	~55	2000
JP-7	54.0	55-40	50-57	55-40	1000
		~55	~55	~55	2000
JP-8	41.4	47-37	45-35	~40	1000
		~40	~40	47-37	2000
Type I Referee	27.8	~35	~20	~20	1000
		~15	~20	~15	2000
Type II Referee	40.2	42-47	~40	~40	1000
		~40	~40	30-40	2000
5-cSt Hydrocarbon Blend	48.5	55-40	55-40	50-40	1000
		~50	~50	~50	2000
12-cSt Hydrocarbon Blend	55.8	57-47	60-47	57-47	1000
		67-57	60-57	60-57	2000
19-cSt Hydocarbon Blend	53.8	~55	~57	~57	1000
		57-47	~57	~57	2000
Sunflower Oil	35.8	60-47	45-57	~45	1000
		~57	~57	~50	2000
Sunflower Ethylester	59.9	67-55	~57	~57	1000
		~57	~57	~60	2000

the regression equation. The development and verification, through cold start experiments, of such an equation would provide the engine basis (mentioned previously) for an improved ignition quality index.

IV. SUMMARY AND CONCLUSIONS

In comparing the CVCB and engine results for the same fuels, it appears that both techniques agree in most cases in indicating ignition quality that is either better or worse than is indicated by the ASTM D 613. This observation is based on comparison of the apparent cetane numbers measured in both apparatus for the D 613 value. This is particularily true for N-octane, N-hexane, and Type I Referee fuel, all of which revealed poorer ignition quality in both apparatus than in D 613. In addition, JP-4 displayed better ignition quality in both techniques than is indicated by D 613.

As indicated previously, it is felt that the reliability of both techniques will improve with the development of larger data bases which include many more fuels and broader ranges of test conditions. The development of an ignition quality index is dependent upon the generation of much larger data bases, including an engine cold start data base. It is envisioned that the index would be based on a variety of readily available reference fuels, including variations in hydrocarbon type, which could change in response to changes in the available diesel fuel. In this procedure, engine manufacturers would define the ignition/combustion quality requirements in terms of this family of reference fuels and the ignition delay data from the CVCB. In an inverse fashion, the fuel refiners would control quality based on either the CVCB or the VCR engine ignition/combustion characteristics as compared to the same family of reference fuels. For the CVCB techniques, the reference fuels could be almost anything because the index would be based on absolute ignition delay time versus temperature relationships. In the VCR engine, some care may be necessary in the selection of the reference fuels because it is possible that the physical delay (and possibly the physical properties of the fuels) has not been completely eliminated as a variable in this procedure.

In addition to advancing the development of two new ignition quality rating techniques, the work performed in this program has resulted in the development of several

58

conclusions regarding ignition and the continued utilization of the cetane number scale. These include:

1. The CVCB technique offers the very attractive possbility of providing an indication of cetane number. This is attractive because the technique is much simplier and easier to incorporate into an Army mobile or laboratory-based quality control apparatus.

2. For currently available diesel fuels, it appears that the CVCB technique can predict cetane numbers to within 2 CN and possibly better using the data checking procedure that was described.

3. The CVCB technique has been demonstrated as a method for rating ignition quality as a function of temperature. This offers the attractive opportunity of developing direct correlations with engine cold start data.

4. The CVCB technique has been successfully used to develop ignition delay data at various temperatures. This is a very convenient method for developing ignition data for almost any fuel over a very broad range of both temperature and pressure.

5. The VCR engine has been demonstrated as a viable tool in evaluating engine ignition quality of a wide variety of fuels.

6. In the engine, ignition delay time was found to be primarily a function of compression ratio and cetane number. Air/fuel ratio had a minor effect on the ignition delay time. This effect was most probably related to changes in the operating temperatures corresponding to changes in the air/fuel ratio.

7. Both the CVCB and the engine techniques pointed out fuels that had different ignition characteristics than indicated by the ASTM D 613 procedure. The significance of this finding will be more apparent when corresponding cold start experiments are performed.

V. RECOMMENDATION

The work described in this report has resulted in the development of several conclusions which could have immediate application, including the development of a new (CVCB) technique for determining the cetane number of diesel fuels. The successful long-term application of this technique depends on the continued development of the data base. In addition, the broader application as an ignition/combustion quality analyzer depends on the continued improvement of the technique as well as on the development of a broader data base that includes engine ignition delay and cold start data bases. For immediate future use, the CVCB should be transitioned from a research device to an Army mobile or laboratory-based quality control apparatus. It is felt that the VCR engine facility offers unique capabilities for developing both data bases. In addition, the unique design, including the variable compression ratio and the optical access, offers the opportunity to develop a basic understanding of the processes occurring during the ignition delay times. The opportunities are particularily interesting in terms of using the optical access to examine the injection, atomization, and ignition processes during cold start.

VI. REFERENCES

1. Boerlage, G.D. and Broeze, J.J., "Ignition Quality of Diesel Fuels as Expressed in Cetane Numbers," SAE Journal, Vol. 31, 1932.

2. Schweitzer, P.H., "Methods of Rating Diesel Fuels," Chemical Reviews, Vol. 22, 1938.

3. Henein, N.A., Fragoulis, A.N., and Luo, L., "Correlations Between Physical Properties and Autoignition Parameters of Alternate Fuels," SAE 850266, 1985.

4. Gulder, O.L., Glavincevski, B., and Burton, G.F., "Ignition Quality Rating Methods for Diesel Fuels — A Critical Appraisal," Diesel Fuel Quality and Trends, SAE, p. 45, October 1985.

5. LeBreton, M.D., "Repeatability Test on the CFR Cetane Engine," SAE 841340, 1984.

6. Glavincevski, B., Gulder, O.L., and Gardner, L., "Cetane Number Estimation of Diesel Fuels From Carbon Type Structural Composition," SAE 841341, 1984.

7. Needham, J.R. and Doyle, D.M., "The Combustion and Ignition Quality of Alternative Fuels in Light Duty Diesels," SAE 852101, 1985.

8. Hurn, R.W. and Hughes, K.J., "Combustion Characteristics of Diesel Fuels as Measured in a Constant-Volume Bomb," SAE Quarterly Trans., Vol. 6, No. 1, p. 24.

9. Hardenberg, H.O. and Ehnert, E.R., "Ignition Quality Determination Problems With Alternative Fuels for Compression Ignition Engines," SAE 811212, 1981.

10. Tavacha, J.W. and Cliffe, J.O., "The Effects of Cetane Quality on the Performance of Diesel Engines," SAE 821232, 1982.

11. Siebers, D.L., "Ignition Delay Characteristics of Alternative Diesel Fuels: Implications on Cetane Number," SAE 852102, 1985.

12. Yu, T.C., Uyehara, O.A., Myers, P.S., Collins, R.N., and Mahadevan, K., "Physical and Chemical Ignition Delay in an Operating Diesel Engine Using the Hot-Motored Technique," SAE Trans., Vol. 64, p. 690, 1956.

13. Tsao, K.C., Myers, P.S., and Uyehara, O.A., "Gas Temperatures During Compression in Motored and Fired Diesel Engines," SAE Trans., Vol. 70, p. 136, 1962.

14. Hardenberg, H.O. and Hase, F.W., "An Empirical Formula for Computing the Pressure Rise Delay of a Fuel From Its Cetane Number and From the Relevant Parameters of Direct-Injection Diesel Engines," SAE 790493, 1979.

15. Parker, T.E., Forsha, M.D., Stewart, H.E., Hom, K., Sawyer, R.F., and Oppenheim, A., "Induction Period for Ignition of Fuel Sprays at High Temperatures and Pressures," SAE 850087, 1985.

16. Walsh, G. J. and Cheng, W.K., "Effects of Highly Heated Fuel on Diesel Combustion," SAE 850088, 1985.

17. Elliott, M.A., "Combustion of Diesel Fuel," SAE Quarterly Trans., Vol. 3, No. 3, p. 490.

18. El Wakil, M.M., Myers, P.S., and Uyehara, O.A., "Fuel Vaporization and Ignition Lag in Diesel Combustion," SAE Trans., Vol. 64, p. 712, 1956.

19. Rao, K.V.L. and Lefebvre, A H., "Spontaneous Ignition Delay Times of Hydrocarbon Fuel/Air Mixtures."

20. Chiang, C.W., Myers, P.S., and Uyehara, O.E., "Physical and Chemical Ignition Delay in an Operating Diesel Engine Using the Hot-Motored Techinique -- Part II," SAE Trans. Vol. 68, p. 562, 1960.

21. Cox, R.A. and Cole, J.A., "Chemical Aspects of the Autoignition of Hydrocarbon/Air Mixtures," Combustion and Flame, Vol. 60, p. 109, 1985.

22. Saeed, M.N. and Henein, N.A., "Ignition Delay Correlations for Neat Ethanol DF-2 Blends in a DI Diesel Engine," SAE 841343, 1984.

23. Dobovisek, Z. and Savery, C.W., "Ignition Delay of Selected Alternative Fuels in IC Engines," SAE 859225, 1985.

24. Hardenberg, H.O. and Ehnert, E.R., "Ignition Quality Determination Problems With Alternative Fuels for Compression Ignition Engines," SAE 811212, 1981.

25. Bowden, J.N. and Frame, E.A., "Effect of Organic Sulfur Compounds on Cetane Number," Am. Chem. Soc., Miami Beach Meeting, 28 April - 3 May 1985.

26. Olreed, R.M. and Lenane, D.L., "Diesel Combustion Cetane Number Effects," SAE 840108, 1984.

27. Collins, J.M. and Unzelman, G.H., "Alternatives for Meeting Cetane Quality in the Next Decade," API 48th Midyear Refining Meeting, 10 May 1983.

28. Unzelman, G.H., "New Cetane Data Reveal Surprises, Challenges," Oil and Gas Journal, Nov. 14, p. 178, 1983.

29. Oren, D.C., Washiduzzaman, S., and Ferguson, C.R., "A Diesel Combustion Bomb --Proof of Concept," SAE 841358, 1984.

30. Collins, J.M. and Unzelman, G.H., "Diesel Trends Emphasize Cetane Economics, Quality, and Prediction," API 47th Midyear Refining Meeting, 11 May 1982.

31. Kloptenstein, W.E., "Estimation of Cetane Index for Esters of Fatty Acids," JAOCS, Vol. 59, No. 12, p. 531, December 1982.

32. Murphy, M.J., "An Improved Cetane Number Predictor for Alternative Fuels," SAE 831746, 1983.

33. Steere, D.E., "Development of the Canadian General Standards Board (CGSB) Cetane Index," SAE 841344, 1984.

34. Bailey, B.K., Russell, J.A., Wimer, W.W., and Buckingham, J.P., "Cetane Number Prediction Modeling," SwRI Internal Research Report No. SwRI-9435, 1986.

35. Ryan, T.W., III, and Dodge, L.G., "Diesel Engine Injection and Combustion of Slurries of Coal, Charcoal, and Coke in Diesel Fuel," SAE Paper 840119, 1984.

36. Callahan, T.J., Ryan, T.W., III, Dodge, L.G., and Schwalb, J.A., "Effects of Fuel Properties on Diesel Spray Characteristics," to be presented at the 1986 SAE Fuels and Lubricants Meeting, Philadelphia, PA, October 1986.

37. Bair, R., Boggs, D., Borman, G., and Foster, D., "Diesel Combustion and Ignition Properties of Fuels with Different Volatile Fraction Constituents," SAE Paper 861539, October 1986.

38. Ryan, T.W. III, "Correlation of Physical and Chemical Ignition Delay to Cetane Number," SAE Paper 852103, October 1985.

39. Spadaccini, L.J. and TeVelde, J.A., "Autoignition Characteristics of Aircraft Type Fuels," Combustion and Flame, Vol. 46, pp. 283-300, 1982.

40. Hamming, R.W., Digital Filters, Prentice-Hall, Englewood Cliffs, NJ, 1977.

APPENDIX A

DATA REDUCTION PROCEDURES

DATA REDUCTION PROCEDURES

The CVCB data are stored in files on the HP-1000 computer. Each file consist of five columns, the first of which represents the time track of the digital oscilloscope through the course of the experiment. The second and third columns contain the chamber pressure and needle lift data for one test. The fourth and fifth columns contain the chamber pressure and needle lift data for a second test. Each fuel is tested six times, which results in a total of three files for a particular fuel at a given condition.

A computer program (BSTEST) reads the file names of the test data from a separate file (FILESLIST). This file consists of two columns, the first of which is the file name of an air environment test, while the second contains the file name of the correpond-ing nitrogen environment test. After reading the first two file names, the program then reads the data from those files into a pair of two-dimensional arrays.

The chamber pressure and needle lift are plotted versus time for both the air and nitrogen environment arrays in order to distinguish the desired points of interest (see Fig. 7 of the text). These points of interest were used to determine the ignition delay times.

Due to the amount of noise encountered and to the sensitivity required to locate the desired points on the pressure and needle lift curves, the data were passed through a smoothing routine. The selection of the proper digital filter for this routine involved the determination of the ratio of the noise to the sampling rate of the data. The ratio was found to be 0.20 to 0.33, which suggested that the digital filtering method known as "3's and 5's" would be effective.(40) The data in an array are passed through the filter, and a new, smoothed array is created using the equation (40),

$$ I' = \frac{(I-3) + 2(I-2) + 3(I-1) + 3I + 3(I-1) + 2(I+2) + (I+3)}{15} \tag{A-1} $$

where I' smoothed point

I (I-ith) data point

67

The newly created arrays replace the original arrays for the remainder of the data reduction process. An example of the improvement of the filtered data over the original data can be seen in Fig. A-1.

During the preliminary assessment of the data, it became apparent that the matching air nitrogen environment tests did not always begin at the same pressure or at the same needle lift rise time. However, due to the required precision of the measurements, it was necessary for the air and nitrogen data pairs to have identical starting points. A subroutine was developed to set the initial pressure so that all chamber pressure arrays would begin at the same pressure level.

In order to adjust the time base of a pair of curves, it was necessary to choose a common point on both curves and adjust the time scale from that point. The time when the chamber pressure drop occurred was chosen as the common point. Thus, a subroutine was developed that could identify this point repeatably, and with some precision. The routine that is used compares the slopes at various points along the chamber pressure curve. As soon as these slopes reach a specified steepness, the routine reads the corresponding value in the time array. The data for the air and nitrogen environment files are run through this routine individually so that each returns a chamber pressure drop time. The difference between the two is obtained by subtracting the drop time of the nitrogen curve from that of the air curve. A subroutine then takes this time difference and adds it to every point in the nitrogen time array so that the air and nitrogen curves have the same pressure drop times.

In order to calculate the delay times which were defined previously, it was necessary to develop subroutines that would identify the times when needle lift and minimum pressure occurred. Subroutines were also needed to find the time when the air nitrogen environment pressure curves deviated due to combustion, and also the time when the air environment pressure curve rose above the initial pressure. The subroutine to determine the needle lift rise time simply returns the value of the time array which corresponds to the first value in the needle lift array that was greater than 0.01 mm. Similarly, another subroutine returns the time value which corresponds to the point on the air environment pressure curve when the given initial pressure is crossed.
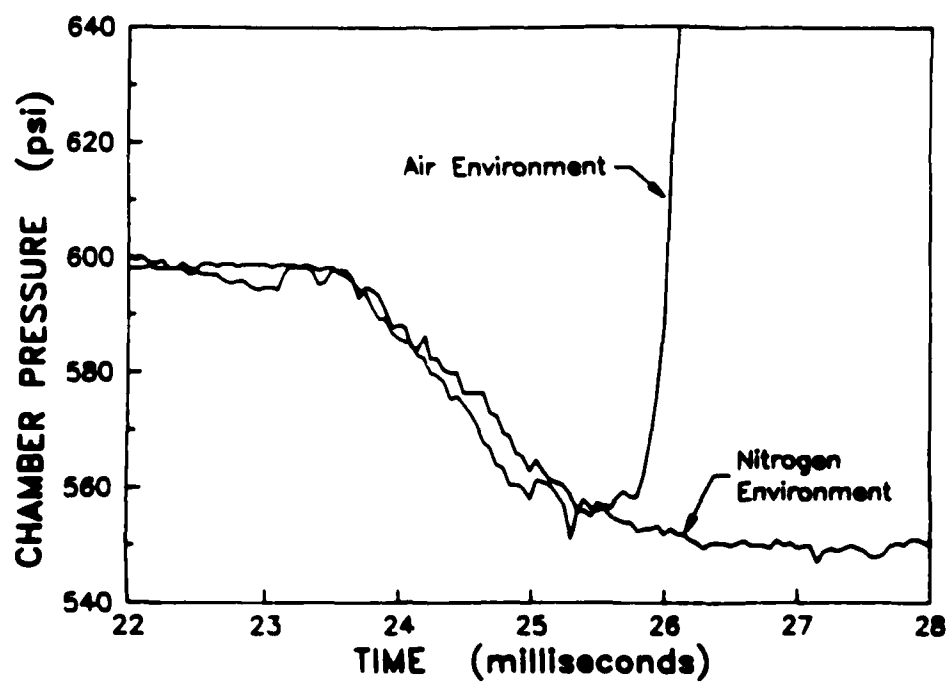
a. Unfiltered signals
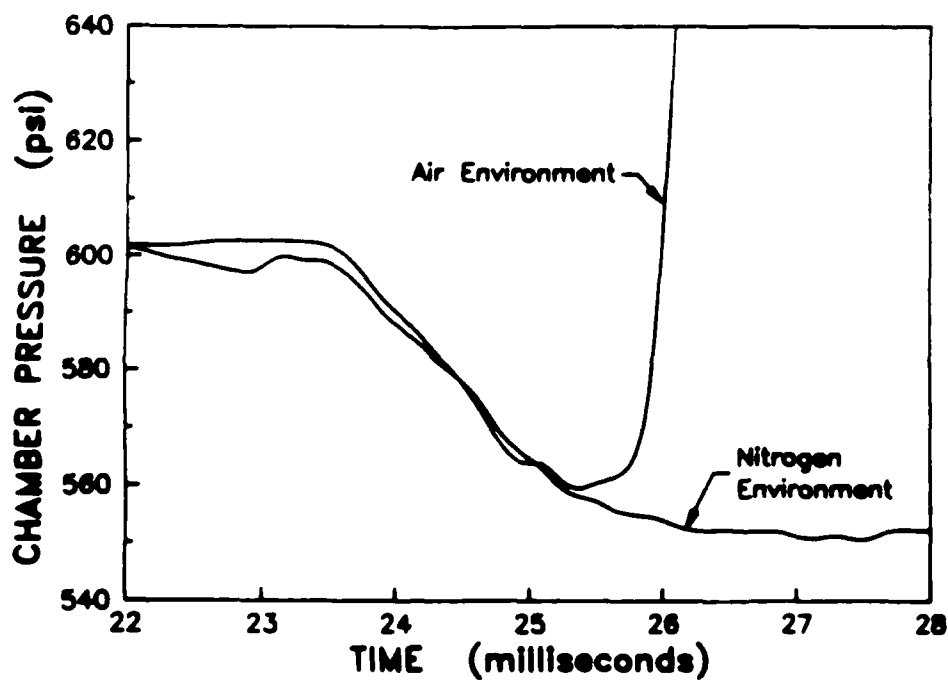
b. Filtered signals

Figure A-1. Effects of digital filtering on the data signals

The subroutine that is used to calculate the point at which the air and nitrogen environment pressure curves deviate from each other is also used to compare the values in the two pressure arrays until they differ by a given percentage of the nitrogen environment pressure. It then returns the corresponding value from the air file's time array. The subroutine, therefore, starts at the point in the air atmosphere pressure array when the initial pressure is crossed. It then reads the array from that point in reverse order until it comes to the place in the pressure curve where the slopes became negative. This point is assumed to be the minimum point on the curve, and the corresponding value of the time array is returned to the main program.

The main program takes the values for the time when the needle lift rises, the minimum pressure occurs, the air and nitrogen environment pressure curves deviate, and the air environment pressure rise above the initial pressure. These values are then used to calculate the delay times mentioned previously. The program performs this function for all of the files read from FILESLIST and writes the values for all of the delay times to a printer. The delay times of tests that are performed at identical conditions are then evaluated to find the average and standard deviation of the results.

APPENDIX B

VARIABLE COMPRESSION-RATIO ENGINE DATA

TABLE B-1. Variable Compression-Ratio Engine Data— Hexadecane (Fuel 6)

Run Number	A/F	Injection Timing, deg.	Power, kW	Sp. Fuel Cons., kg/kW-h	τ_d TC, ms
1000 rpm					
264	19.50	6.8	2.30	0.48	1.13
269	30.27	6.9	1.63	0.46	1.15
271	39.71	7.7	1.08	0.53	1.28
270	59.99	8.4	0.82	0.46	1.40
261	17.55	4.4	2.63	0.46	0.74
262	18.05	4.2	2.61	0.46	0.70
263	19.27	5.0	2.50	0.44	0.83
268	30.19	4.8	1.68	0.44	0.80
272	40.04	6.0	1.12	0.51	1.00
265	19.50	3.0	2.98	0.37	0.50
266	25.91	3.2	2.25	0.37	0.54
267	29.80	3.6	1.96	0.38	0.60
273	39.86	3.2	1.32	0.43	0.54
2000 rpm					
279	19.74	12.4	2.95	0.66	1.03
278	25.00	12.4	2.73	0.58	1.03
277	30.69	12.1	1.76	0.74	1.01
285	40.00	12.7	0.51	1.93	1.06
280	20.33	6.7	3.04	0.63	0.56
276	30.84	7.7	1.54	0.85	0.64
284	39.79	10.6	0.63	1.59	0.88
281	20.39	5.6	3.69	0.52	0.47
275	31.15	5.5	1.99	0.66	0.46
282	35.42	5.2	1.65	0.69	0.43
283	39.53	6.4	1.02	1.00	0.53

TABLE B-2. Variable Compression-Ratio Engine Data—
75% Hexadecane 25% Heptamethylnonane (Fuel 8)

Run Number	A/F	Injection Timing, deg.	Power, kW	Sp. Fuel Cons., kg/kW-h	τ_d TC, ms
1000 rpm					
288	19.88	8.9	2.19	0.49	1.49
293	30.62	9.0	1.54	0.47	1.51
294	36.56	9.7	1.18	0.52	1.61
296	40.02	9.8	0.99	0.56	1.63
286	19.25	5.8	2.36	0.46	0.96
287	19.91	5.9	2.33	0.46	0.99
292	30.62	6.4	1.59	0.46	1.07
297	40.19	6.4	1.02	0.55	1.06
289	20.07	4.1	2.67	0.40	0.68
291	30.34	3.8	1.79	0.40	0.64
298	40.19	4.3	1.13	0.49	0.72
2000 rpm					
301	19.72	13.7	3.24	0.60	1.14
303	29.06	16.1	1.79	0.74	1.34
310	42.88	18.5	0.57	1.63	1.54
300	19.98	10.2	3.52	0.55	0.85
304	29.06	11.6	1.93	0.68	0.97
309	43.30	11.9	0.68	1.36	0.99
299	20.18	5.9	3.92	0.50	0.49
305	29.67	6.7	2.28	0.58	0.56
308	43.30	7.4	0.79	1.17	0.62
307	47.03	7.8	0.63	1.36	0.65

TABLE B-3. Variable Compression-Ratio Engine Data—
50% Hexadecane 50% Heptamethylnonane (Fuel 9)

Run Number	A/F	Injection Timing, deg.	Power, kW	Sp. Fuel Cons., kg/kW-h	τ_d TC, ms
1000 rpm					
313	20.85	10.4	2.40	0.43	1.73
314	30.32	11.0	1.73	0.04	1.83
319	41.41	12.8	1.04	0.52	2.13
312	20.85	7.6	2.56	0.41	1.27
315	30.69	8.0	1.75	0.41	1.33
318	41.41	7.4	1.08	0.51	1.24
311	20.85	4.2	2.84	0.37	0.70
316	30.69	5.0	1.93	0.37	0.83
317	40.04	5.0	1.24	0.45	0.84
2000 rpm					
320	17.92	21.4	3.47	0.60	1.78
321	19.46	22.0	3.21	0.60	1.83
328	29.01	23.4	2.13	0.61	1.95
333	42.74	25.2	0.74	1.84	2.10
322	19.90	14.2	3.86	0.49	1.18
326	29.82	13.8	2.42	0.24	1.15
329	29.01	14.6	2.25	0.27	1.22
332	42.96	16.3	1.02	0.89	1.36
323	20.11	7.3	3.98	0.48	0.61
325	29.22	8.5	2.84	0.47	0.71
330	29.32	9.2	2.61	0.50	0.77
331	41.49	9.6	1.11	0.84	0.80

TABLE B-4. Variable Compression-Ratio Engine Data—
25% Hexadecane 75% Heptamethylnonane (Fuel 10)

Run Number	A/F	Injection Timing, deg.	Power, kW	Sp. Fuel Cons., kg/kW-h	τ_d TC, ms
1000 rpm					
336	20.51	24.7	2.36	0.44	4.12
337	30.34	20.6	1.59	0.46	3.44
335	20.12	17.2	2.39	0.43	2.86
338	31.19	12.8	1.75	0.41	2.14
344	40.67	14.6	1.12	0.49	2.44
334	19.99	6.6	2.78	0.38	1.10
339	31.19	6.5	1.89	0.38	1.09
343	40.67	7.2	1.22	0.45	1.20
2000 rpm					
348	19.69	37.3/47.1	2.75	0.70	3.92
347	19.10	22.1	3.89	0.50	1.84
350	28.87	28.8	2.47	0.54	2.40
355	40.00	30.0	0.68	0.80	2.50
346	20.23	10.8	4.12	0.47	0.90
349	29.23	13.6	2.67	0.49	1.13
353	38.42	13.8	1.48	0.69	1.15
354	41.35	13.1	1.25	0.76	1.09

TABLE B-5. Variable Compression-Ratio Engine Data—
100% Normal Octane (Fuel 11)

Run Number	A/F	Injection Timing, deg.	Power, kW	Sp. Fuel Cons., kg/kW-h	τ_d TC, ms
1000 rpm					
210	21.60	10.0	2.30	0.44	1.67
211	19.29	10.6	2.47	0.46	1.76
208	28.97	12.8	1.70	0.44	2.14
217	43.15	15.5	1.60	0.33	2.58
212	19.29	7.1	2.69	0.42	1.18
205	29.18	8.0	1.89	0.40	1.34
218	42.76	9.6	1.59	0.33	1.60
213	19.50	3.5	1.52	0.72	0.58
207	29.03	5.0	2.01	0.38	0.84
206	28.00	5.0	2.03	0.39	0.83
214	33.20	5.0	1.55	0.43	0.84
215	42.41	5.2	1.57	0.33	0.86
216	42.57	5.0	1.58	0.33	0.85
2000 rpm					
222	17.50	18.6	3.49	0.63	1.55
229	20.90	20.2	3.04	0.60	1.68
227	28.23	20.2	2.39	0.59	1.68
230	38.44	20.3	1.31	0.79	1.69
221	20.48	12.8	4.04	0.49	1.07
220	23.49	12.6	5.71	0.30	1.05
226	28.70	13.3	2.56	0.55	1.11
231	39.58	15.7	1.42	0.71	1.31
223	18.15	--	4.15	0.54	
228	21.57	6.8	3.69	0.49	0.57
225	29.03	7.8	--		0.65
232	39.22	9.2	1.13	0.90	0.77

TABLE B-6. Variable Compression-Ratio Engine Data—
Normal Hexane (Fuel 13)

Run Number	A F	Injection Timing, deg.	Power kW	Sp. Fuel Cons. kg/kW·h	ms
1000 rpm					
243	22.90				
244					
240					
241					
245					
248					
242					
246					
247					
2000 rpm					

(remaining data illegible)

TABLE B-7. Variable Compression-Ratio Engine Data—
19-cSt Hydrocarbon Blend (Fuel 18)

Run Number	A F	Injection Timing, deg.	Power, kW	Sp. Fuel Cons., kg/kW-h	τ_d TC, ms
1000 rpm					
580	19.94	11.9	1.68	0.61	1.98
582	30.66	11.5	1.11	0.63	1.92
590	39.83	11.7	0.55	1.00	1.95
579	19.94	6.24	1.73	0.59	1.04
583	30.66	6.50	1.28	0.55	1.08
584	39.83	8.3	0.74	0.75	1.39
578	19.99	4.9	2.06	0.50	0.82
584	30.66	4.4	1.42	0.49	0.74
586	35.76	4.6	1.13	0.54	0.77
588	39.63	4.7	0.94	0.59	0.78
2000 rpm					
594	19.40	20.0	2.53	0.76	1.67
595	29.32	21.6	1.40	0.93	1.80
601	40.01	21.6	2.73	0.69	1.98
593	19.70	11.6	1.51	0.85	0.97
596	29.82	13.6	0.46	2.12	1.13
600	40.01	14.9	3.66	0.58	1.24
591	17.94	7.1	3.24	0.59	0.59
592	19.81	7.7	1.54	0.83	0.64
597	29.76	7.9	0.99	1.06	0.66
598	36.39	8.6	0.71	1.38	0.72
599	39.48	8.8	1.82	0.55	0.73

TABLE B-8. Variable Compression-Ratio Engine Data—
12-cSt Hydrocarbon Blend (Fuel 19)

Run Number	A/F	Injection Timing, deg.	Power, kW	Sp. Fuel Cons., kg/kW-h	τ_d TC, ms
1000 rpm					
559	20.67	10.6	1.24	0.58	1.76
560	30.19	10.2	0.69	0.79	1.70
567	40.78	11.7	1.92	0.52	1.95
558	20.67	8.4	1.24	0.58	1.40
561	29.68	6.6	0.77	0.71	1.10
566	40.78	7.8	2.26	0.45	1.30
557	20.30	5.2	1.98	0.43	0.87
550	24.70	4.9	1.28	0.57	0.81
562	29.68	5.2	0.94	0.58	0.86
565	40.68	5.3	0.85	0.60	0.88
564	43.16	5.7	2.61	0.72	0.95
2000 rpm					
571A	19.59	17.2	1.45	0.86	1.43
571B	30.16	20.3	--	12.79	1.69
577	40.39	21.7	2.73	0.69	1.81
570	19.95	11.9	1.48	0.83	0.99
572	30.50	12.8	0.43	2.24	1.07
576	40.39	14.0	3.16	0.60	1.17
569	20.37	7.2	1.73	0.71	0.60
573	30.66	8.6	0.71	1.35	0.72
575	40.39	8.9	0.46	1.98	0.74
574	42.94	9.5	2.06	0.48	0.79

**TABLE B-9. Variable Compression-Ratio Engine Data—
5-cSt Hydrocarbon Blend (Fuel 20)**

Run Number	A/F	Injection Timing, deg.	Power, kW	Sp. Fuel Cons., kg/kW-h	τ_d TC, ms
1000 rpm					
540	21.18	10.50	2.06	0.48	1.75
541	30.50	11.88	1.42	0.51	1.98
546	40.82	14.2	0.85	0.64	2.37
539	20.76	8.94	2.09	0.48	1.49
542	30.50	7.02	1.43	0.50	1.17
545	40.82	9.4	0.90	0.61	1.57
538	20.82	5.40	2.29	0.43	0.90
543	29.84	6.00	1.51	0.49	1.00
544	40.24	5.94	0.96	0.57	0.99
2000 rpm					
549	20.08	24.2	2.81	0.66	2.02
550	30.81	26.5	1.28	0.96	2.21
555	39.80	24.6	0.28	3.37	2.35
548	20.08	14.2	2.75	0.68	1.18
551	30.68	16.1	1.40	0.88	1.34
554	39.80	18.1	0.62	1.54	1.51
547	20.81	7.9	2.81	0.65	0.66
552	30.84	9.8	1.62	0.76	0.82
553	39.80	10.0	0.74	1.29	0.83

TABLE B-10. Variable Compression-Ratio Engine Data—Sunflower Oil (Fuel 22)

Run Number	A/F	Injection Timing, deg.	Power, kW	Sp. Fuel Cons., kg/kW-h	τ_d TC, ms
1000 rpm					
360	19.22	6.5	1.90	0.58	1.08
365	32.82	11.0	0.07	9.07	1.84
357	17.78	4.3	2.53	0.48	0.72
358	21.20	4.1	2.09	0.49	0.68
359	19.49	5.1	2.33	0.47	0.85
362	27.80	5.1	1.46	0.53	0.85
363	32.59	5.1	1.16	0.57	0.85
364	31.93	5.1	1.26	0.54	0.85
367	39.67	5.5	0.63	0.86	0.91
2000 rpm					
372	17.50	13.4	1.72	1.18	1.12
373	20.68	13.1	1.19	1.47	1.09
375	31.70	13.8	0.14	8.28	1.15
371	19.55	7.3	2.28	0.84	0.61
370	28.09	8.9	0.74	1.88	0.74
376	31.25	8.3	0.66	1.97	0.69
377	37.69	9.6	0.14	7.06	0.80

TABLE B-11. Variable Compression-Ratio Engine Data—Sunflower Ethylester (Fuel 23)

Run Number	A/F	Injection Timing, deg.	Power, kW	Sp. Fuel Cons., kg/kW-h	τ_d TC, ms
1000 rpm					
382	20.33	9.1	1.82	0.58	1.52
383	26.24	10.3	1.32	0.63	1.71
386	32.39	12.5	0.88	0.77	2.09
384	35.43	13.0	0.72	0.87	2.16
391	45.82	11.8	0.01	65.16	1.96
381	20.13	7.5	2.01	0.53	1.25
387	32.39	7.0	0.98	0.70	1.17
393	36.30	7.1	0.88	0.70	1.19
390	45.82	7.4	0.22	2.17	1.24
378	15.25	3.8	2.91	0.47	0.63
380	20.13	4.1	2.31	0.46	0.69
388	32.39	4.7	1.05	0.65	0.79
392	36.30	4.9	1.07	0.58	0.81
389	45.82	4.6	0.38	1.28	0.77
2000 rpm					
395	12.30	13.7	3.10	0.96	1.41
397	20.01	20.0	1.85	0.99	1.67
403	28.91	21.6	0.88	1.51	1.80
398	20.15	12.7	2.22	0.83	1.06
402	29.21	12.1	1.22	1.09	1.01
405	40.00	15.4	0.06	16.14	1.28
399	20.37	7.3	4.13	0.69	0.61
400	24.36	7.8	1.85	0.83	0.65
401	29.13	7.6	1.59	0.83	0.63
406	40.00	7.9	0.14	6.80	0.66

TABLE B-12. Variable Compression-Ratio Engine Data— AL-10583 JP-4 (Fuel 38)

Run Number	A/F	Injection Timing, deg.	Power, kW	Sp. Fuel Cons., kg/kW-h	τ_d TC, ms
1000 rpm					
412	20.35	10.4	1.93	0.54	1.73
413	26.98	11.8	1.51	0.54	1.96
415	32.20	13.0	1.08	0.63	2.17
420	42.69	14.8	0.75	0.70	2.46
411	19.96	8.0	1.98	0.52	1.33
416	32.20	8.4	1.11	0.62	1.40
419	42.69	9.3	0.80	0.66	1.55
407	14.80	8.2	2.39	0.57	1.36
410	20.11	5.7	2.17	0.47	0.95
417	31.90	5.9	1.49	0.46	0.99
418	40.90	5.3	0.91	0.60	0.89
2000 rpm					
424	20.54	21.6	2.78	0.66	1.80
430	31.74	25.0	1.40	0.87	2.08
431	41.26	26.8	0.14	6.58	2.23
425	20.68	13.1	2.95	0.62	1.09
429	31.90	14.4	1.59	0.77	1.20
432	41.49	17.5	0.40	2.36	1.46
426	20.87	6.7	3.33	0.54	0.56
427	25.80	8.2	2.39	0.62	0.68
428	31.34	9.7	1.73	0.71	0.81
433	41.70	9.5	0.51	1.81	0.79

TABLE B-13. Variable Compression-Ratio Engine Data— JP-7

Run Number	A/F	Injection Timing, deg.	Power, kW	Sp. Fuel Cons., kg/kW-h	τ_d TC, ms
1000 rpm					
516	21.26	11.8	2.30	0.44	1.97
515	22.00	12.1	2.20	0.44	2.01
518	28.89	13.8	1.69	0.45	2.30
519	29.96	13.7	1.66	0.44	2.28
526	40.63	14.0	1.05	0.53	2.34
514	21.70	8.9	2.34	0.41	1.49
517	20.96	7.4	2.37	0.43	1.24
520	29.96	7.7	1.70	0.43	1.29
525	40.63	9.2	1.05	0.53	1.53
511	17.60	6.1	2.86	0.41	1.01
512	20.97	5.3	2.67	0.38	0.88
521	29.96	5.0	1.87	0.40	0.83
524	39.47	5.9	1.22	0.46	0.99
522	46.19	6.1	0.84	0.40	1.01
2000 rpm					
529	19.97	23.6	2.89	0.65	1.97
530	29.40	23.9	1.87	0.69	1.99
537	39.46	26.3	0.85	1.16	2.19
528	20.29	14.4	3.49	0.54	1.20
531	31.26	16.0	1.99	0.62	1.34
530	39.77	16.1	0.85	1.16	1.34
527	20.81	7.4	3.61	0.51	0.62
532	31.33	9.5	2.04	0.60	0.79
535	39.35	10.0	0.94	1.07	0.83
533	44.84	9.7	0.43	2.03	0.81

TABLE B-14. Variable Compression-Ratio Engine Data—
AL-14216 JP-8 (Fuel 39)

Run Number	A/F	Injection Timing, deg.	Power, kW	Sp. Fuel Cons., kg/kW-h	τ_d TC, ms
1000 rpm					
438	20.60	17.2	2.13	0.49	2.86
440	30.20	14.4	1.46	0.49	2.74
445	43.80	19.4	0.75	0.68	3.23
437	20.41	10.7	2.29	0.45	1.78
441	30.20	11.2	1.62	0.44	1.87
444	43.80	11.9	0.87	0.59	1.98
436	20.60	6.1	2.66	0.39	1.01
434	24.90	6.4	2.19	0.40	1.07
442	30.20	7.0	1.82	0.40	1.17
443	40.71	6.7	0.98	0.55	1.12
2000 rpm					
450	19.82	30.6	3.27	0.58	2.55
454	30.50	36.4	1.76	0.72	3.03
449	19.69	17.3	3.80	0.50	1.44
453	30.50	21.6	2.10	0.60	1.80
458	40.31	21.7	0.80	1.21	1.81
447	19.56	8.6	3.52	0.56	0.72
451	19.79	8.9	3.55	0.54	0.74
446	20.87	9.2	3.24	0.58	0.77
452	30.42	10.7	2.13	0.60	0.89
455	35.20	11.4	1.51	0.74	0.95
456	41.82	12.1	0.80	1.18	1.01

TABLE B-15. Variable Compression-Ratio Engine Data—AL-10999 Type I Referee Fuel (Fuel 41)

Run Number	A/F	Injection Timing, deg.	Power, kW	Sp. Fuel Cons., kg/kW-h	τ_d TC, ms
1000 rpm					
464	20.55	28.0	2.31	0.45	4.66
466	29.84	32.6	1.51	0.48	5.44
463	20.55	15.5	2.33	0.44	2.58
467	29.84	17.2	1.56	0.47	2.86
471	40.06	17.8	0.88	0.63	2.97
462	20.59	7.8	2.59	0.40	1.30
460	24.25	8.2	2.31	0.39	1.37
468	30.12	9.2	1.73	0.42	1.54
470	40.06	9.7	0.95	0.58	1.62
2000 rpm					
475	20.70	30.3	3.83	0.49	2.52
477	30.34	35.8	2.16	0.60	2.98
474	20.91	14.3	4.12	0.45	1.19
478	31.25	17.0	2.61	0.48	1.42
482	41.00	20.0	0.99	0.96	1.67
480	46.49	19.8	0.74	1.14	1.65

TABLE B-16. Variable Compression-Ratio Engine Data—
AL-14751 Type II Referee Fuel (Fuel 42)

Run Number	A/F	Injection Timing, deg.	Power, kW	Sp. Fuel Cons., kg/kW-h	τ_d TC, ms
1000 rpm					
486	20.62	20.5	2.03	0.51	3.41
487	26.93	19.3	1.54	0.53	3.21
488	30.80	19.5	1.29	0.55	3.25
485	20.62	9.7	2.33	0.44	1.62
489	30.00	11.0	1.60	0.46	1.83
495	40.63	12.8	0.88	0.63	2.13
484	20.12	6.5	2.42	0.43	1.08
490	29.35	6.2	1.72	0.44	1.04
494	40.63	6.7	0.96	0.57	1.11
492	45.52	7.8	0.71	0.69	1.30
2000 rpm					
503	20.10	45.6	--	--	4.09
502	19.70	19.9	3.52	0.54	1.66
505	29.39	24.4	2.10	0.61	2.03
510	40.00	31.6	4.04	0.58	2.74
498	16.50	8.9	3.07	0.63	0.74
501	19.97	8.9	1.87	0.69	0.74
506	29.79	10.1	1.20	0.90	0.84
507	35.80	10.4	0.63	1.53	0.87
509	40.03	11.6	0.51	1.71	0.97
508	43.01	12.0	--	--	1.00

APPENDIX C

TEST FUEL IGNITION DELAY DATA COMPARED TO THE CORRESPONDING REFERENCE FUEL DATA
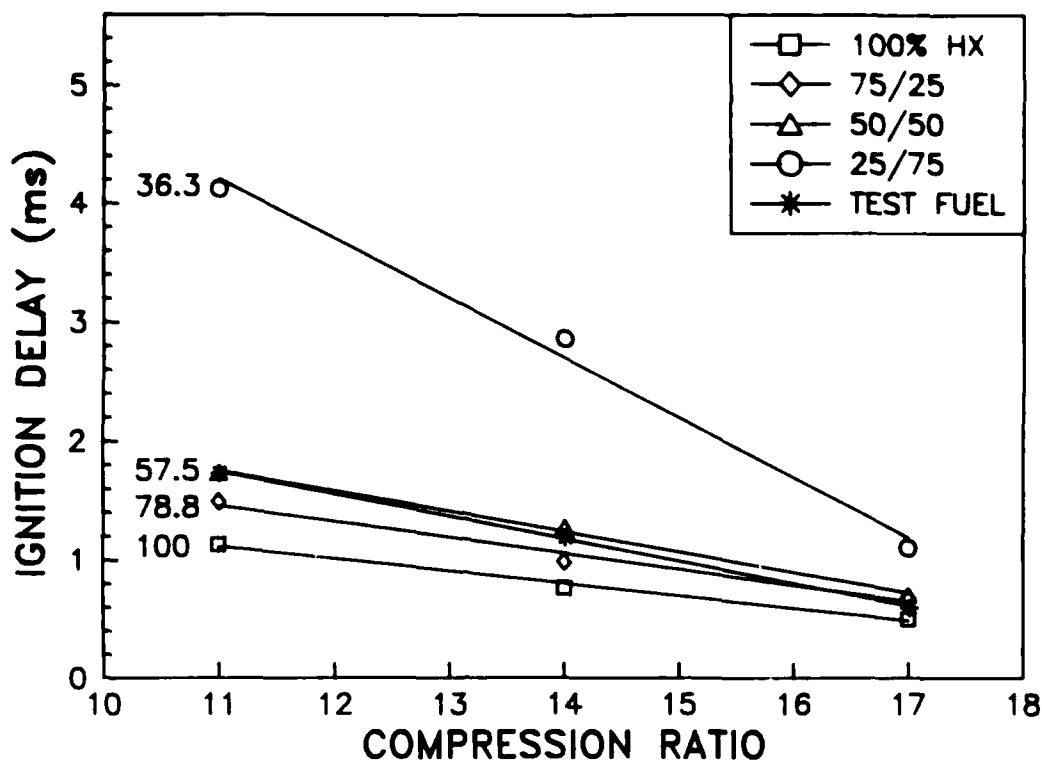
Figure C-1. Normal octane at 1000 rpm, A/F=20
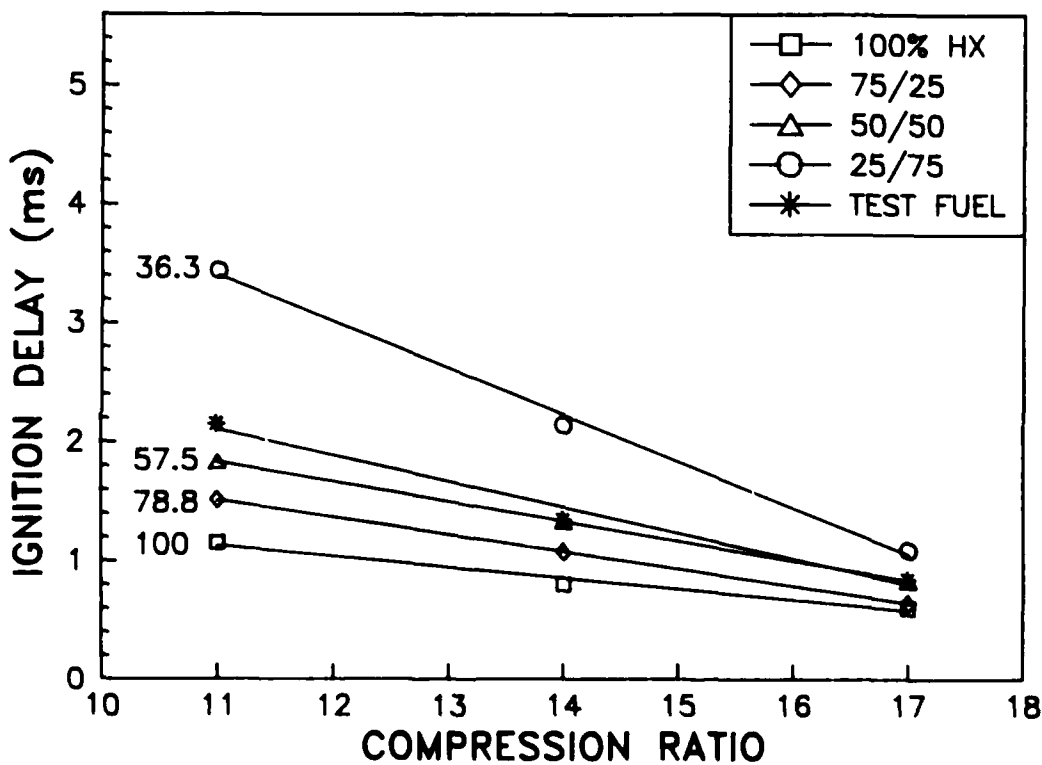
Figure C-2. Normal octane at 1000 rpm, A/F=30
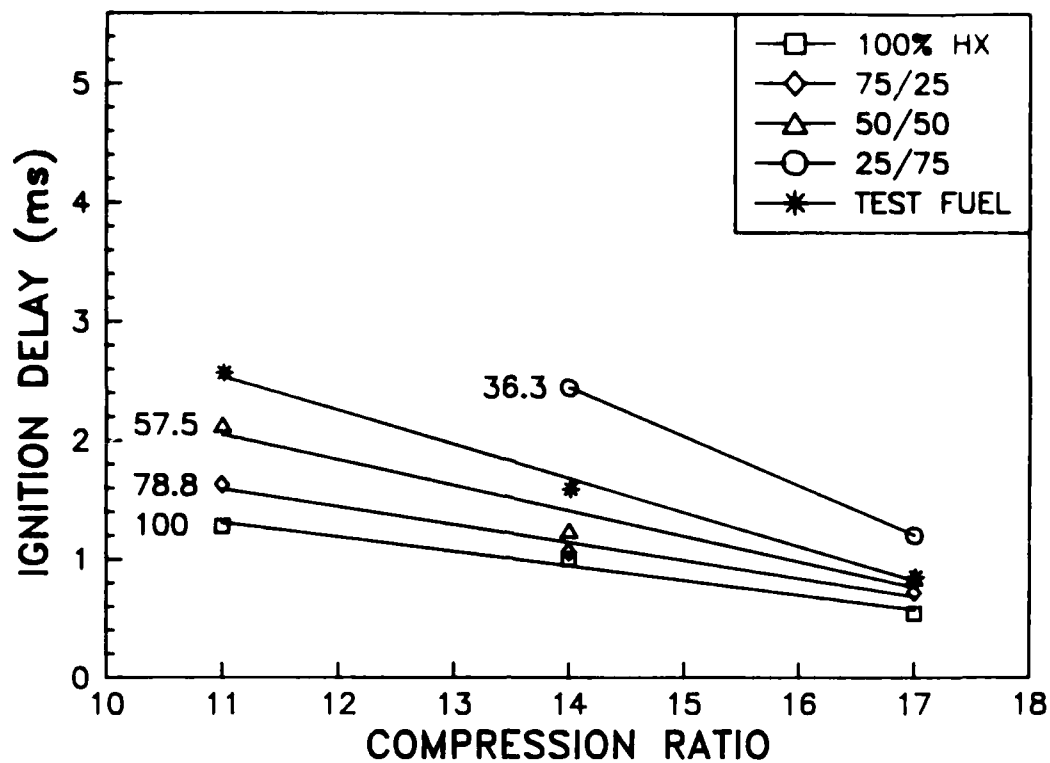
Figure C-3. Normal octane at 1000 rpm, A/F=40
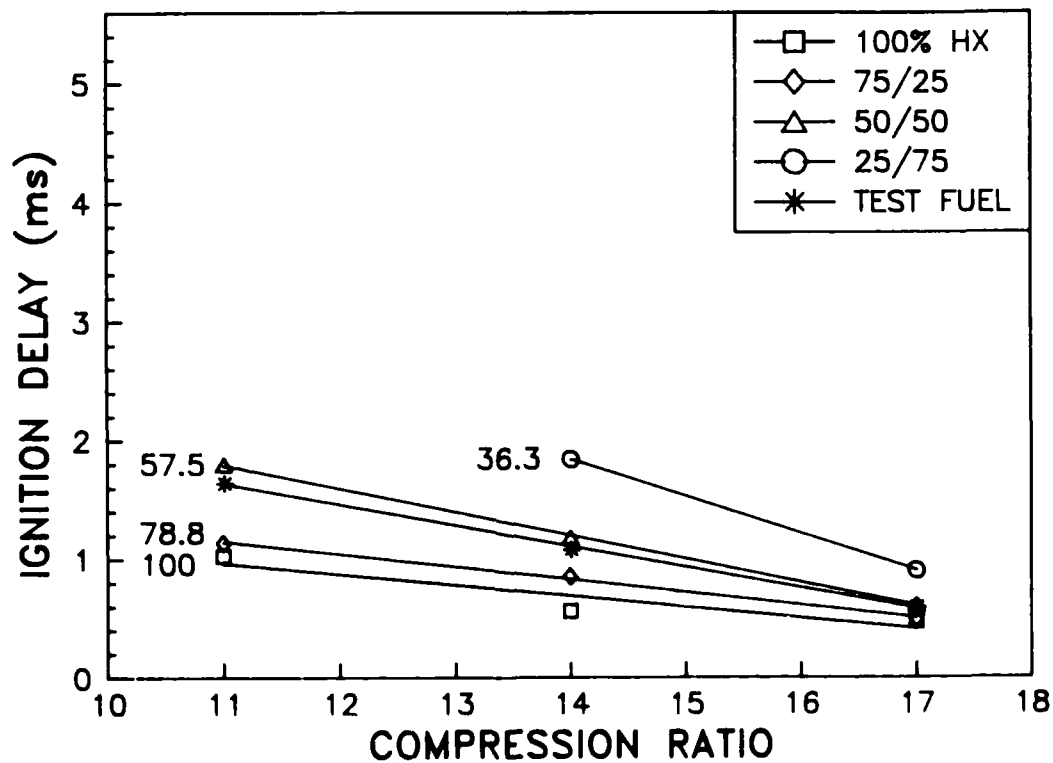
Figure C-4. Normal octane at 2000 rpm, A/F=20
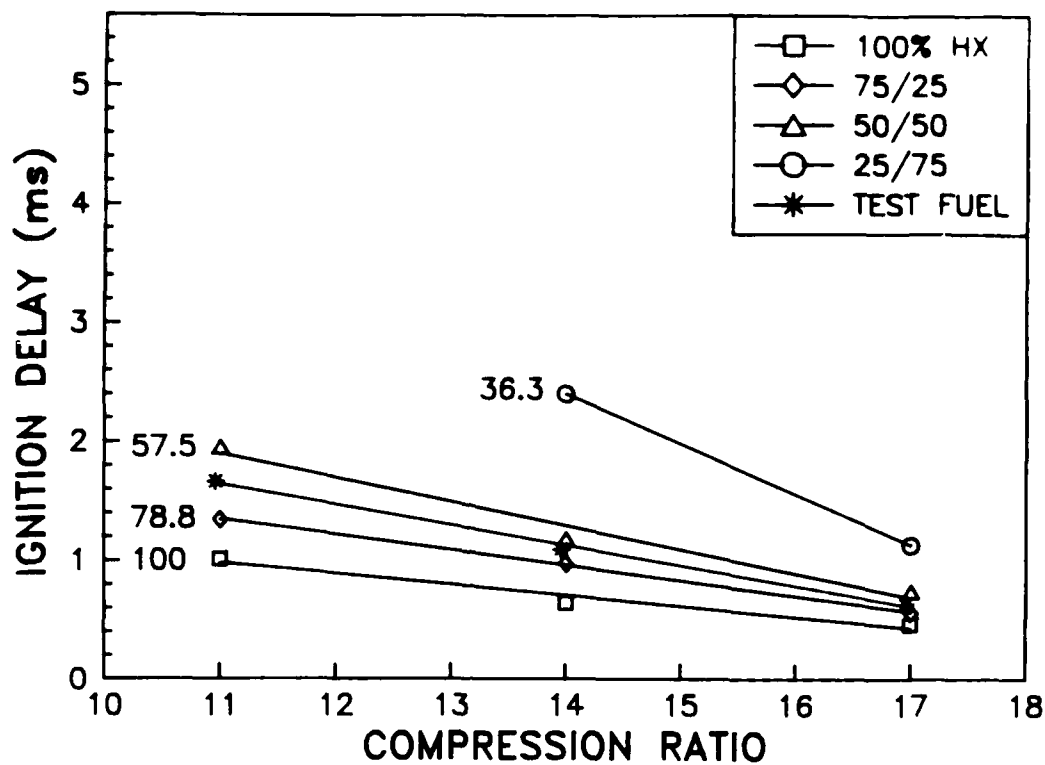
Figure C-5. Normal octane at 2000 rpm, A/F=30
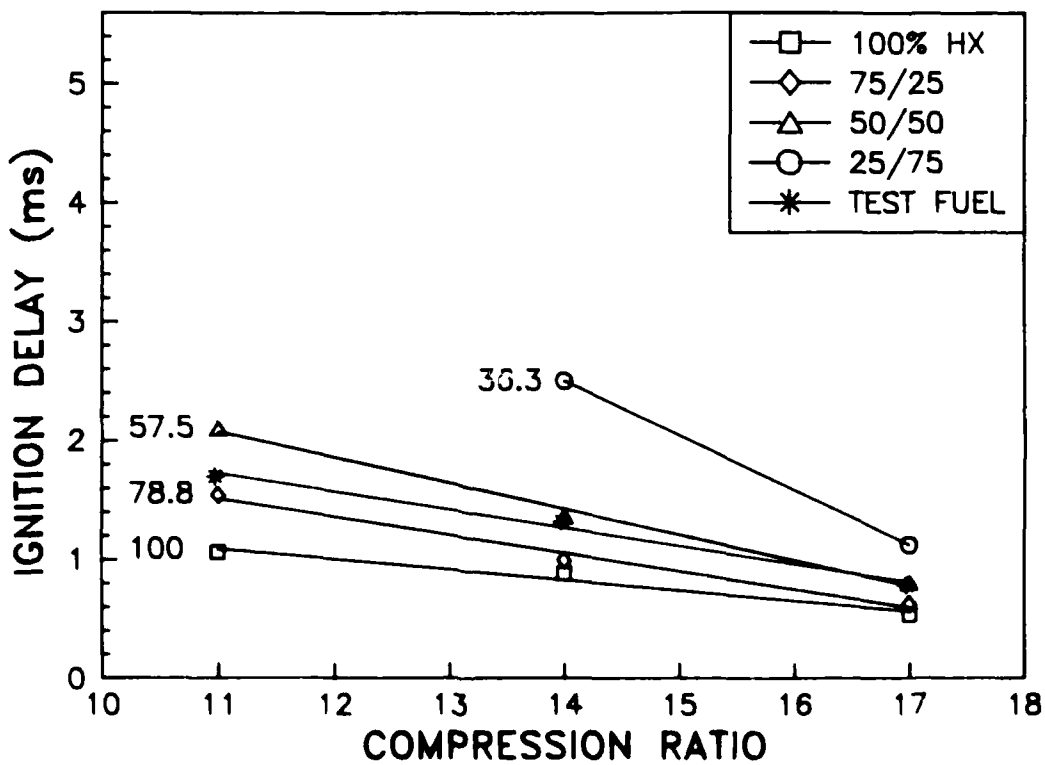
Figure C-6. Normal octane at 2000 rpm, A/F=40

93
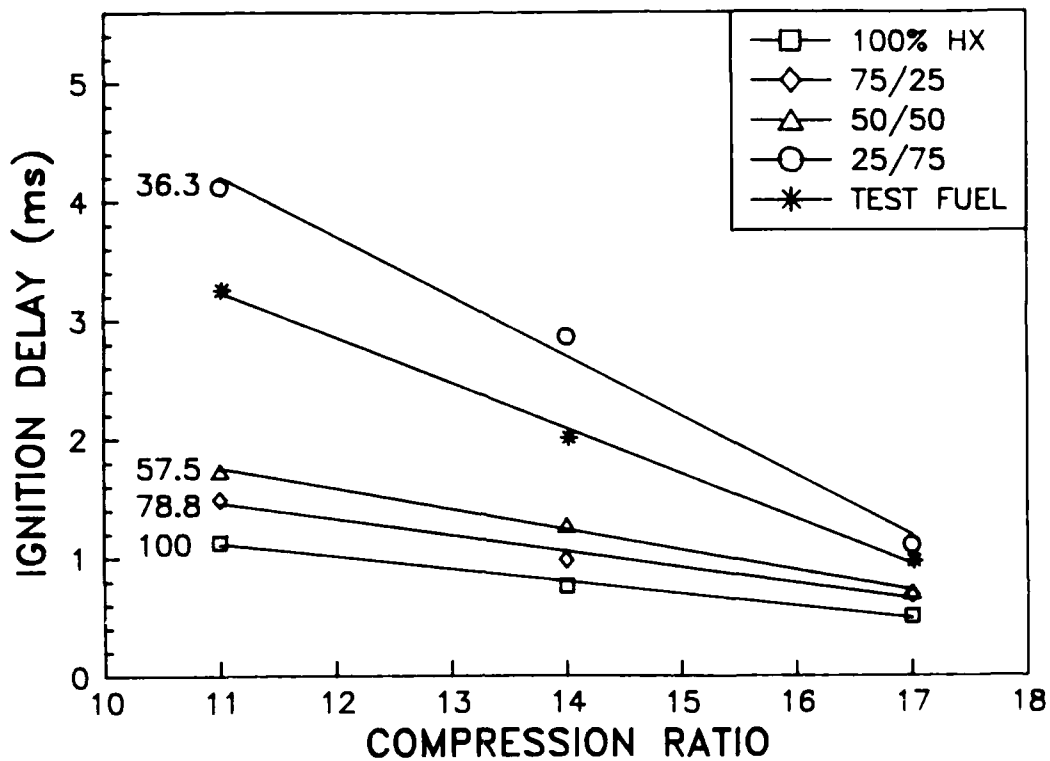
Figure C-7. **Normal hexane at 1000 rpm, A/F=20**
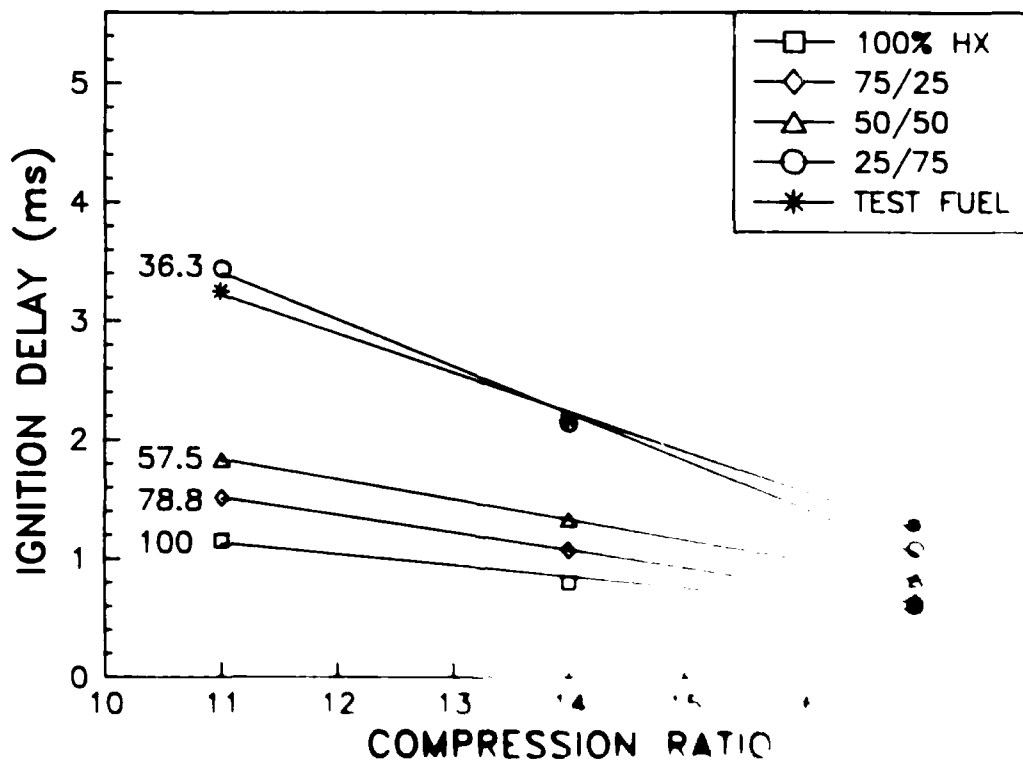
Figure C-8. **Normal hexane at 1000 rpm, A/F 30**
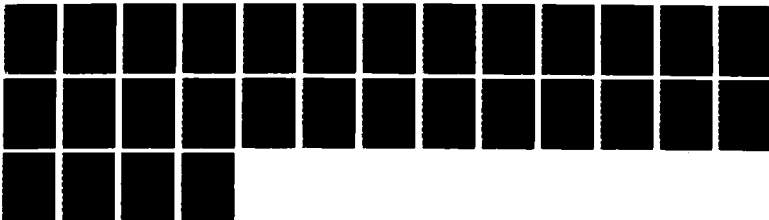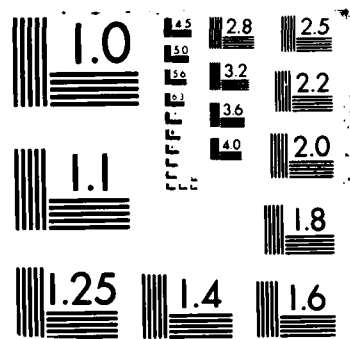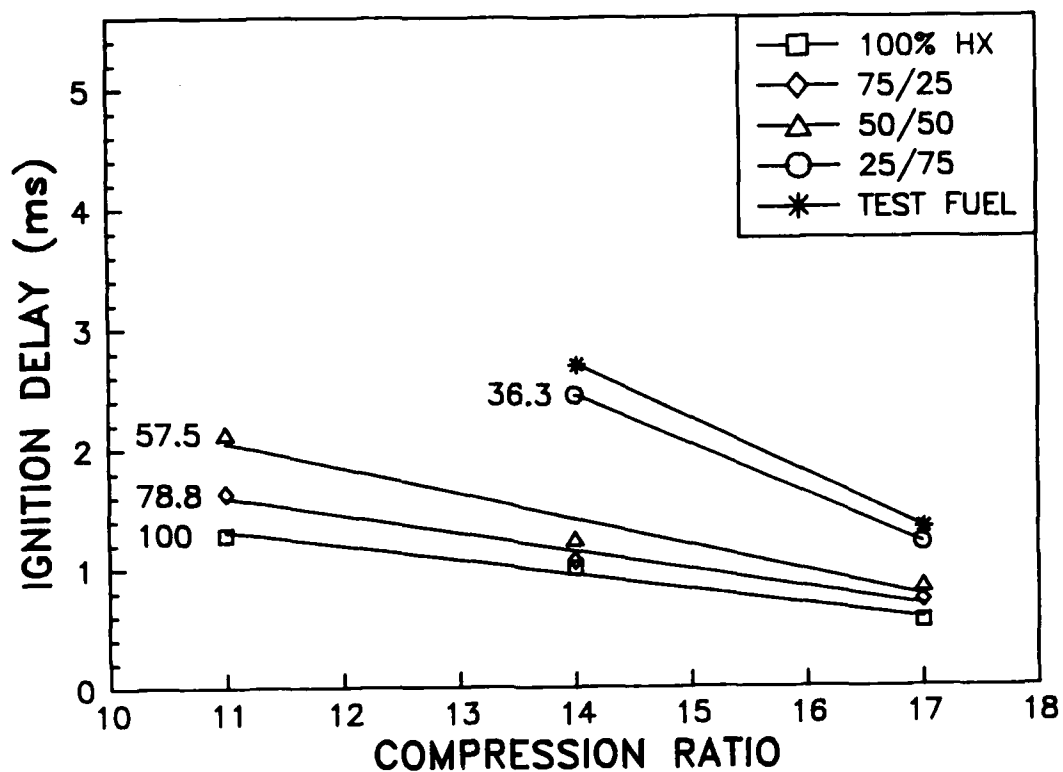
Figure C-9. **Normal hexane at 1000 rpm, A/F=40**
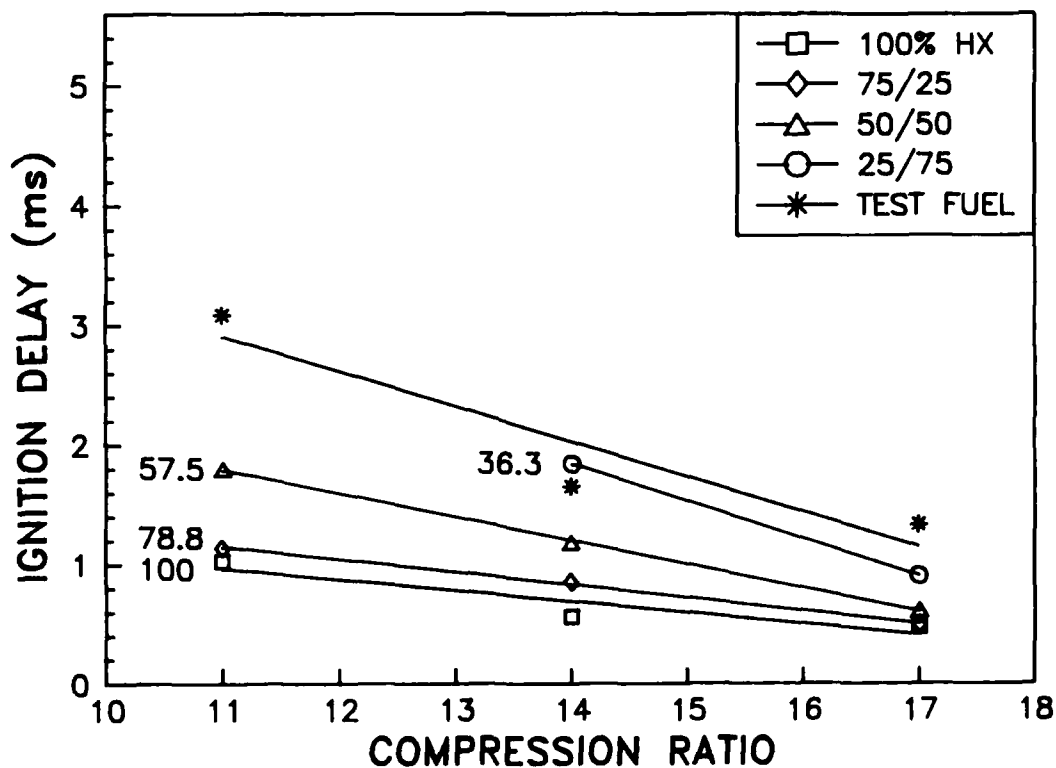
Figure C-10. **Normal hexane at 2000 rpm, A/F=20**

95
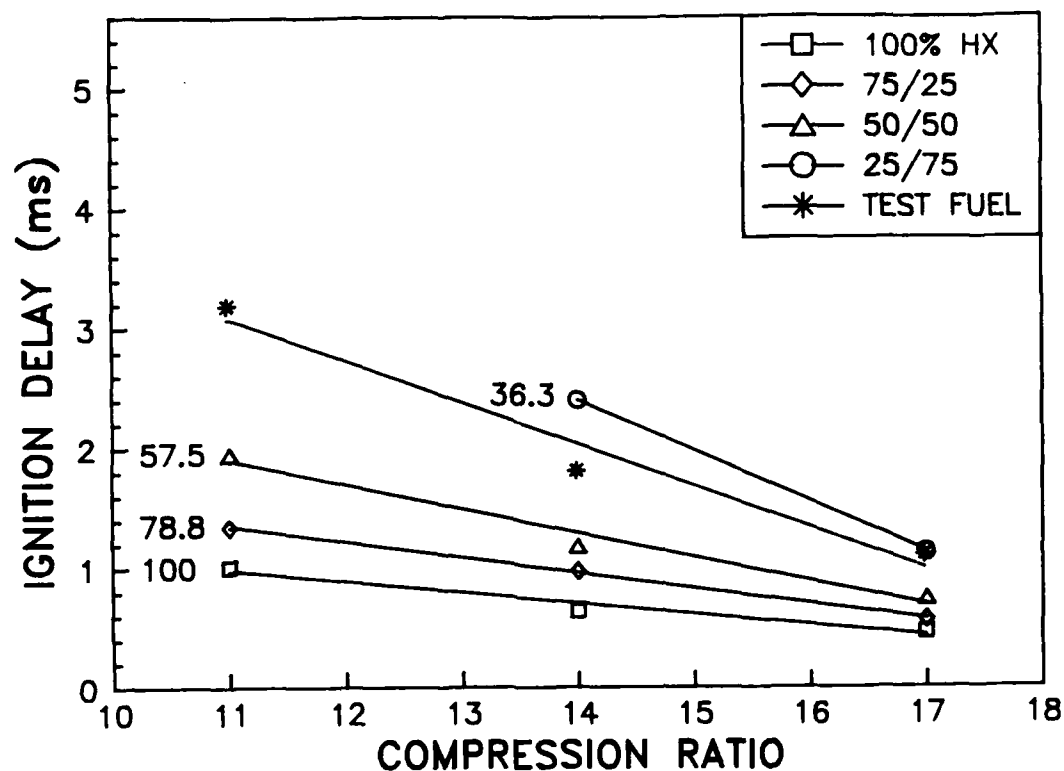
Figure C-11. **Normal hexane at 2000 rpm, A/F=30**
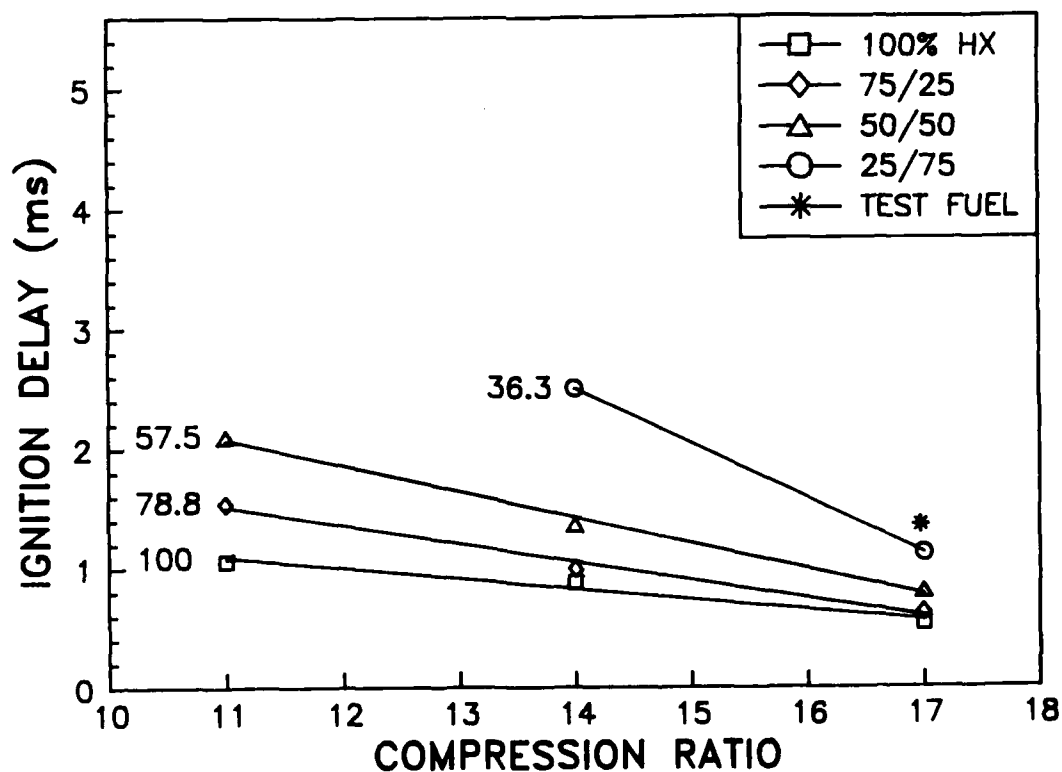
Figure C-12. **Normal hexane at 2000 rpm, A/F=40**
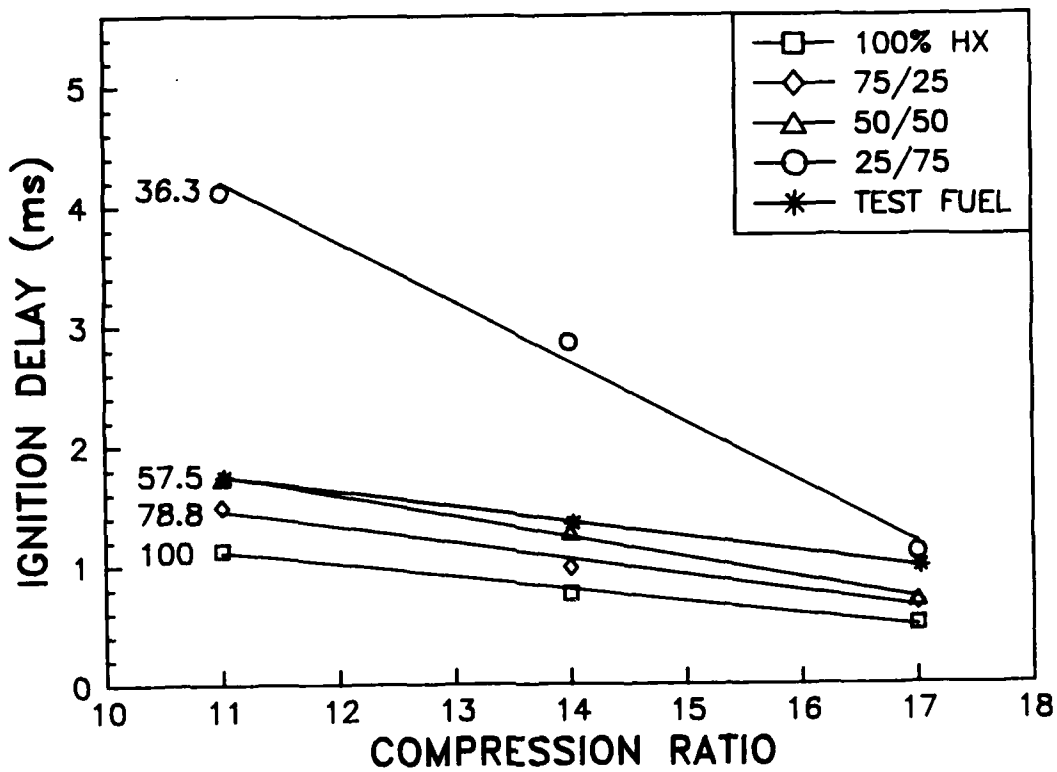
Figure C-13. JP-4 at 1000 rpm, A/F=20
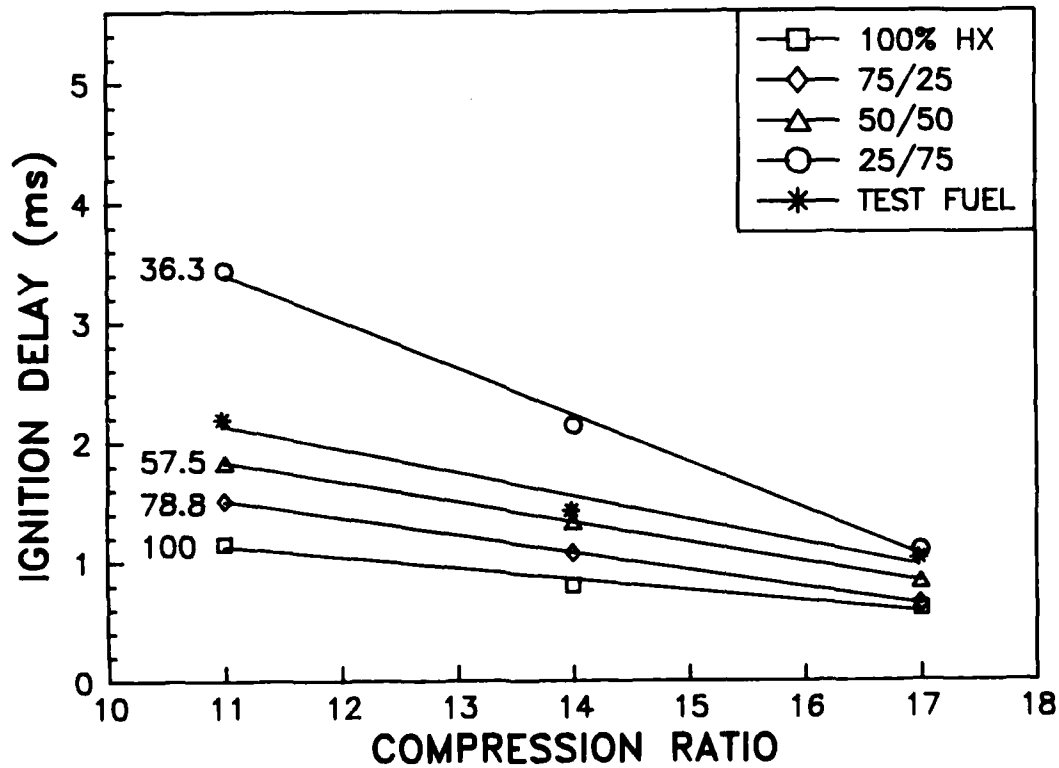
Figure C-14. JP-4 at 1000 rpm, A/F=30

97
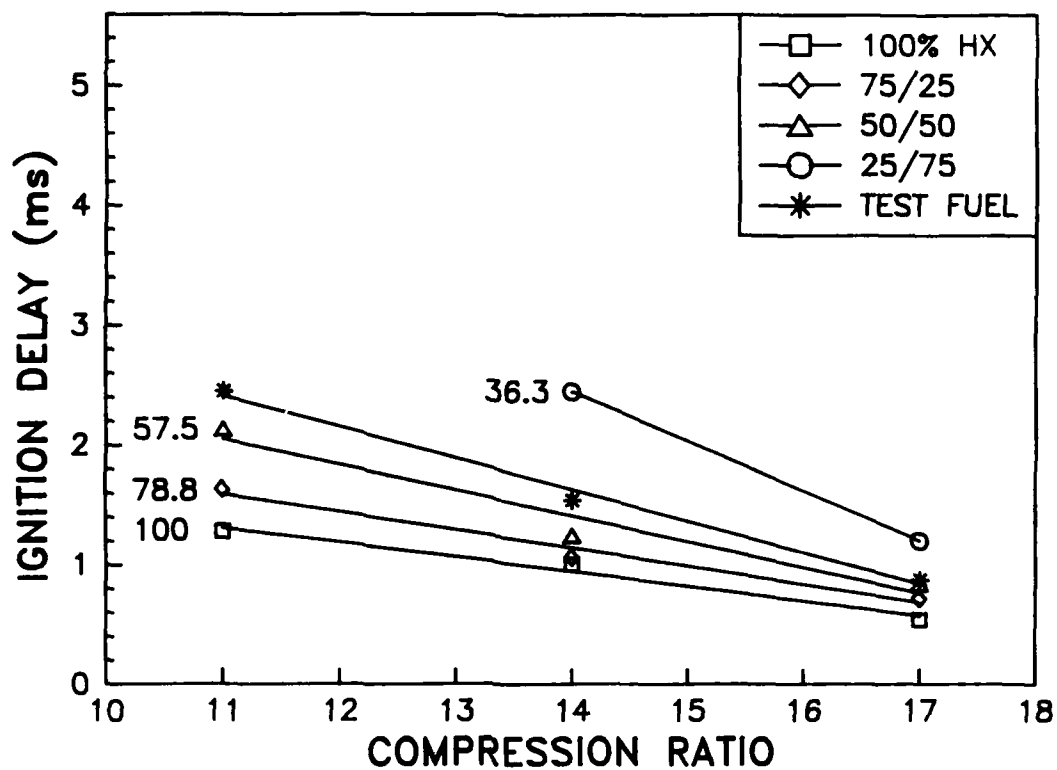
Figure C-15. JP-4 at 1000 rpm, A/F=40
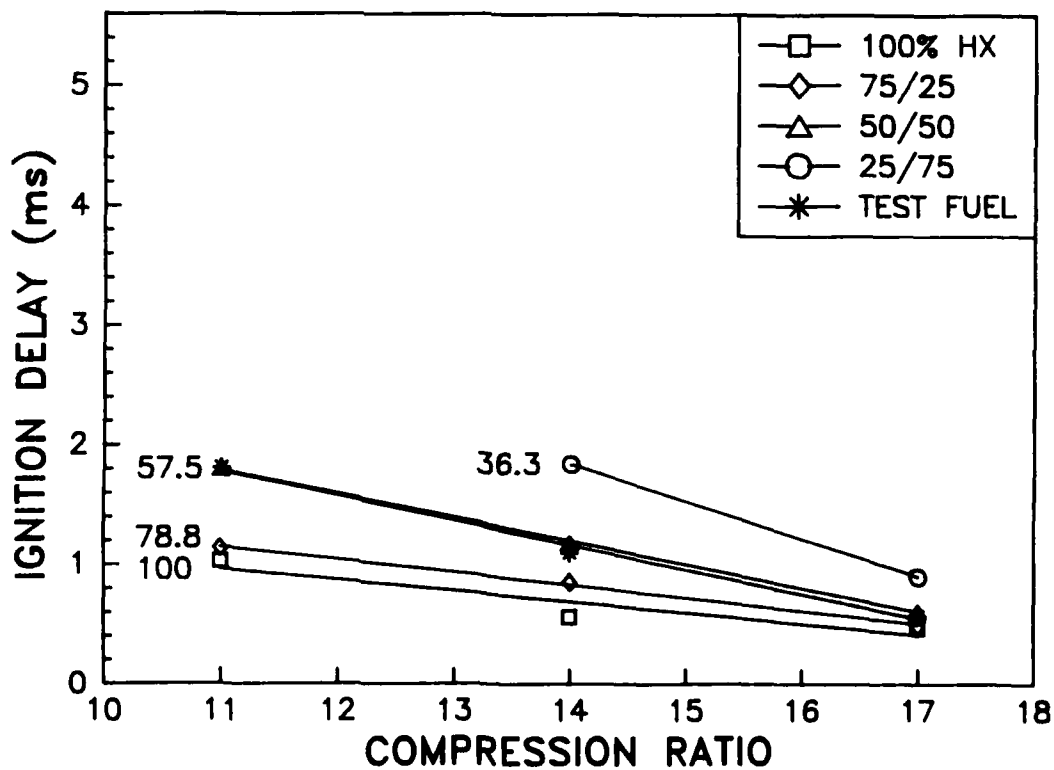
Figure C-16. JP-4 at 2000 rpm, A/F=20

98
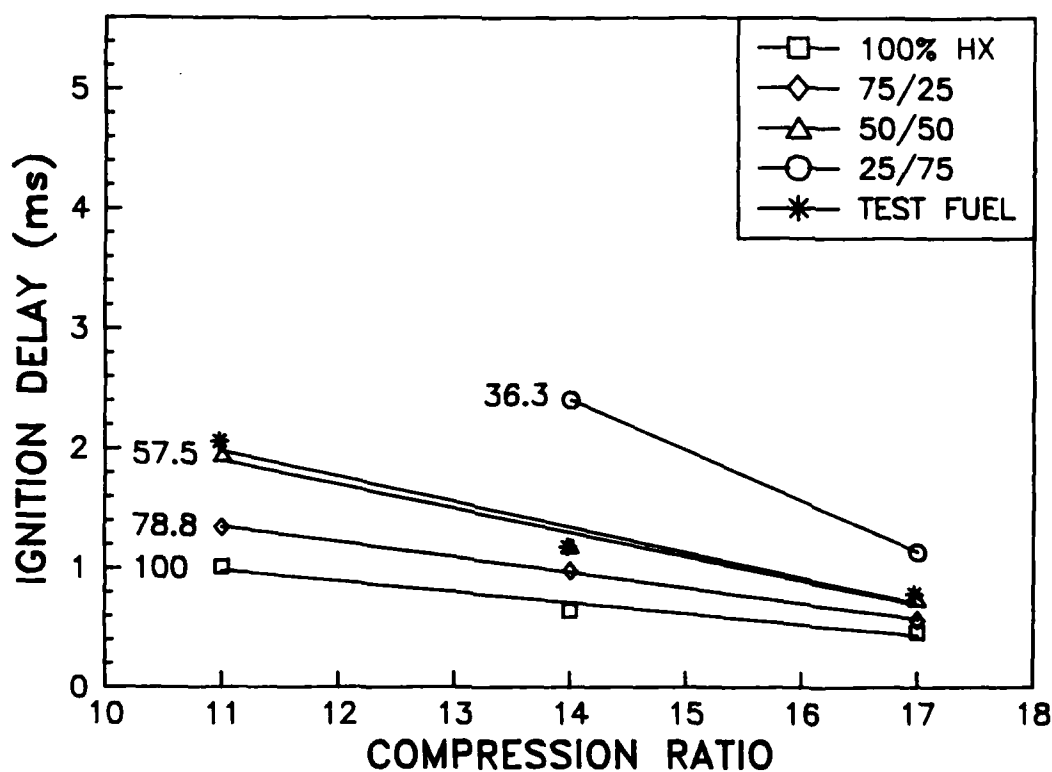
Figure C-17. **JP-4 at 2000 rpm, A/F=30**
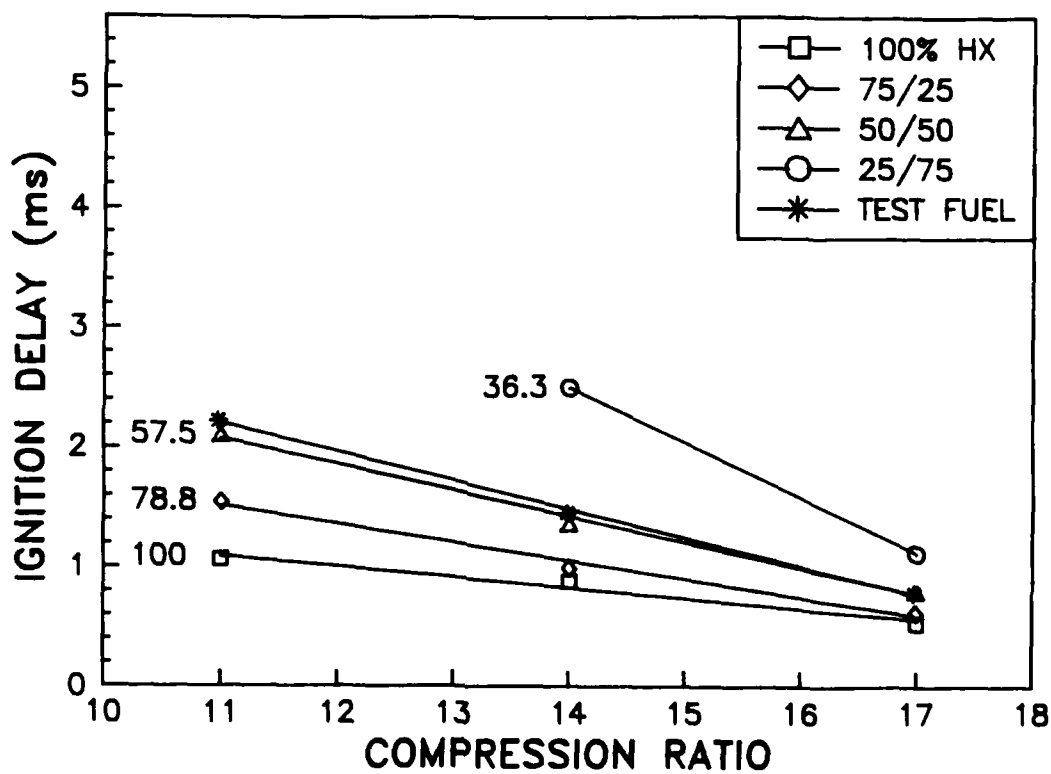
Figure C-18. **JP-4 at 2000 rpm, A/F=40**

99
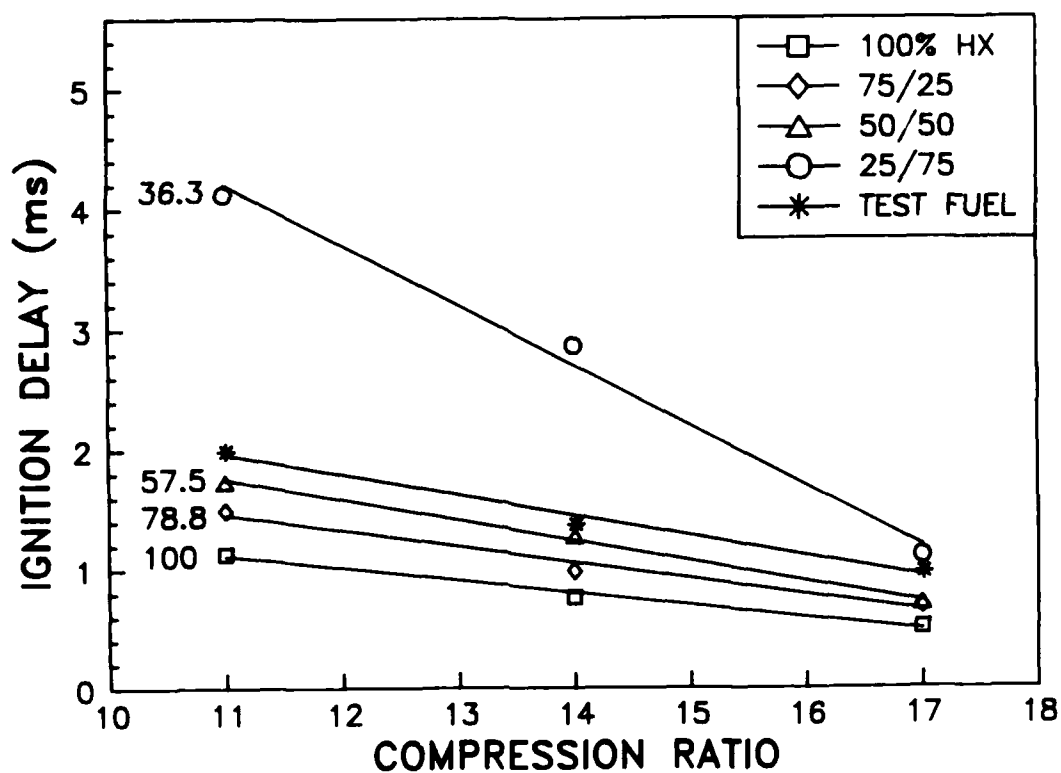
Figure C-19. <u>JP-7 at 1000 rpm, A/F=20</u>
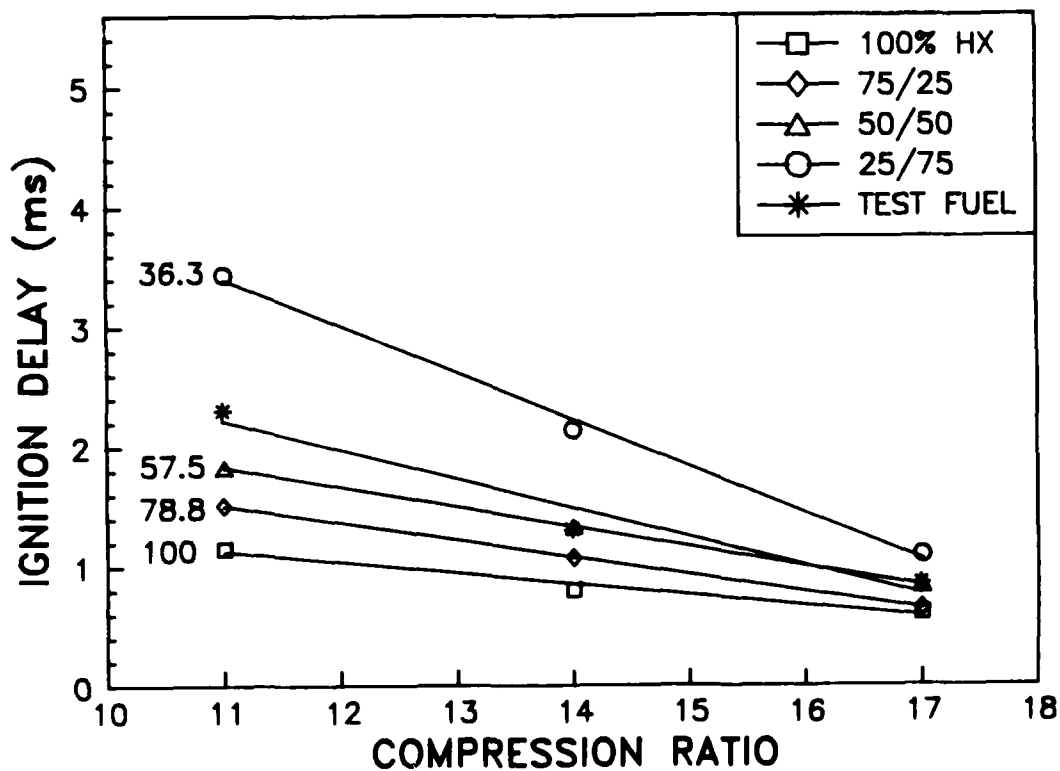
Figure C-20. <u>JP-7 at 1000 rpm, A/F=30</u>

100
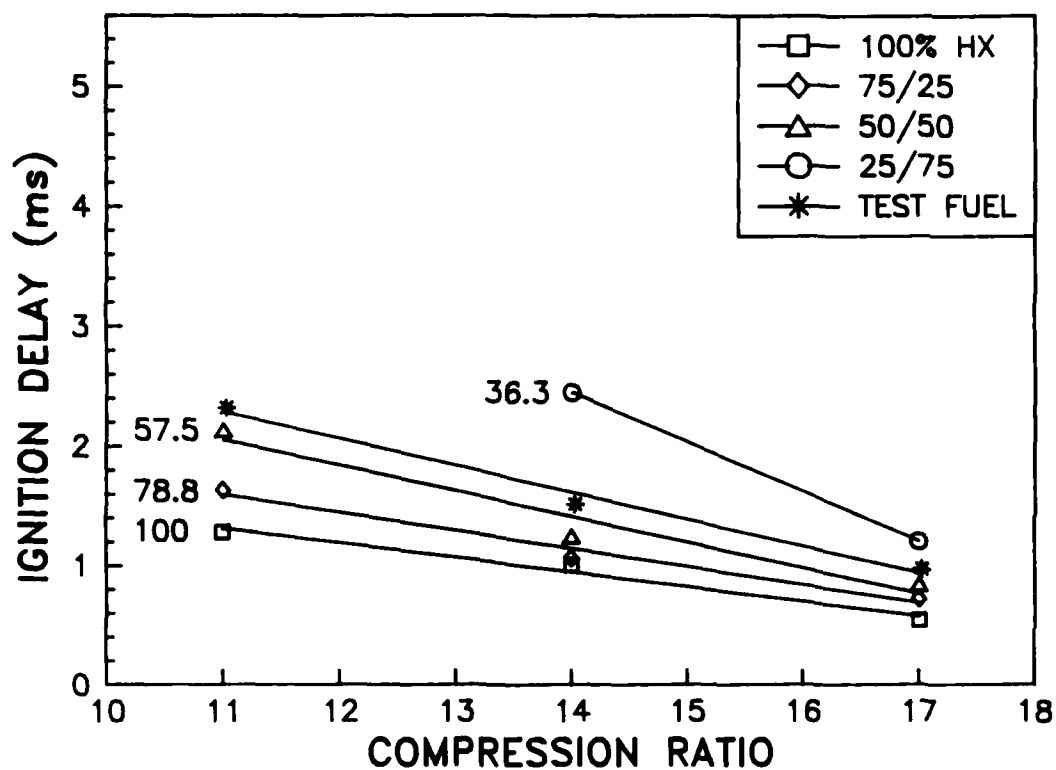
Figure C-21. JP-7 at 1000 rpm, A/F=40
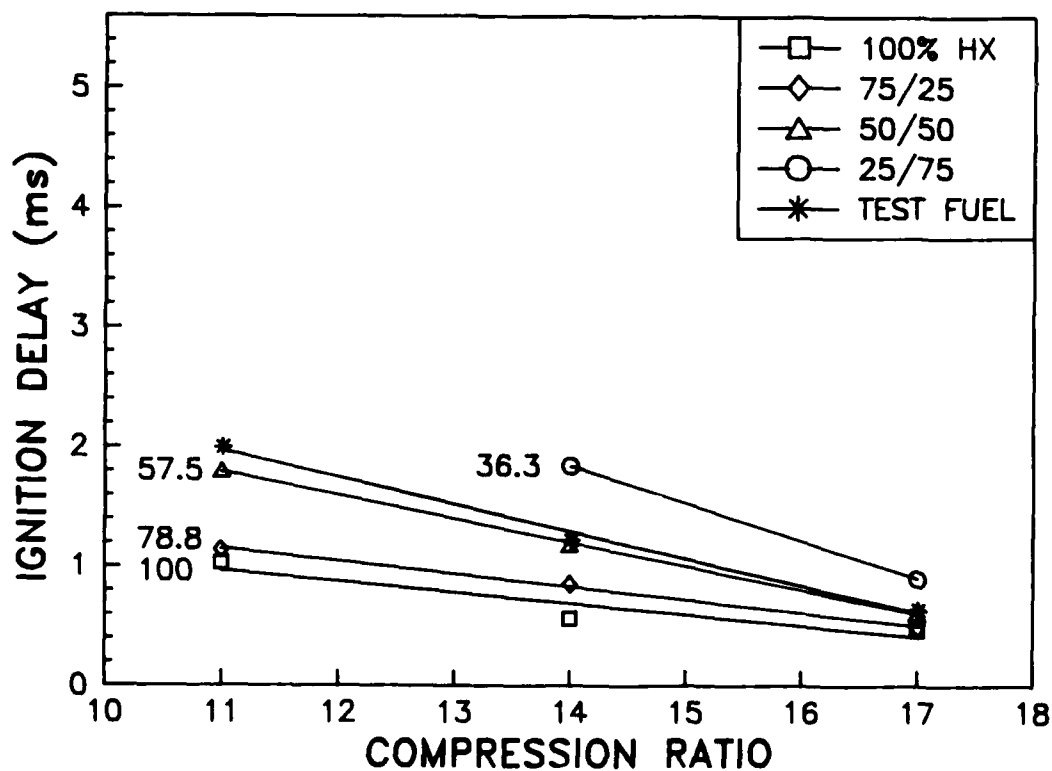
Figure C-22. JP-7 at 2000 rpm, A/F=20

101
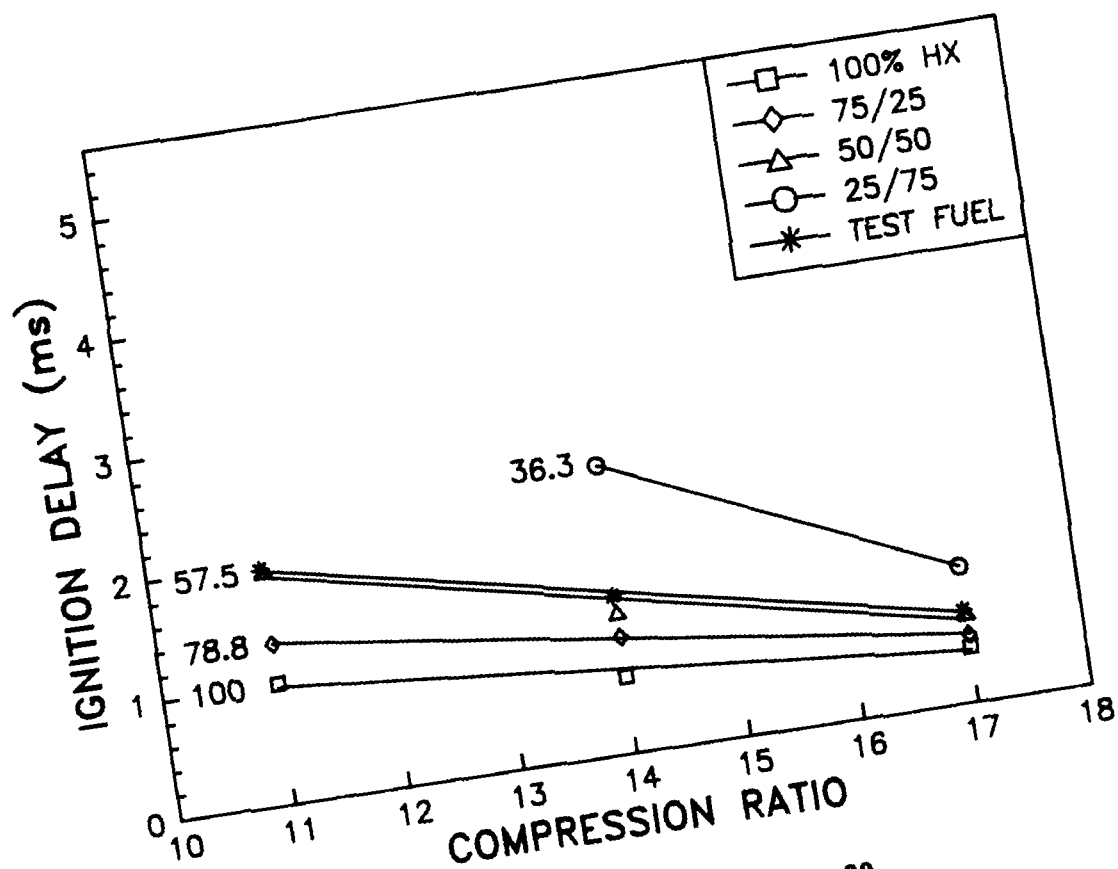
Figure C-23. JP-7 at 2000 rpm, A/F=30
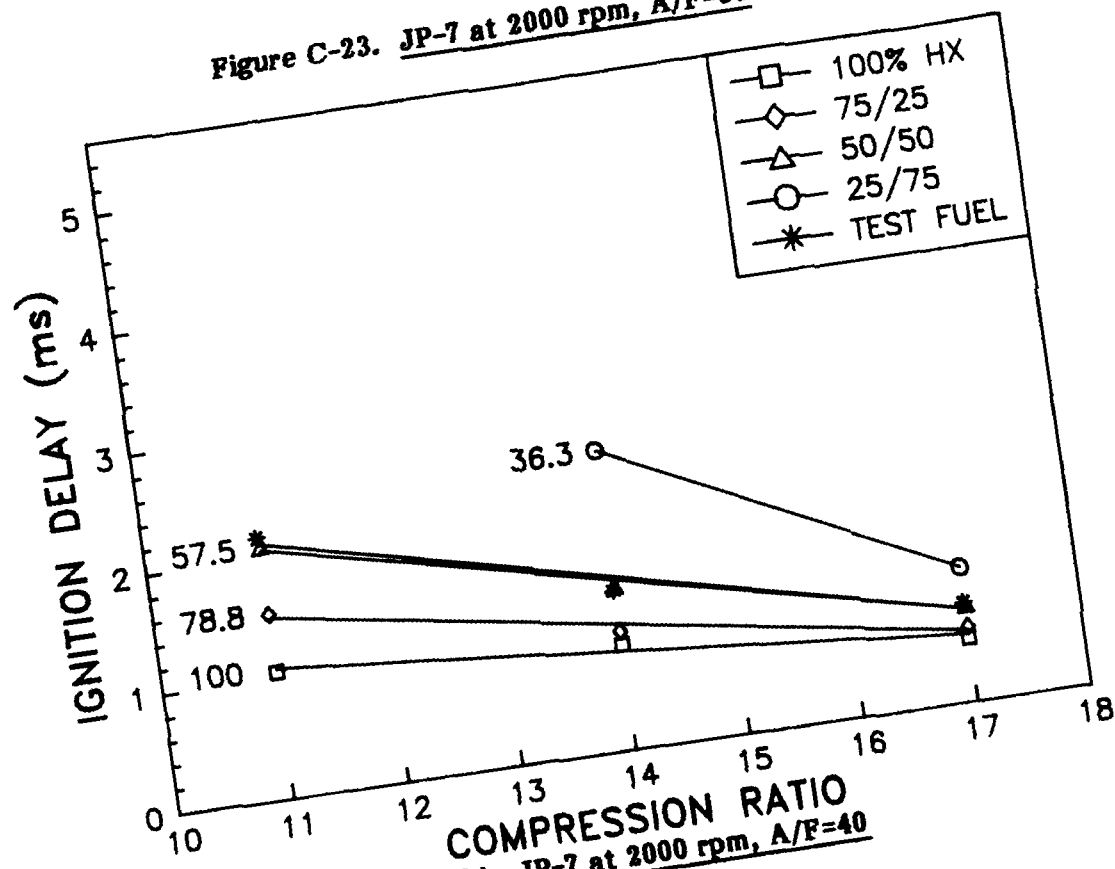
Figure C-24. JP-7 at 2000 rpm, A/F=40

102
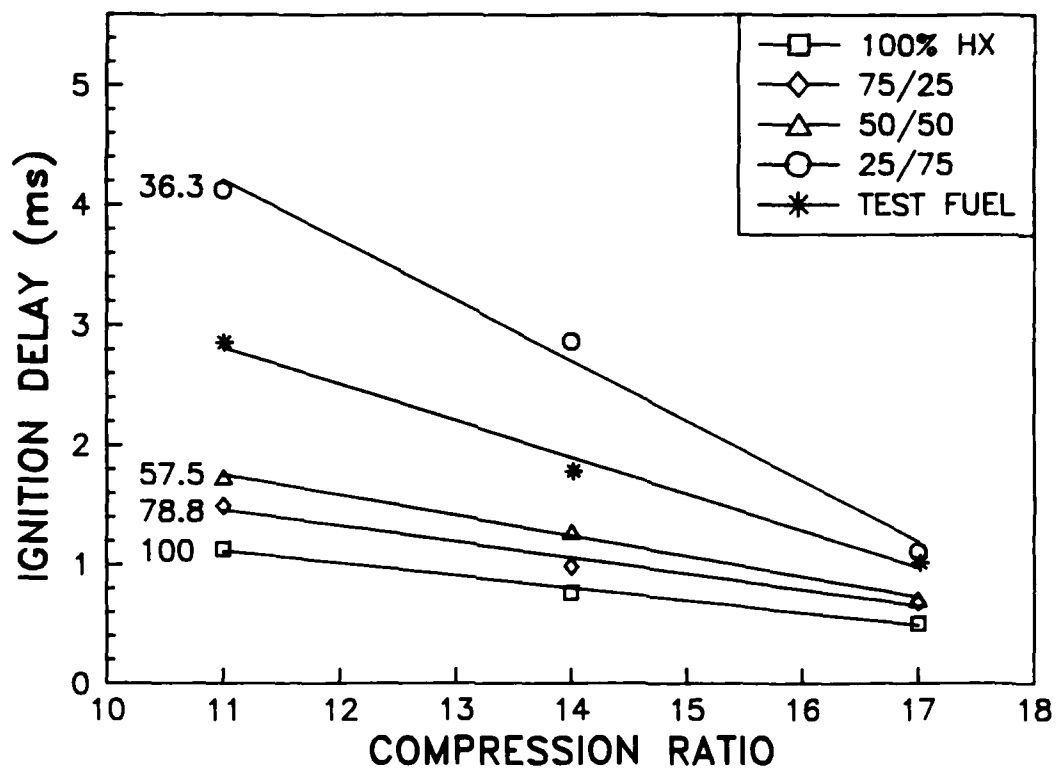
Figure C-25. <u>JP-8 at 1000 rpm, A/F=20</u>
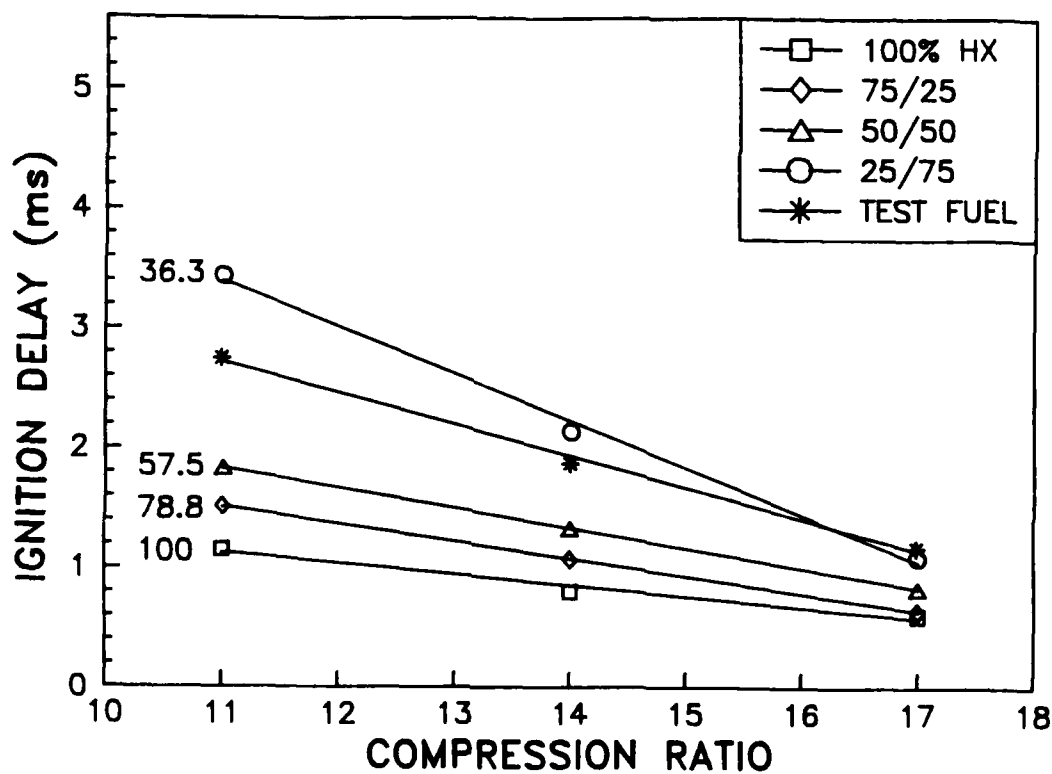
Figure C-26. <u>JP-8 at 1000 rpm, A/F=30</u>

103
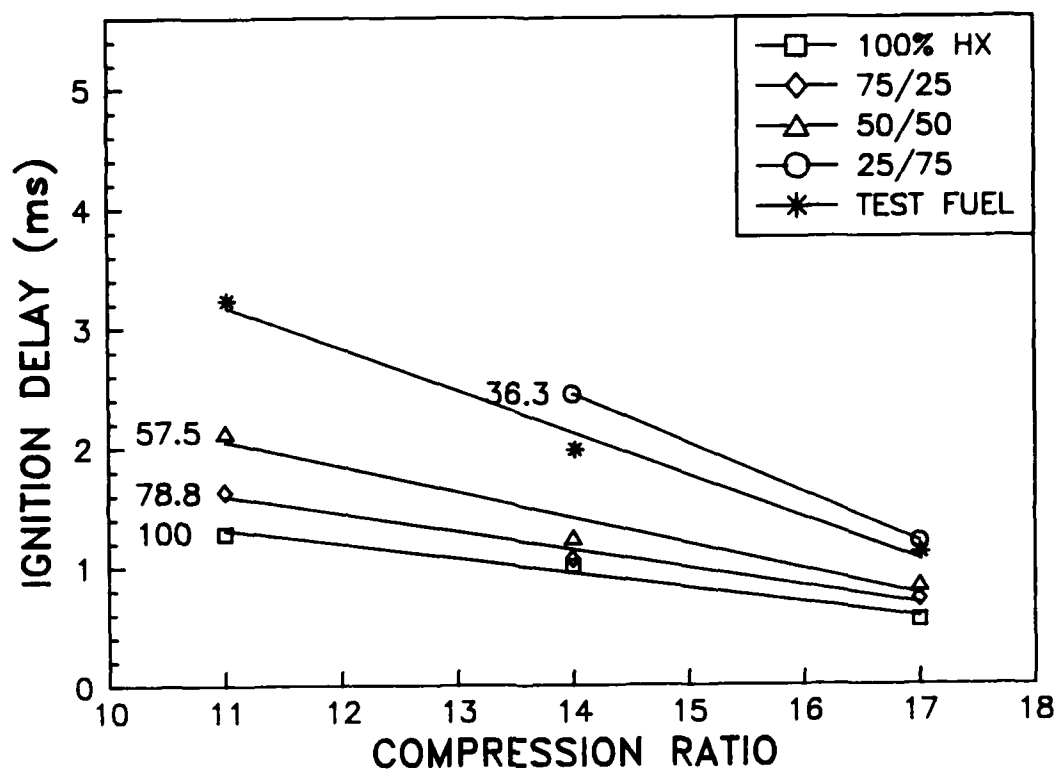
Figure C-27. JP-8 at 1000 rpm, A/F=40
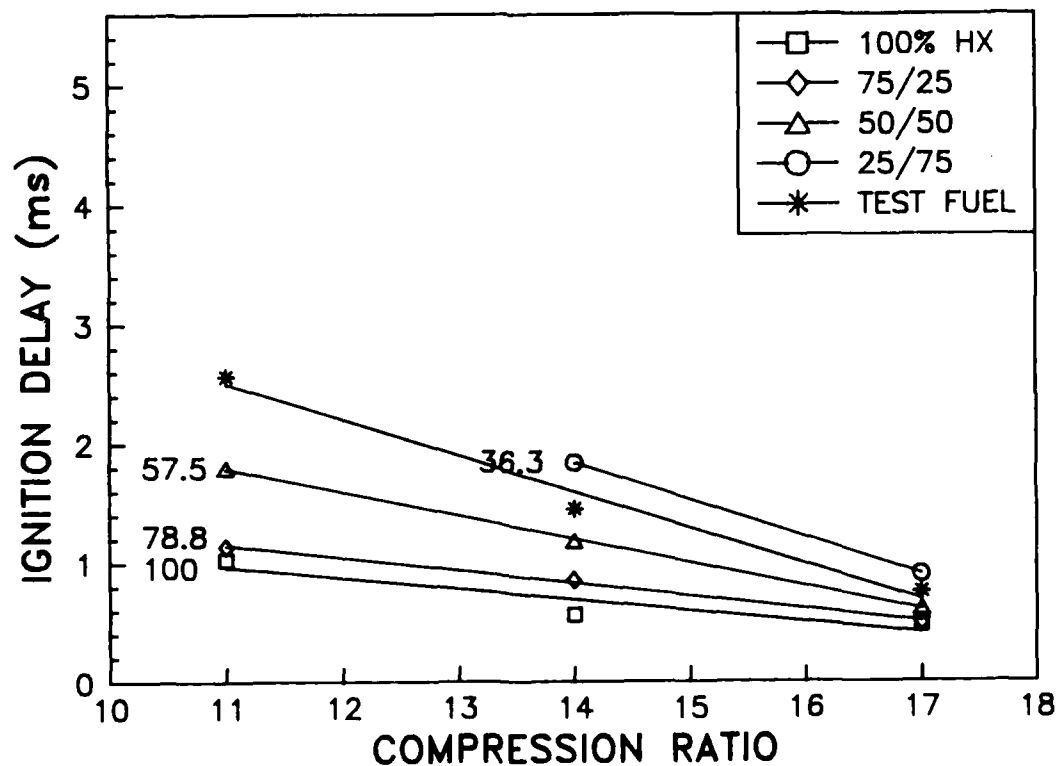
Figure C-28. JP-8 at 2000 rpm, A/F=20
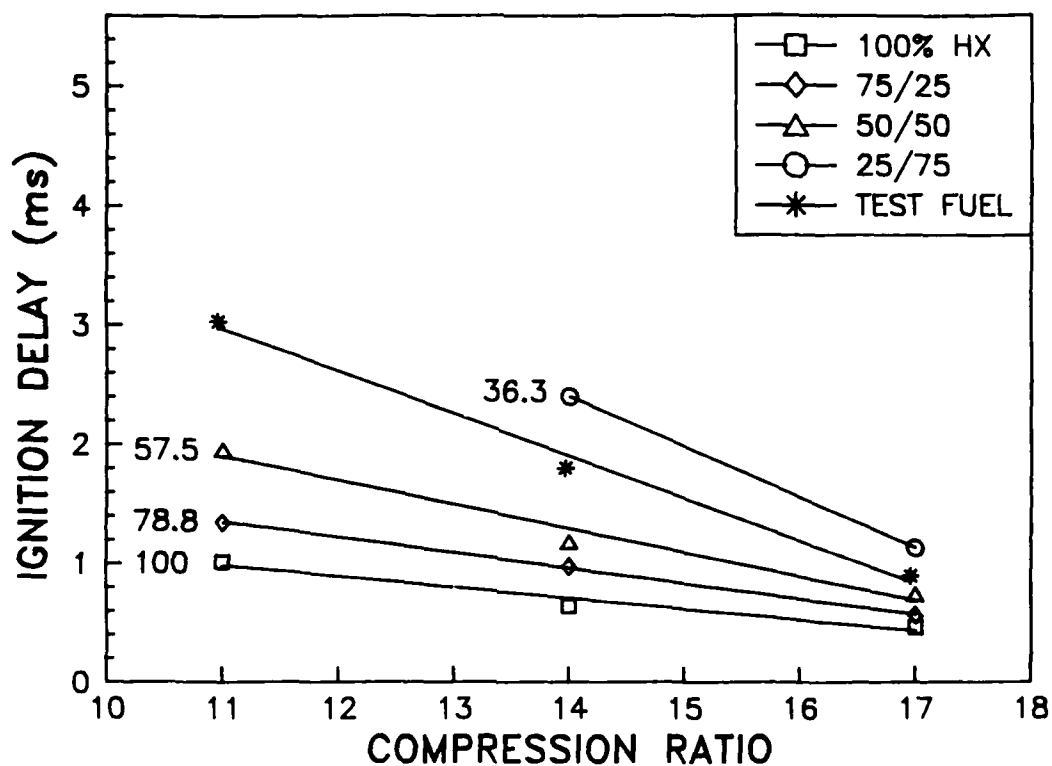
Figure C-29. **JP-8 at 2000 rpm, A/F=30**
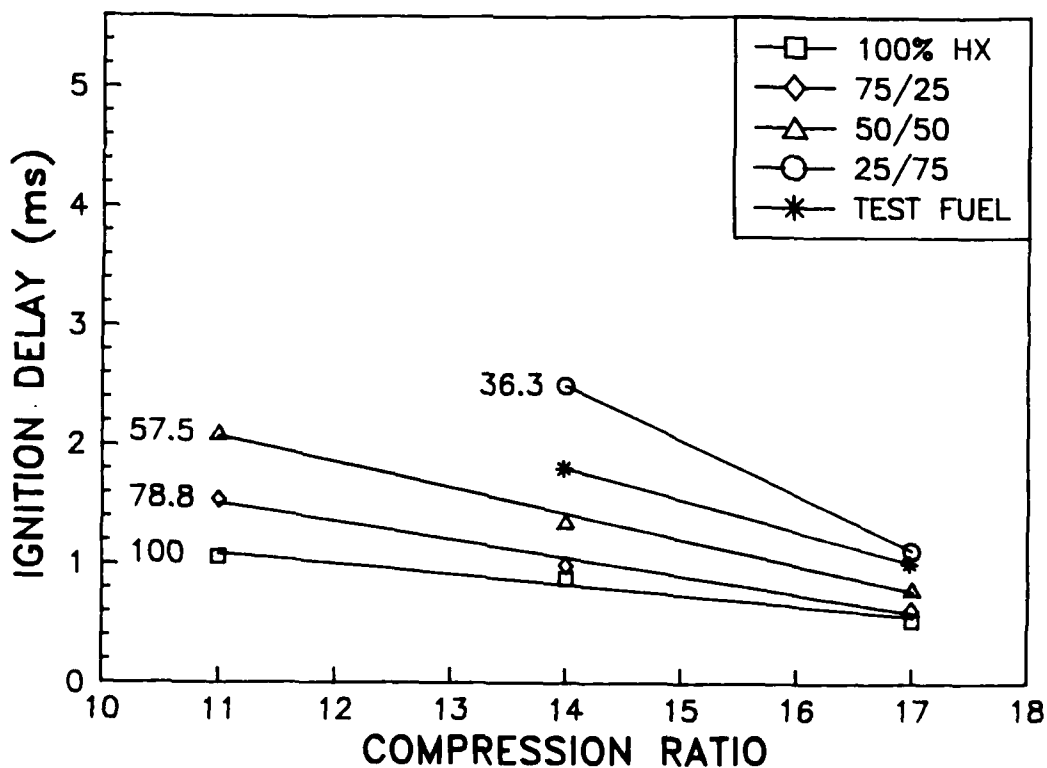
Figure C-30. **JP-8 at 2000 rpm, A/F=40**
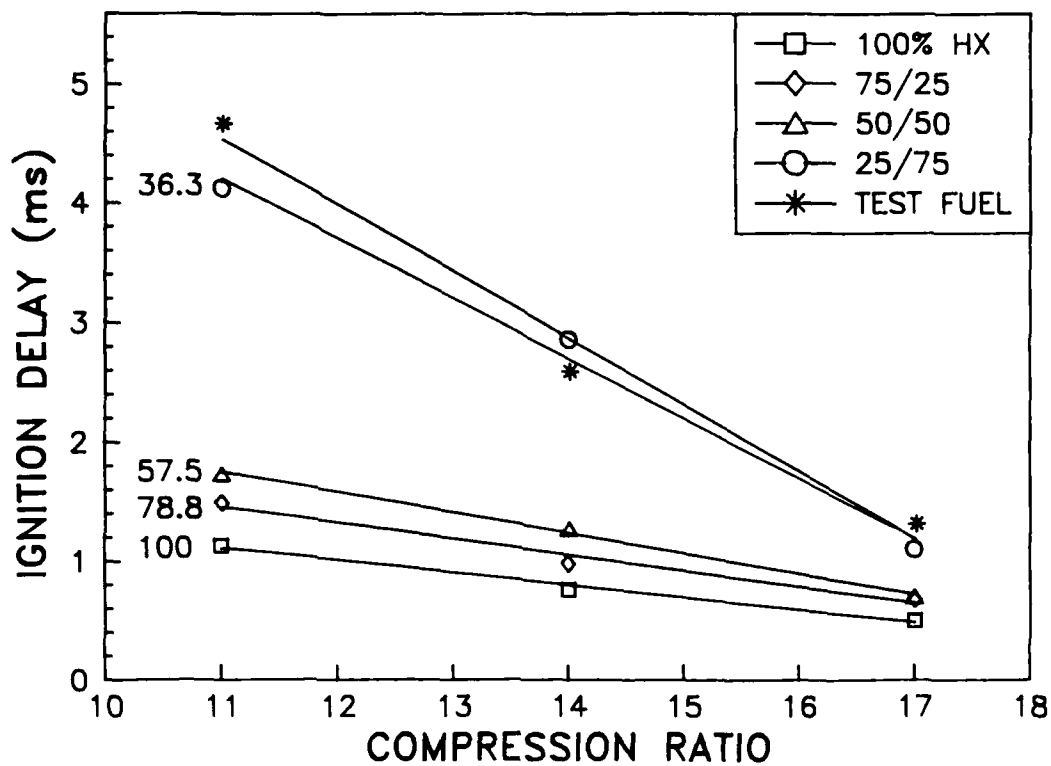
Figure C-31. Referee I at 1000 rpm, A/F=20
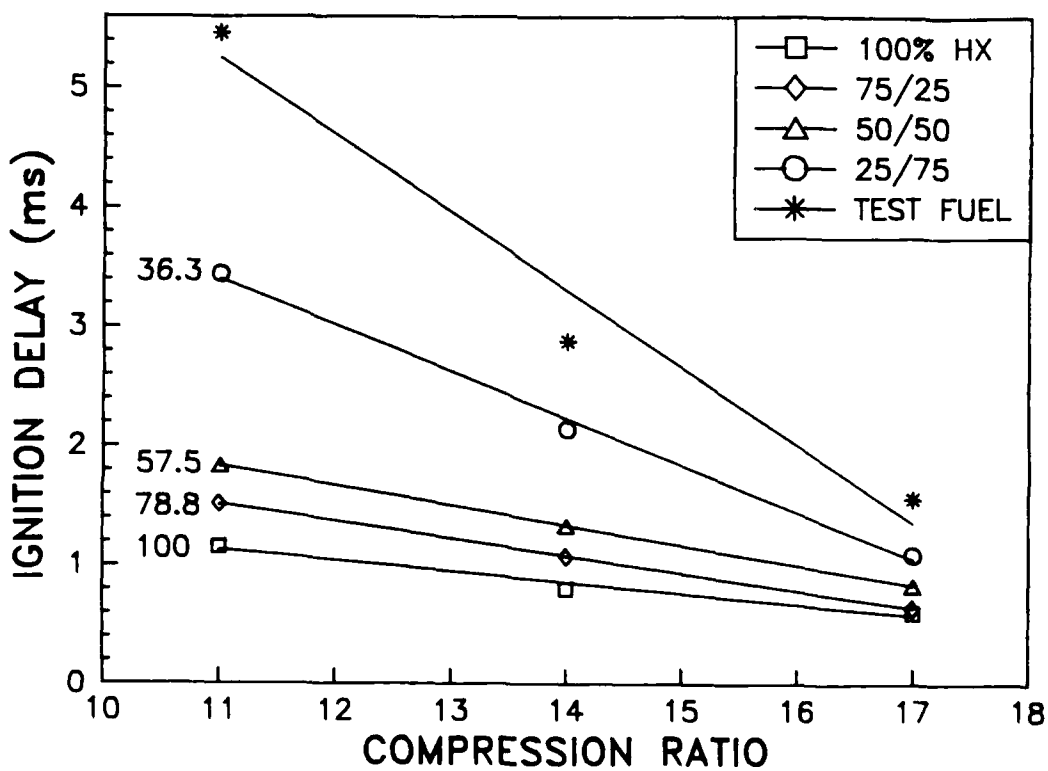
Figure C-32. Referee I at 1000 rpm, A/F=30
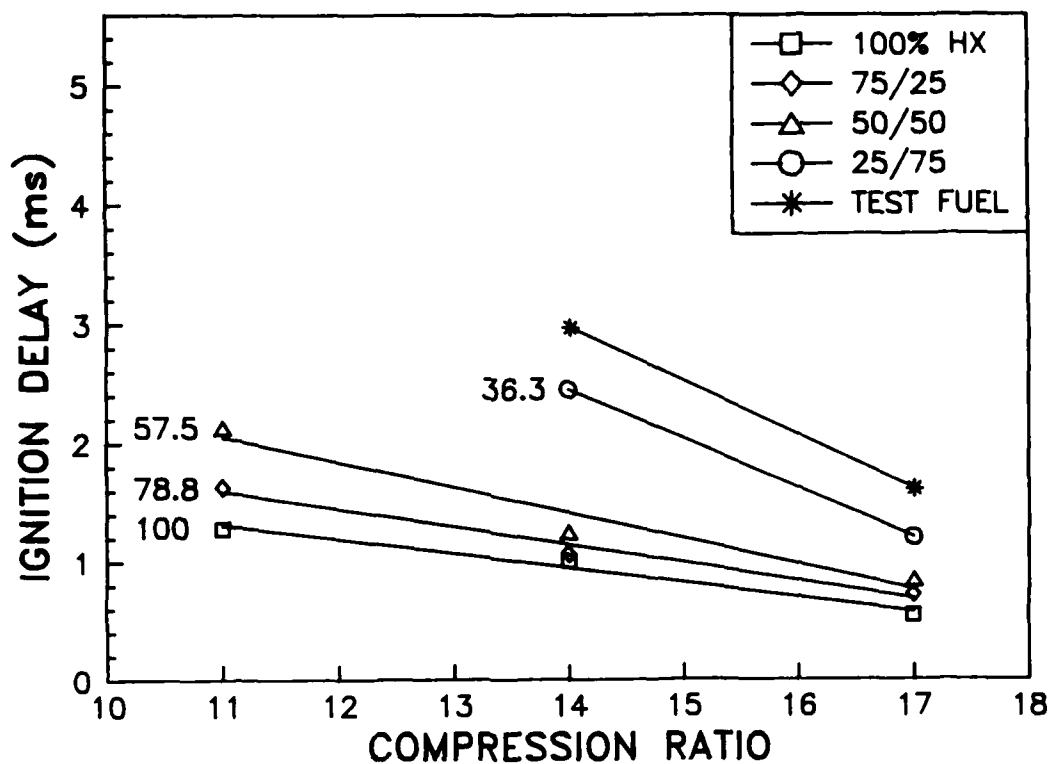
Figure C-33. <u>Referee I at 1000 rpm, A/F=40</u>
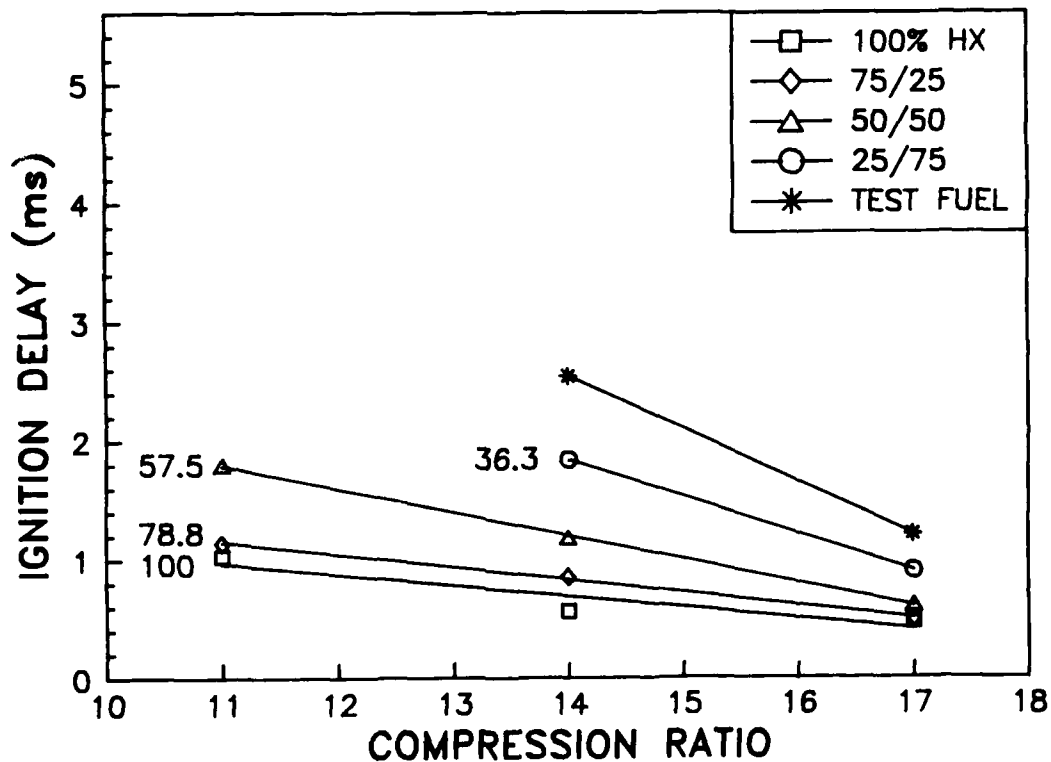
Figure C-34. <u>Referee I at 2000 rpm, A/F=20</u>
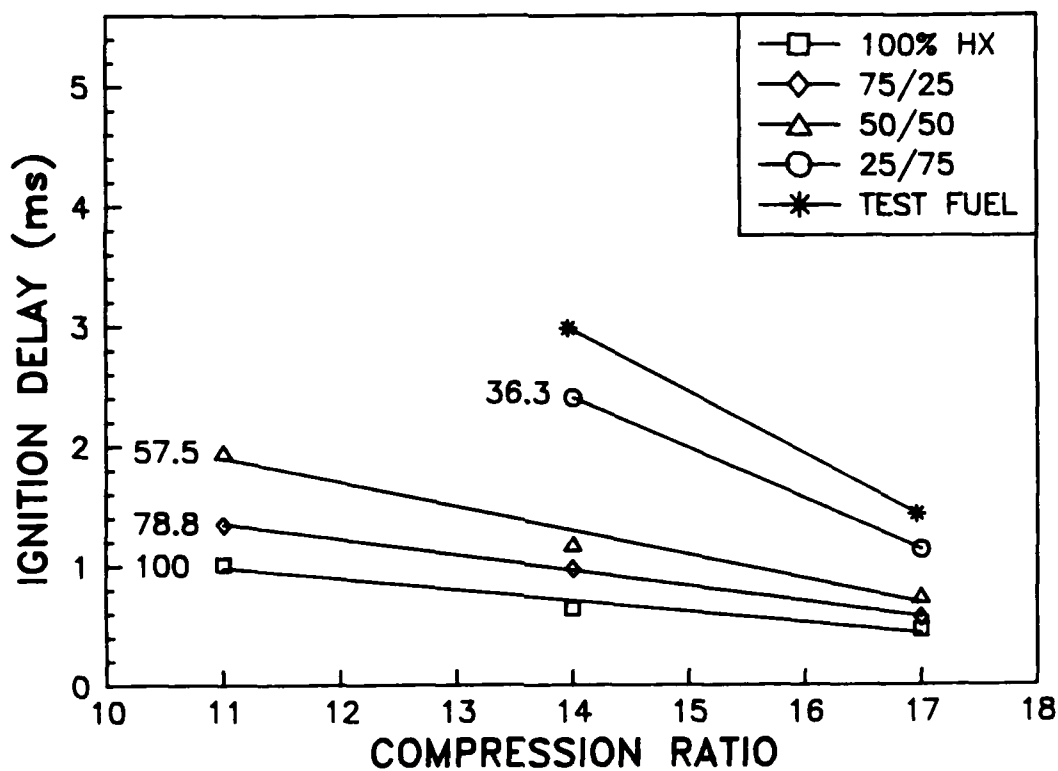
Figure C-35. <u>Referee I at 2000 rpm, A/F=30</u>
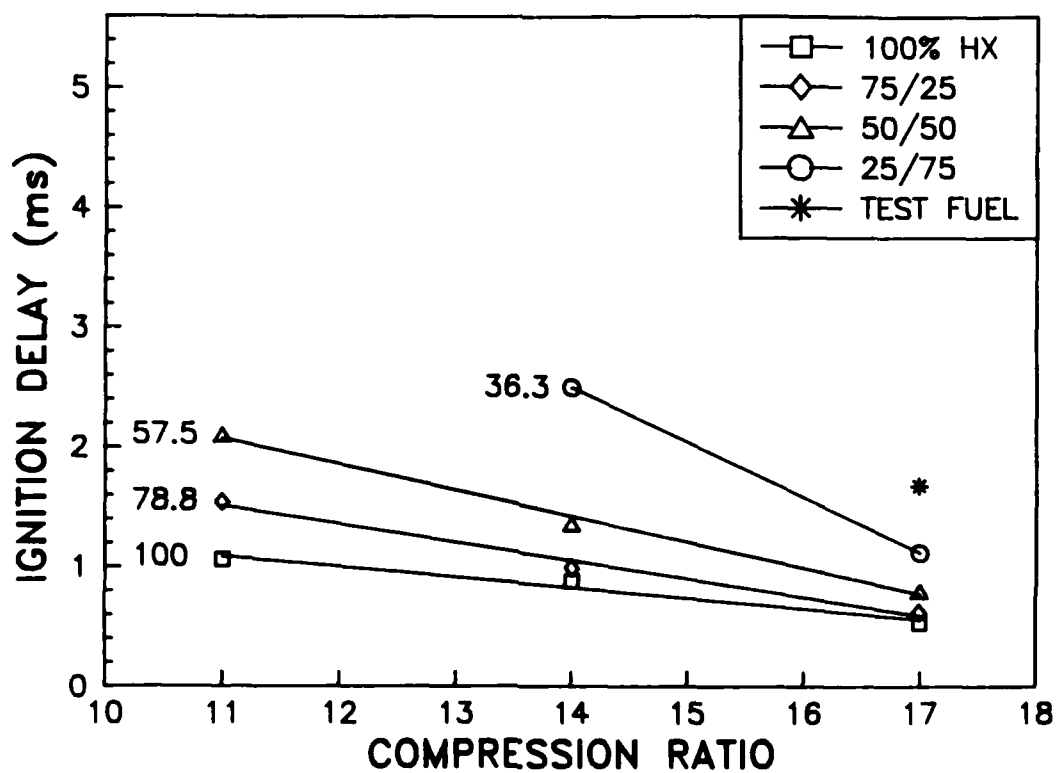
Figure C-36. <u>Referee I at 2000 rpm, A/F=40</u>

108
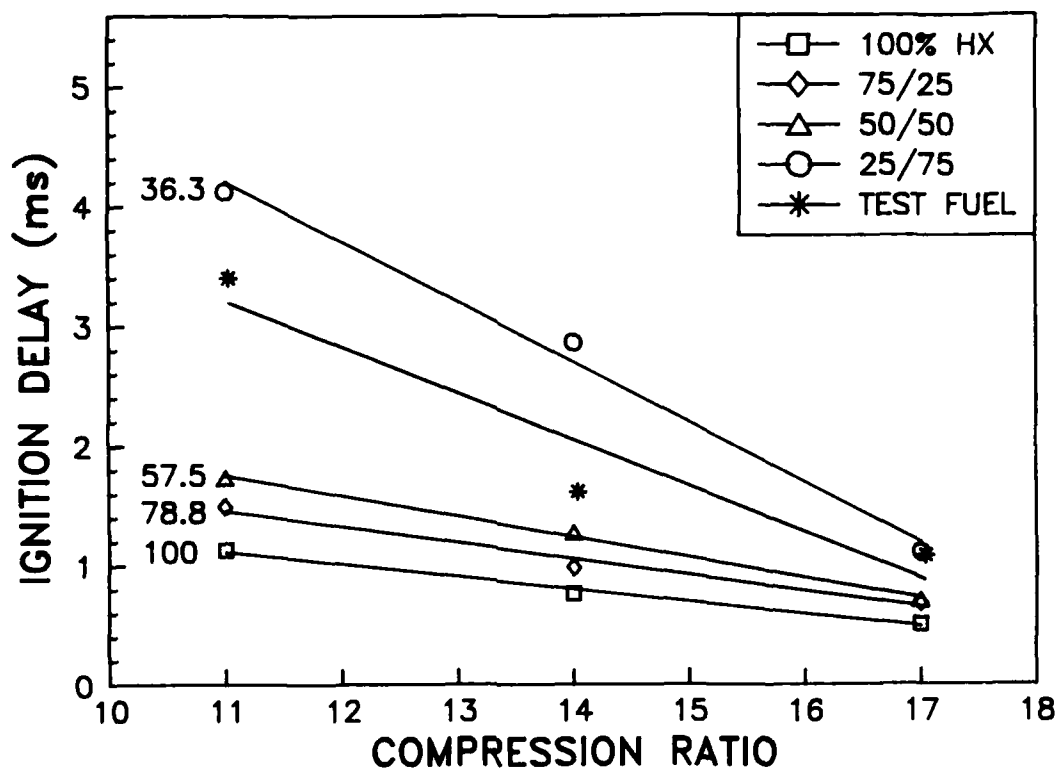
Figure C-37. <u>Referee II at 1000 rpm, A/F=20</u>
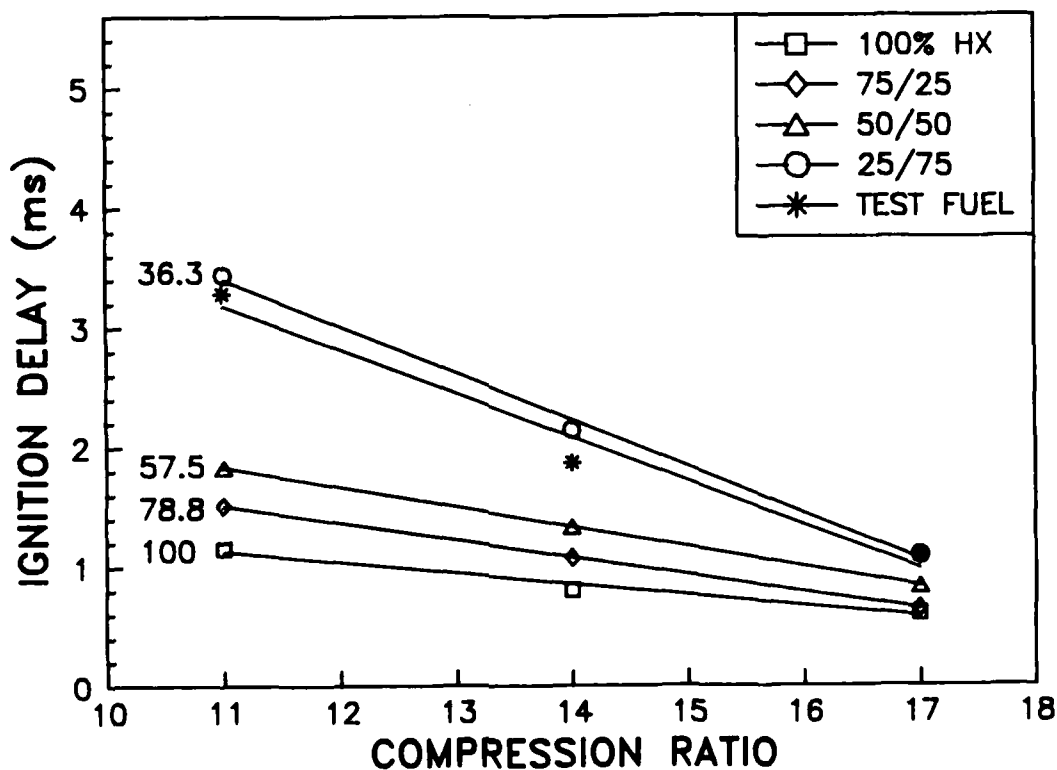
Figure C-38. <u>Referee II at 1000 rpm, A/F=30</u>

109
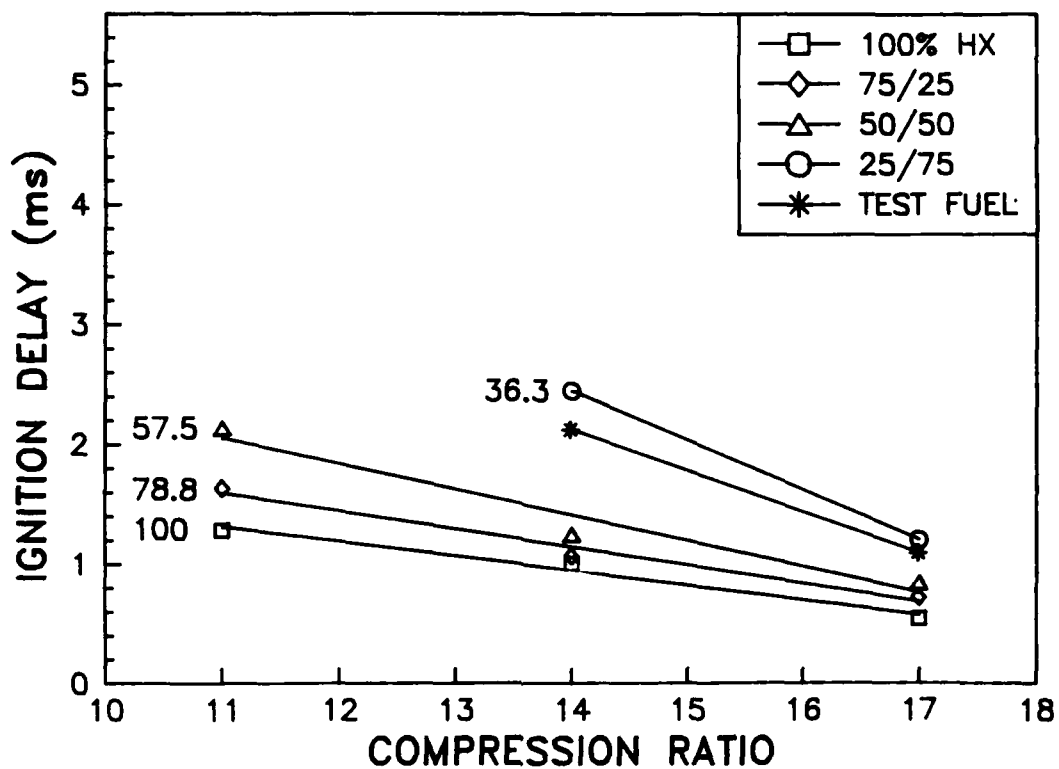
Figure C-39. <u>Referee II at 1000 rpm, A/F=40</u>
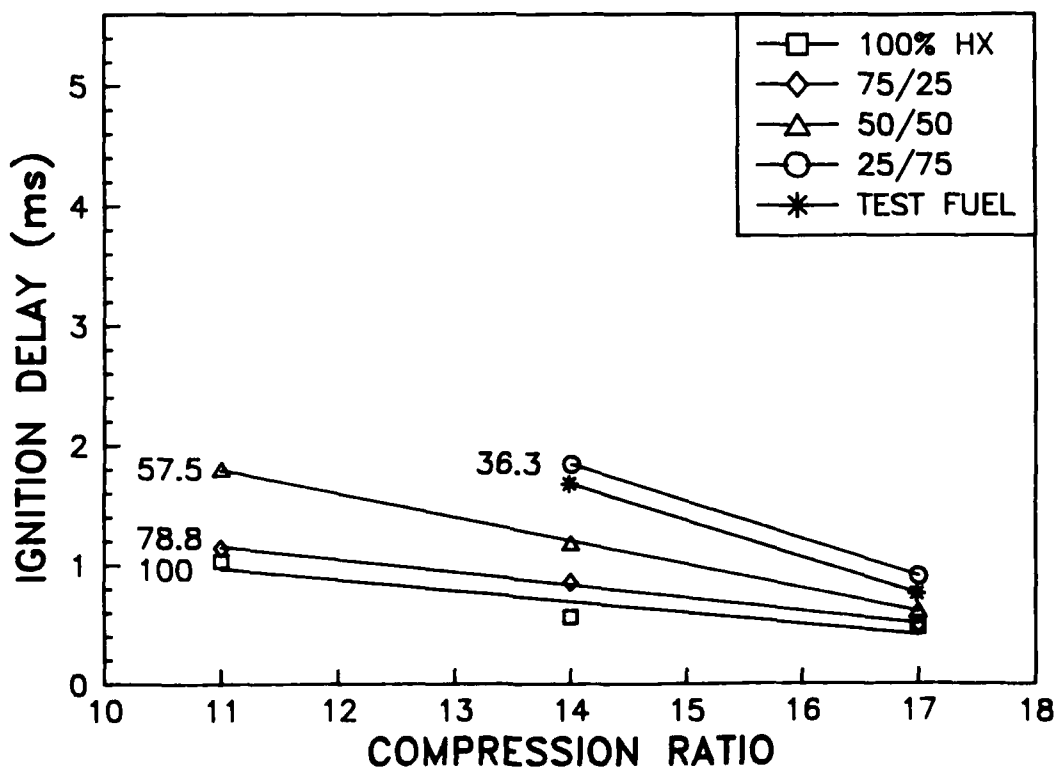
Figure C-40. <u>Referee II at 2000 rpm, A/F=20</u>

110
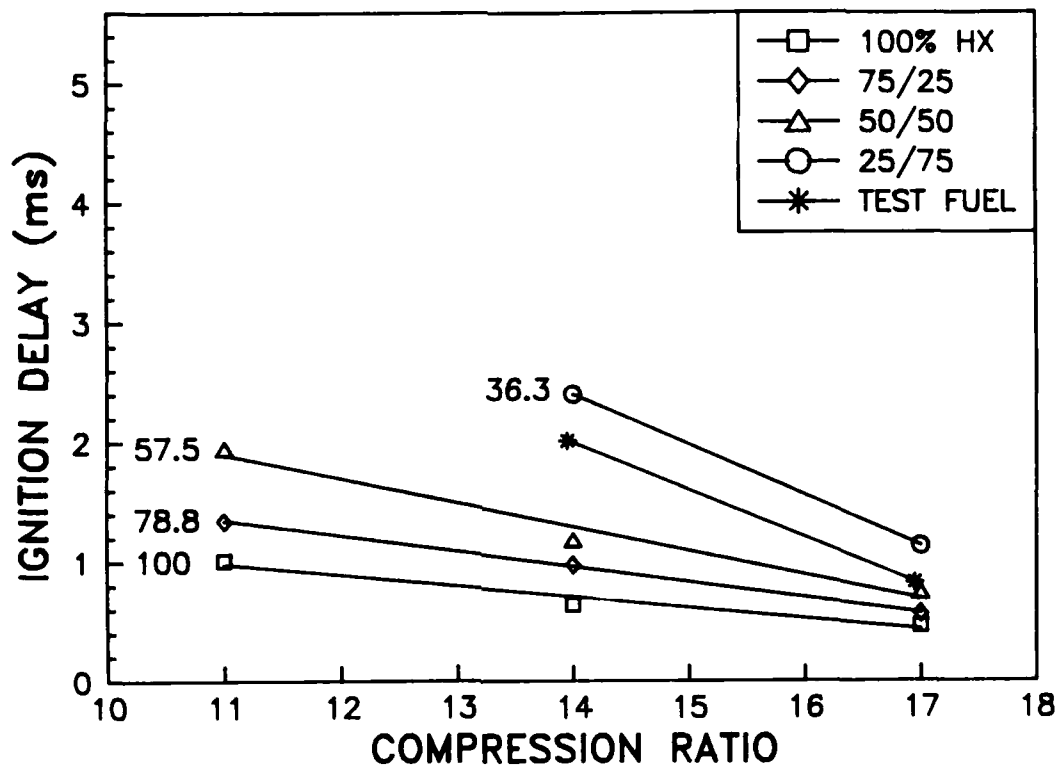
Figure C-41. <u>Referee II at 2000 rpm, A/F=30</u>
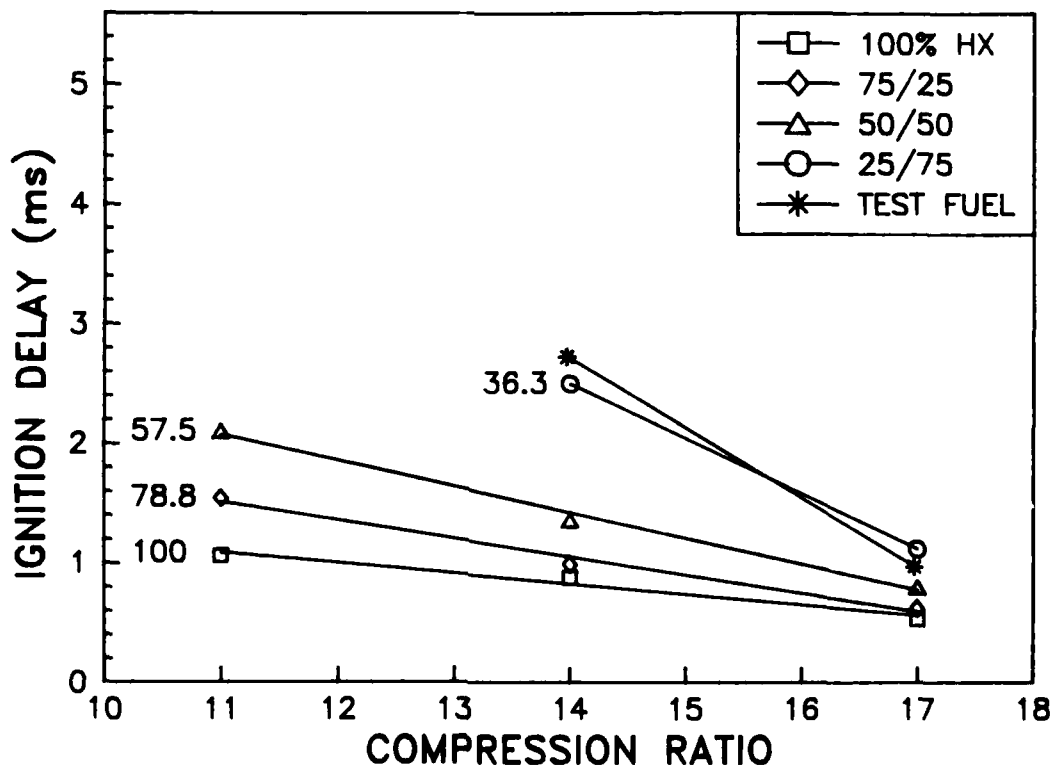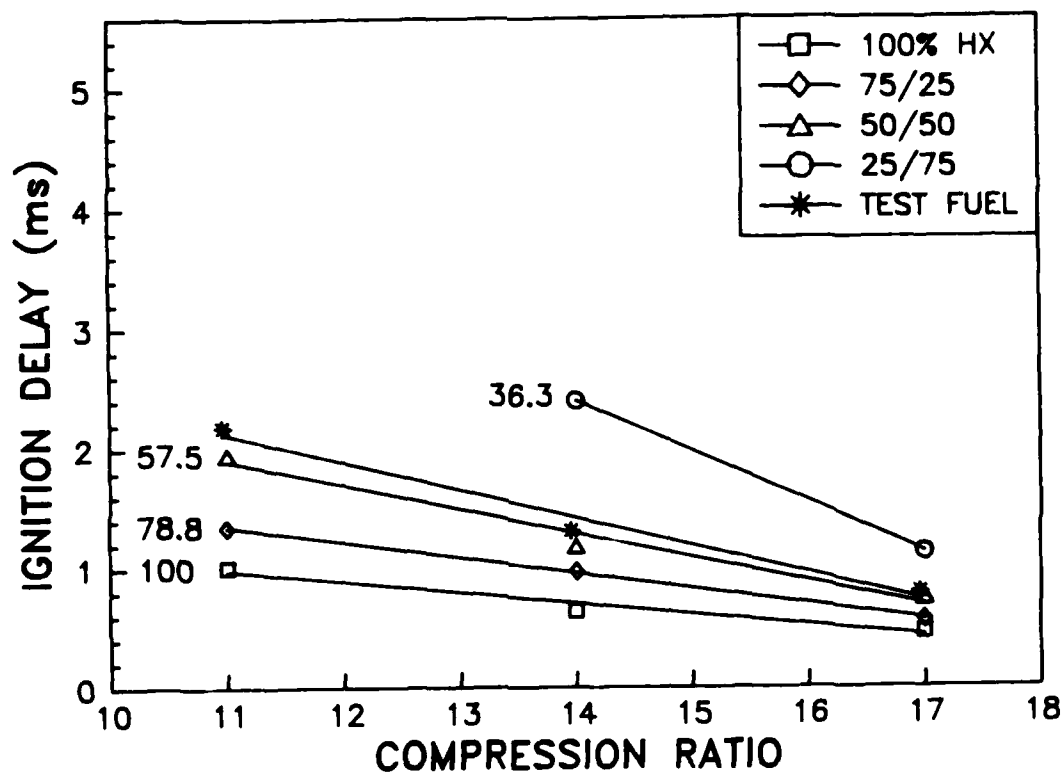

Figure C-42. <u>Referee II at 2000 rpm, A/F=40</u>
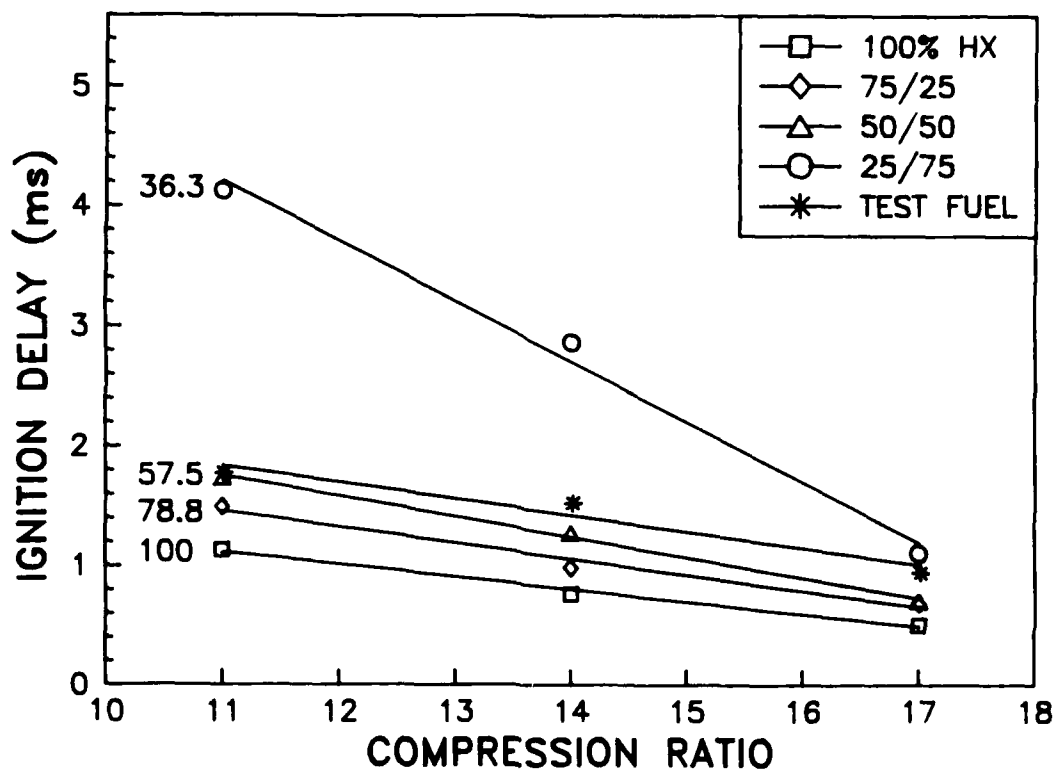
Figure C-43. 5-cSt blend at 1000 rpm, A/F=20
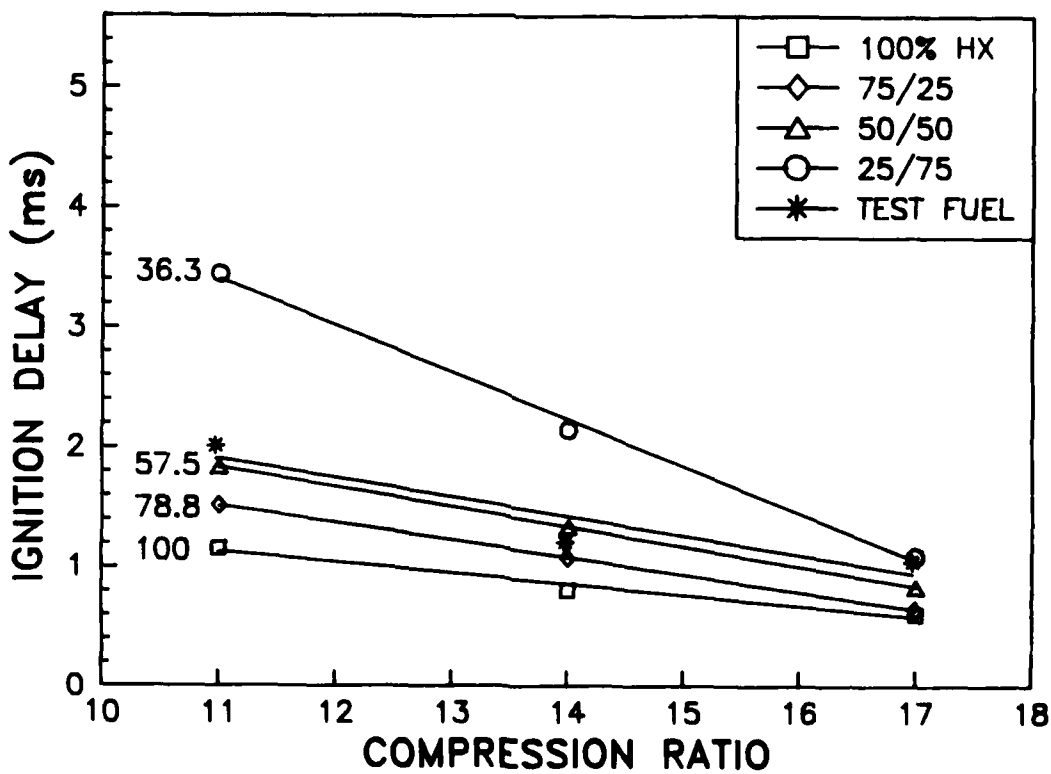
Figure C-44. 5-cSt blend at 1000 rpm, A/F=30

112
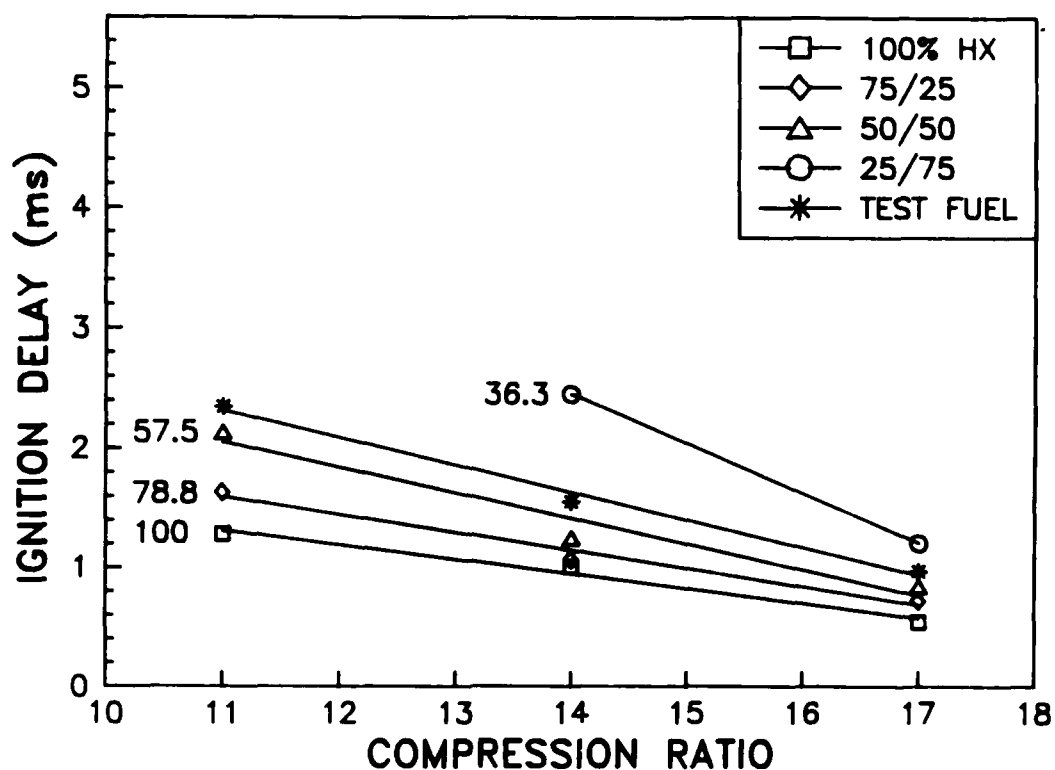
Figure C-45. 5-cSt blend at 1000 rpm, A/F=40
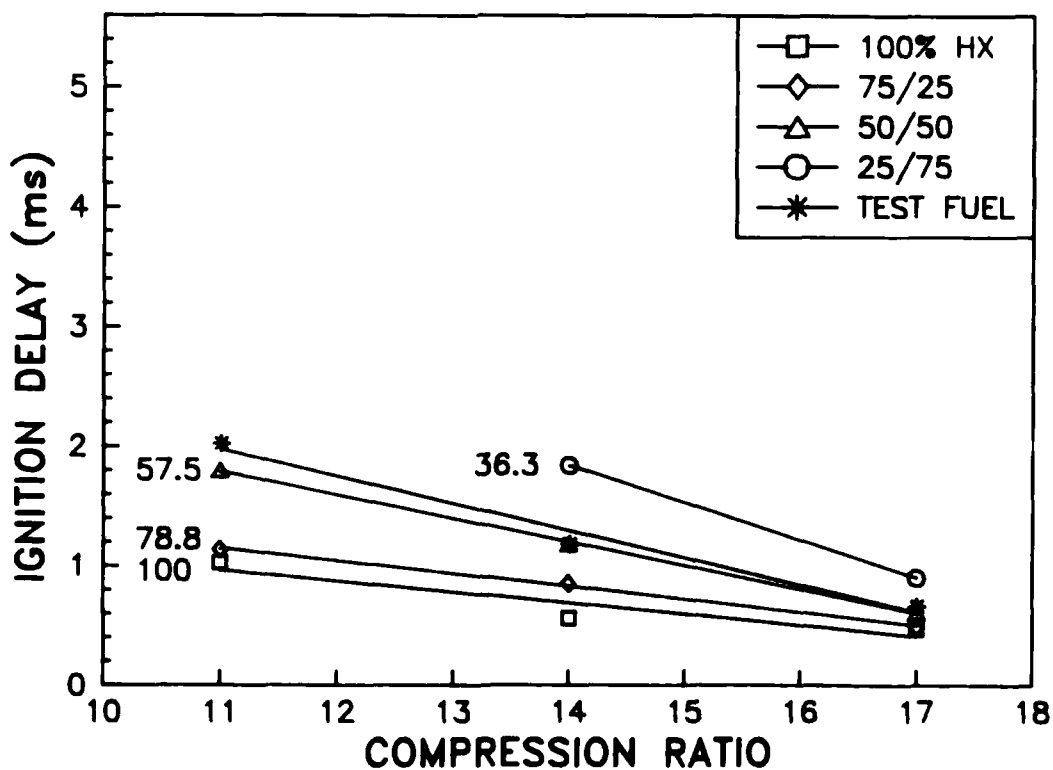
Figure C-46. 5-cSt blend at 2000 rpm, A/F=20
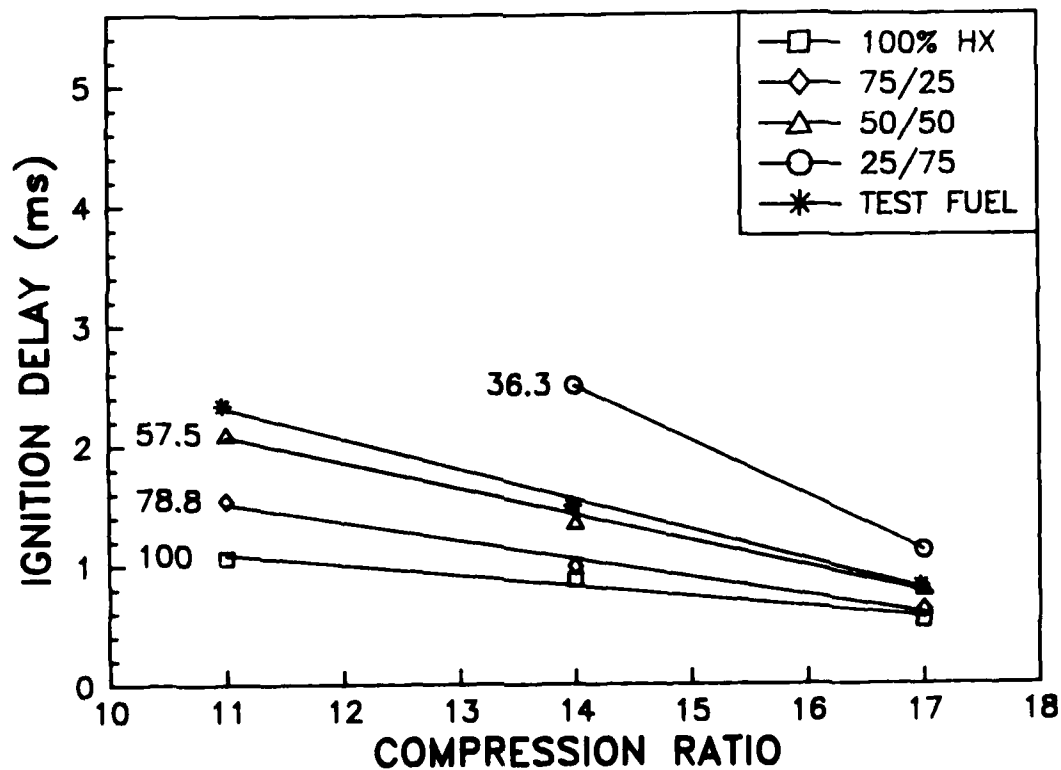
Figure C-47 5-cSt blend at 2000 rpm, A/F=30
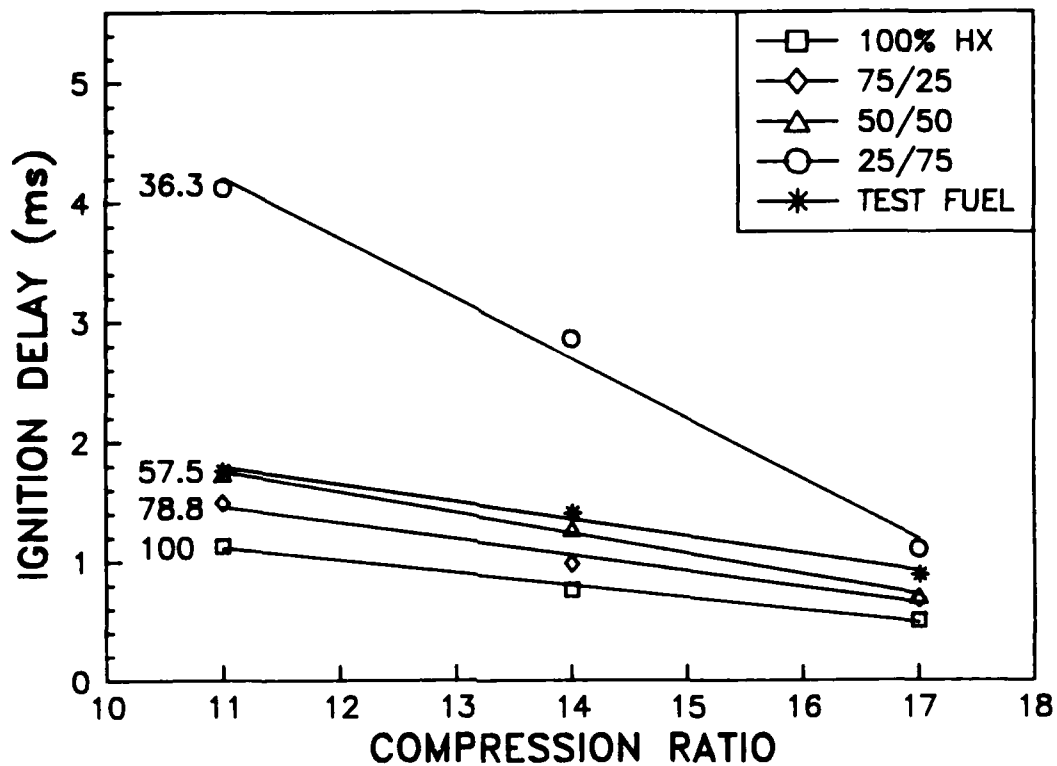

Figure C-48. 5-cSt blend at 2000 rpm, A/F=40

114

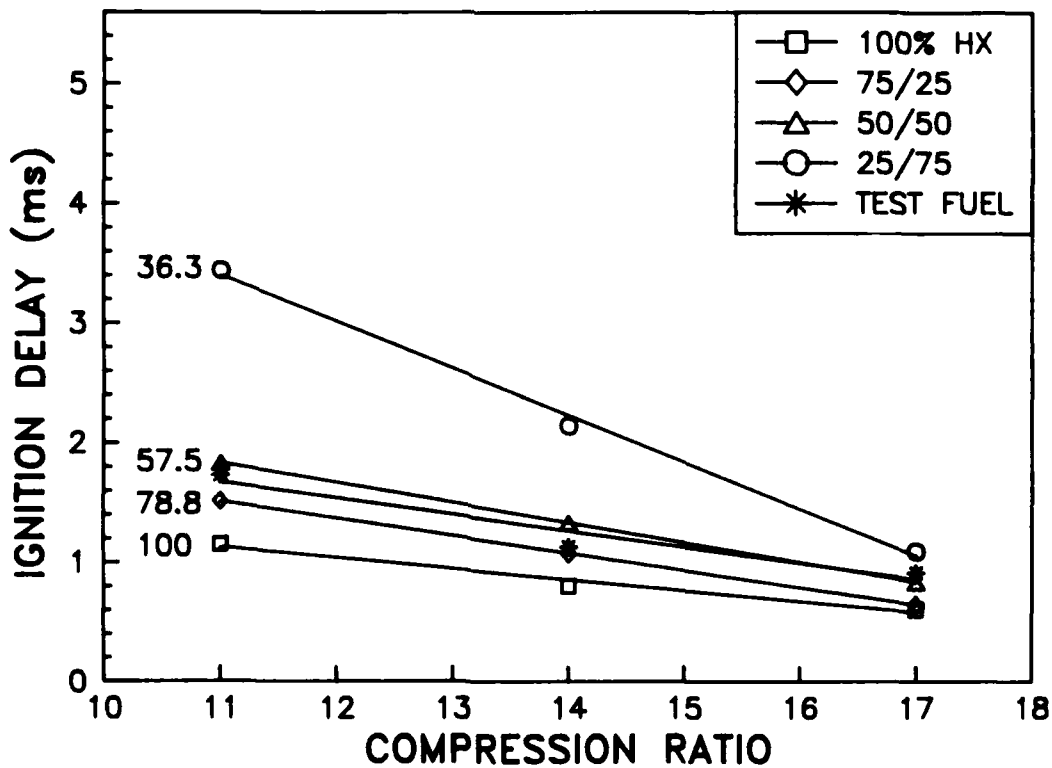**Figure C-49.** 12-cSt blend at 1000 rpm, A/F=20

Figure C-50. 12-cSt blend at 1000 rpm, A/F=30
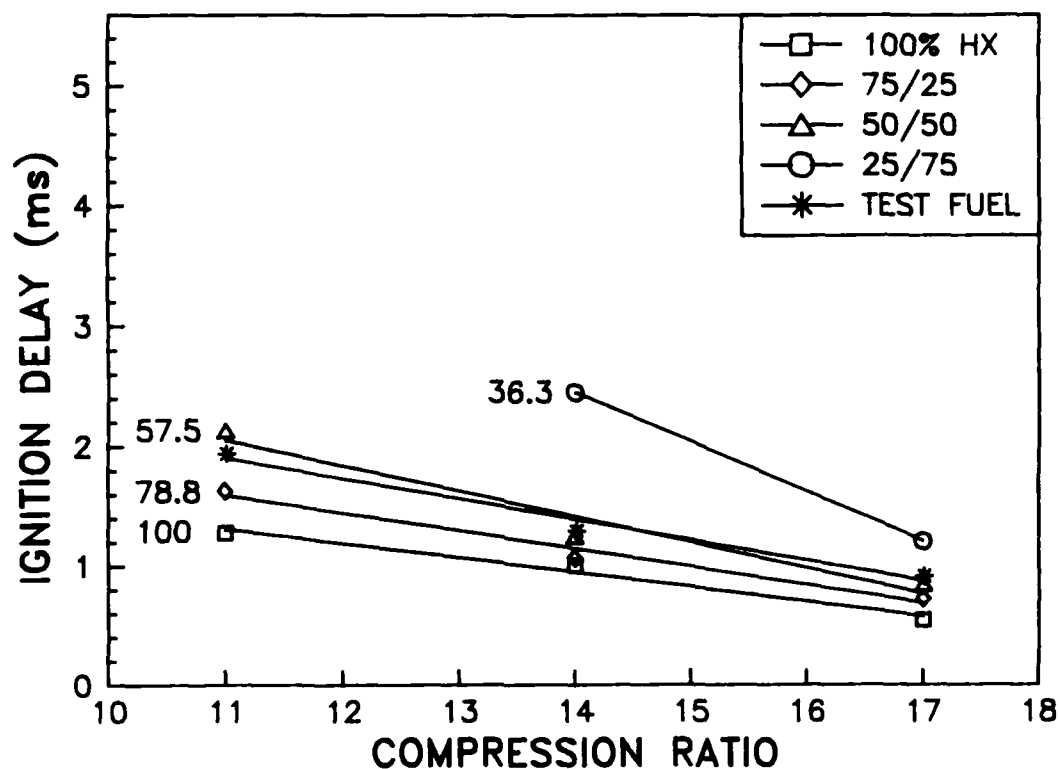
Figure C-51. <u>12-cSt blend at 1000 rpm, A/F=40</u>

Figure C-52. <u>12-cSt blend at 2000 rpm, A/F=20</u>

116

Figure C-53. 12-cSt blend at 2000 rpm, A/F=30

Figure C-54. 12-cSt blend at 2000 rpm, A/F=40

117

Figure C-55. 19-cSt blend at 1000 rpm, A/F=20

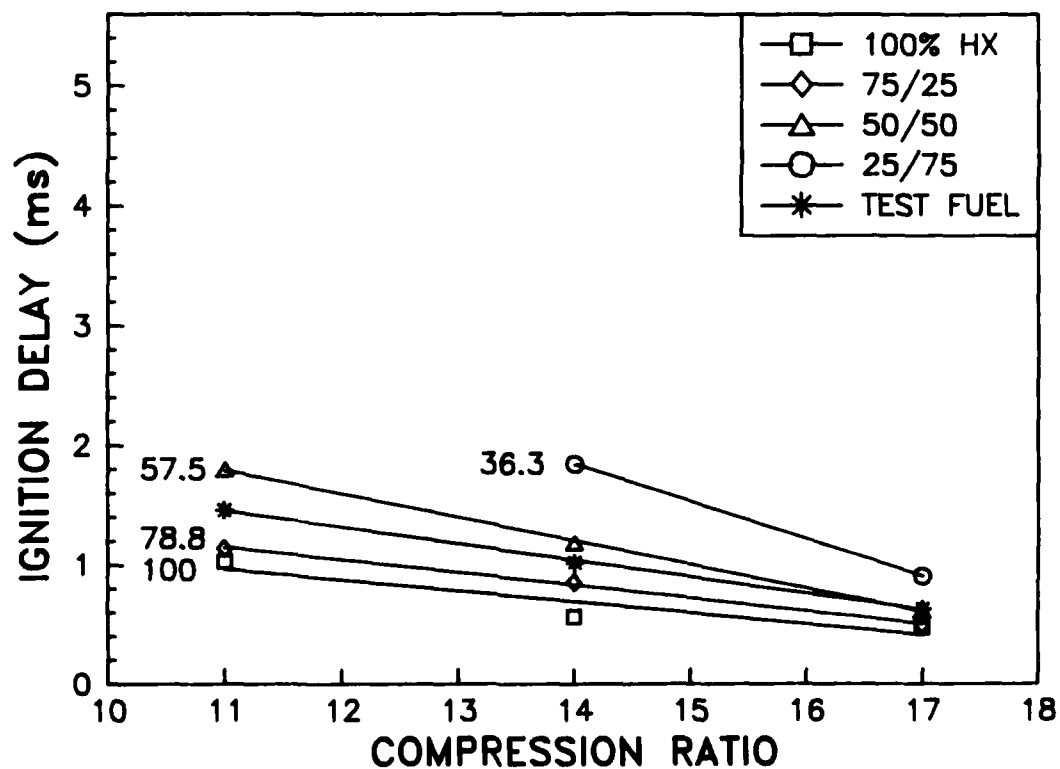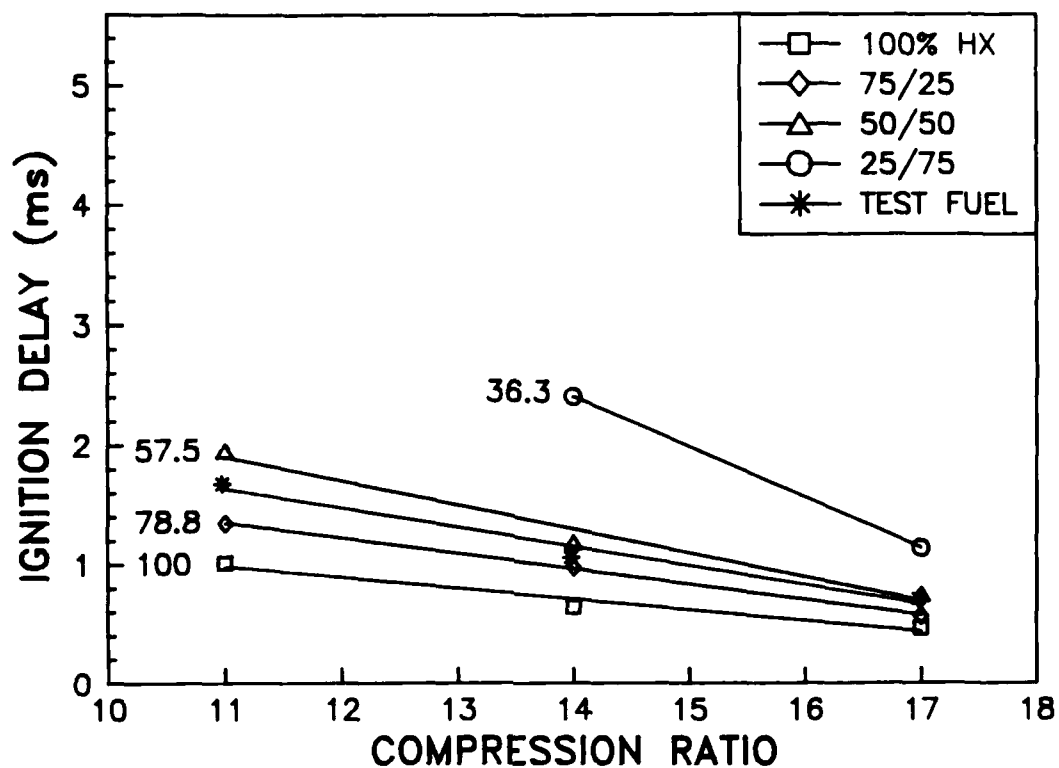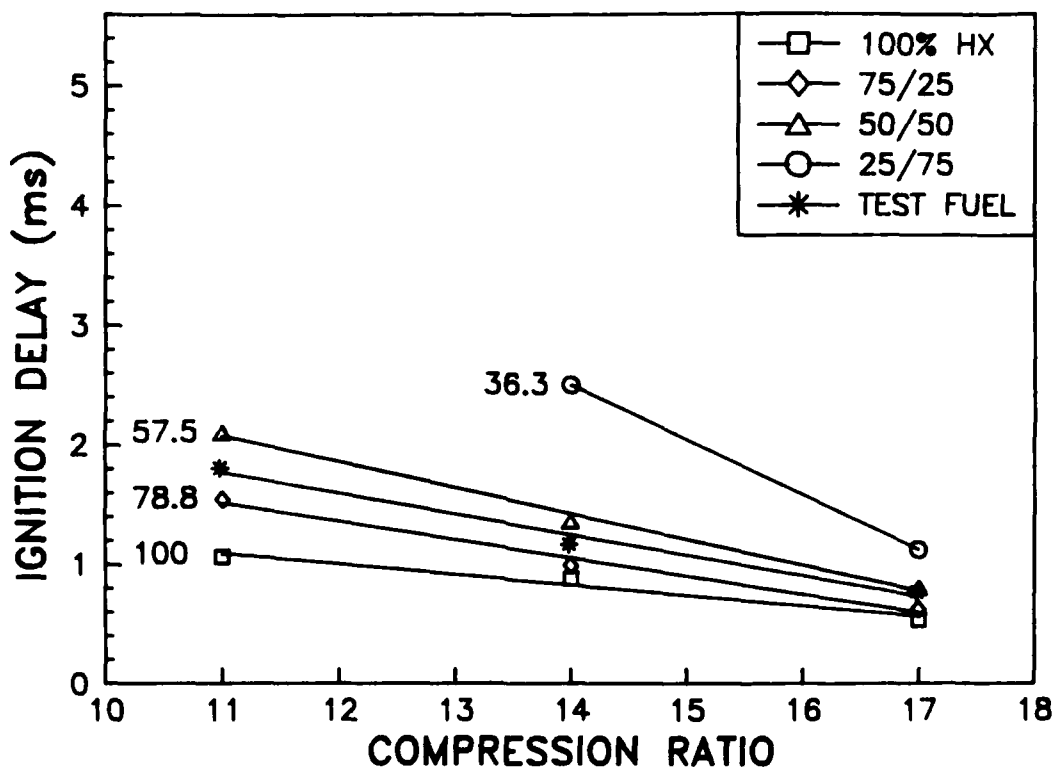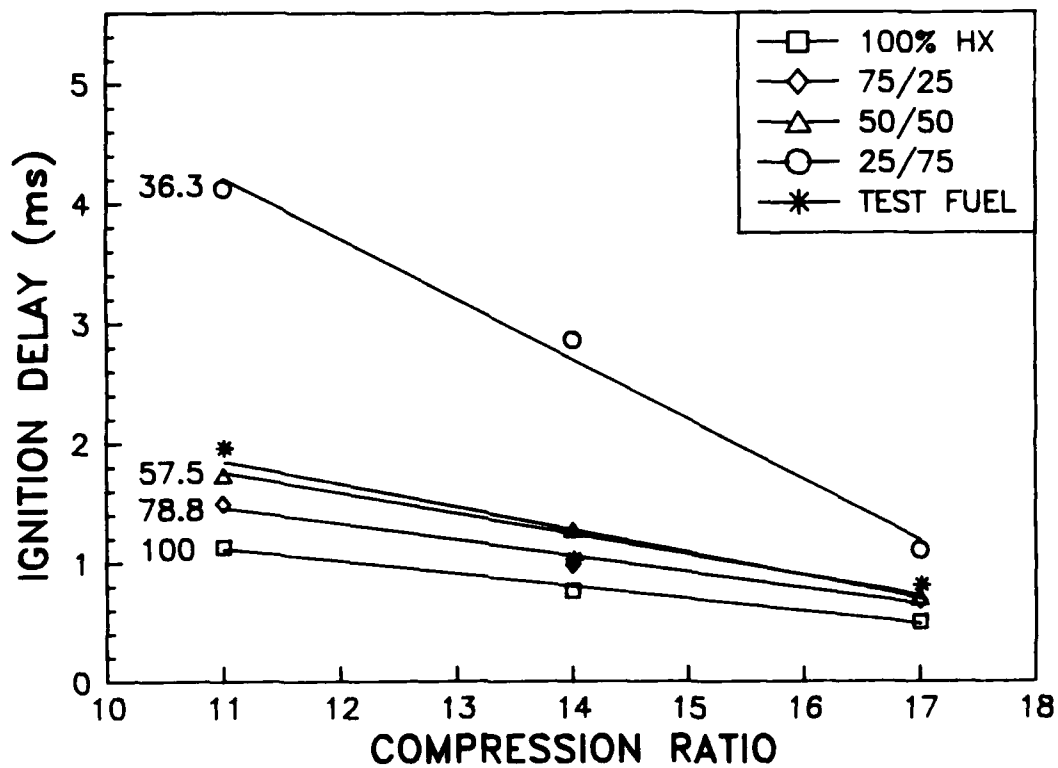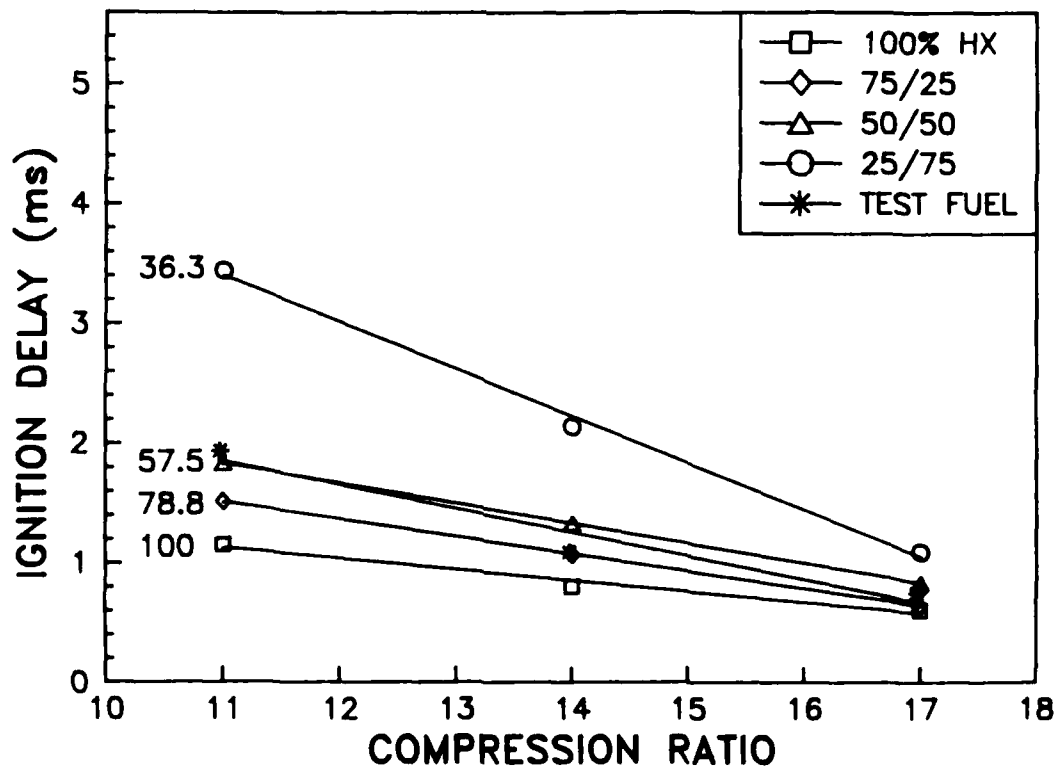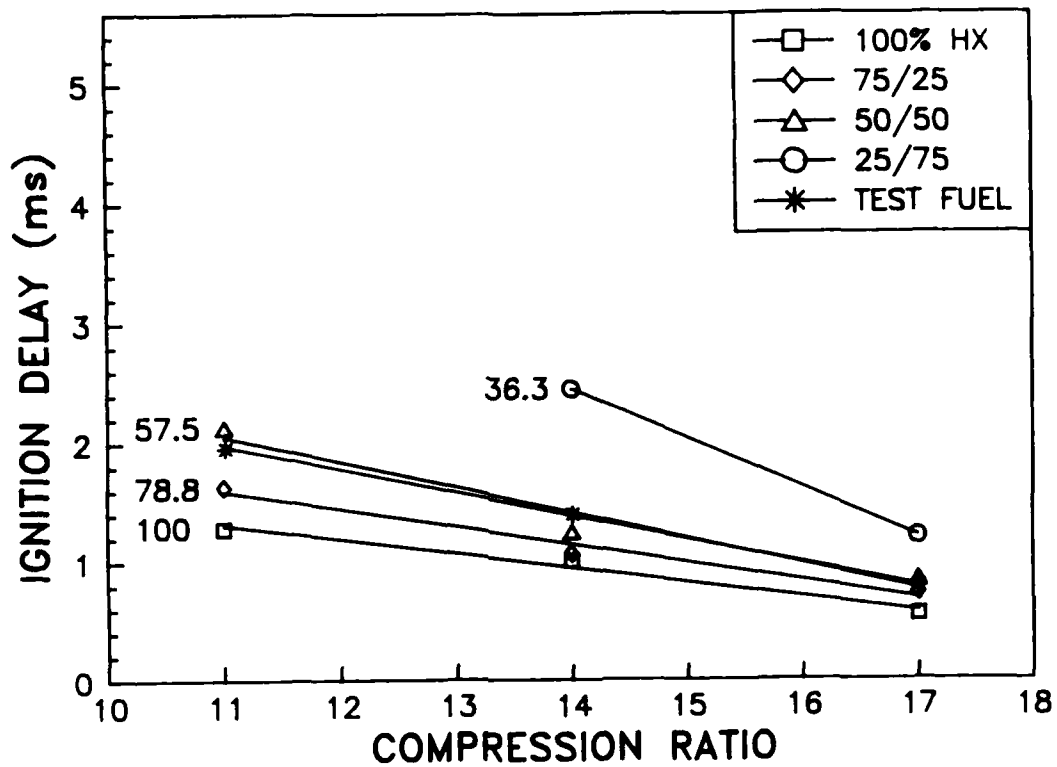Figure C-56. 19-cSt blend at 1000 rpm, A/F=30

118

Figure C-57. 19-cSt blend at 1000 rpm, A/F=40
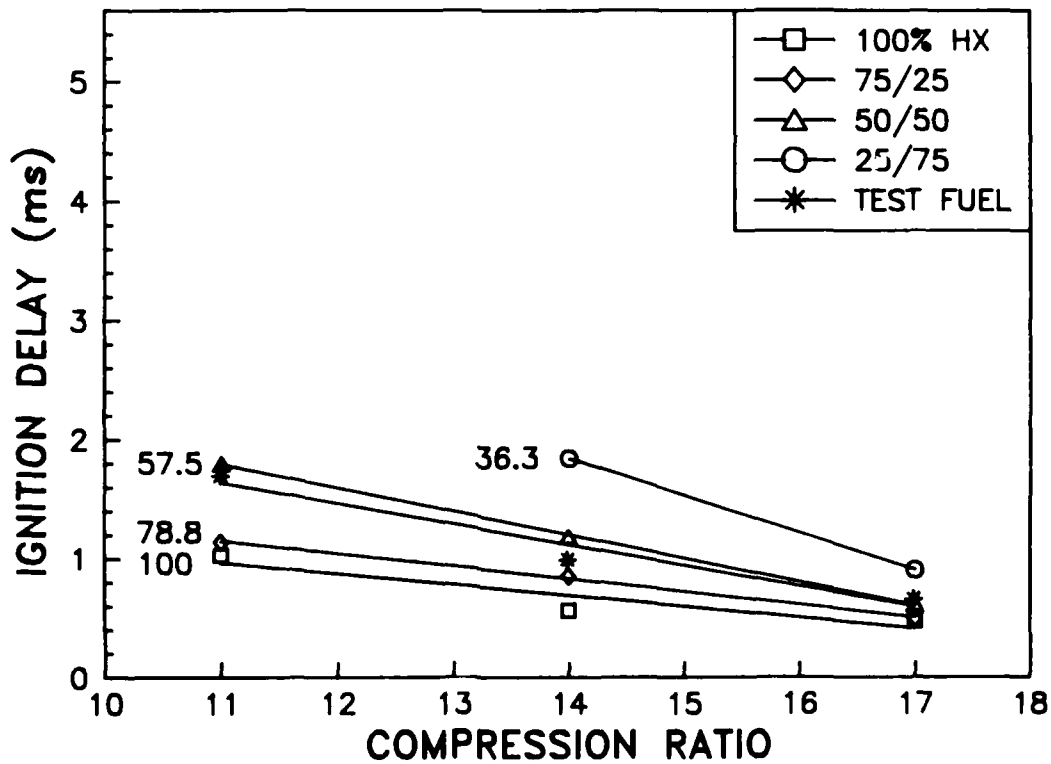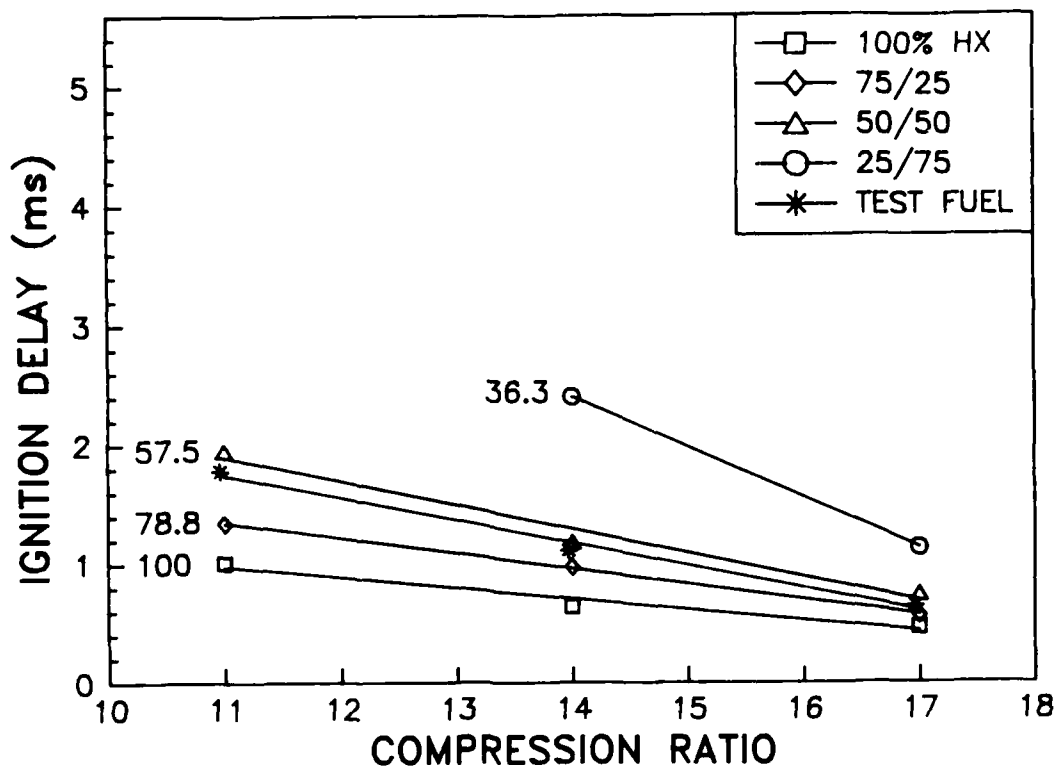

Figure C-58. 19-cSt blend at 2000 rpm, A/F=20

Figure C-59. **19-cSt blend at 2000 rpm, A/F=30**
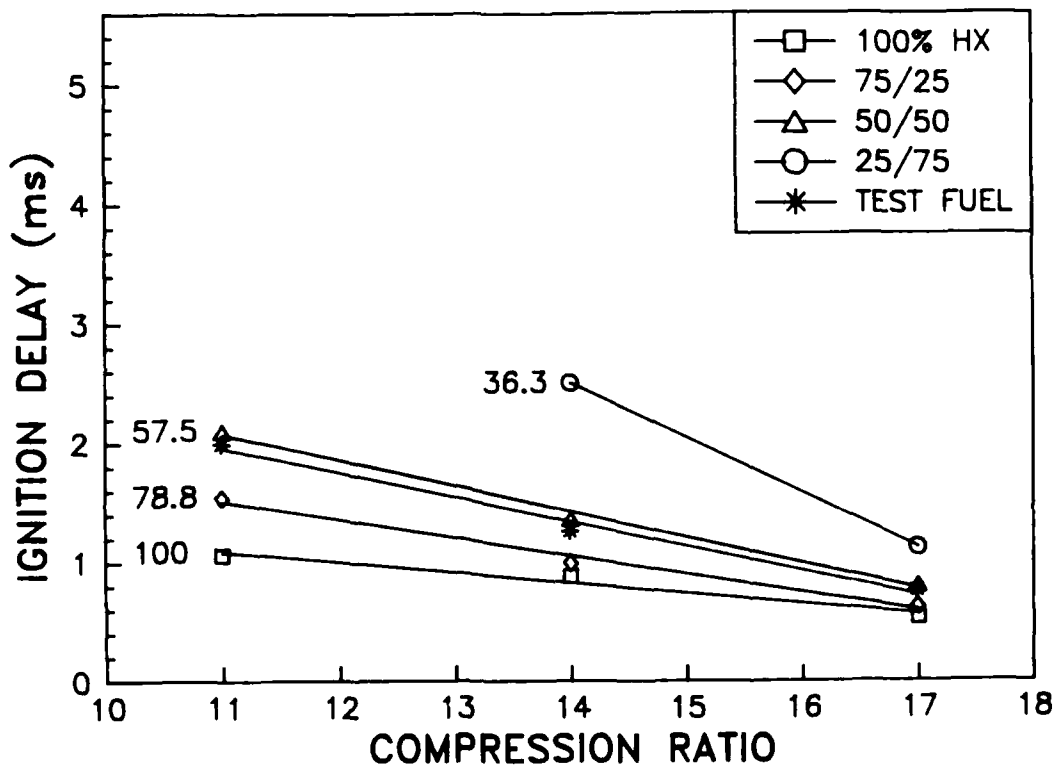

Figure C-60. **19-cSt blend at 2000 rpm, A/F=40**

DISTRIBUTION LIST

DEPARTMENT OF DEFENSE

DEFENSE TECHNICAL INFORMATION
  CTR
CAMERON STATION   12
ALEXANDRIA VA 22314

DEPT. OF DEFENSE
ATTN: OASD/A&L (EP)
        (MR DYCKMAN)   1
WASHINGTON DC 20301-8000

CDR
DEFENSE FUEL SUPPLY CTR
ATTN: DFSC-Q (MR MARTIN)   1
      DFSC-DF (MR FRENCH)   1
CAMERON STATION
ALEXANDRIA VA 22304-6160

DOD
ATTN: DUSDRE (RAT) (DR DIX)   1
ATTN: ROOM 3-D-1089, PENTAGON   1
WASHINGTON DC 20301

DEFENSE ADVANCED RES PROJ
  AGENCY
DEFENSE SCIENCES OFC   1
1400 WILSON BLVD
ARLINGTON VA 22209

DEPARTMENT OF THE ARMY

CDR
U.S. ARMY BELVOIR RESEARCH,
  DEVELOPMENT & ENGINEERING CTR
ATTN: STRBE-VF   10
      STRBE-BT   2
FORT BELVOIR VA 22060-5606

HG, DEPT OF ARMY
ATTN: DALO-TSE (COL BLISS)   1
      DALO-TSZ-B (MR KOWALCZYK)   1
      DALO-AV   1
      DAMO-FDR (MAJ KNOX)   1
      DAMA-ARZ (DR CHURCH)   1
      DAMA-ART (MR APPEL)   1
WASHINGTON DC 20310-0005

CDR
US ARMY MATERIEL COMMAND
ATTN: AMCDE-SS   1
      AMCSM-WST (LTC McKNIGHT)   1
5001 EISENHOWER AVE
ALEXANDRIA VA 22333-0001

CDR
US ARMY TANK-AUTOMOTIVE CMD
ATTN: AMSTA-RG (MR WHEELOCK)   1
      AMSTA-TSL (MR BURG)   1
      AMSTA-MTC (MR GAGLIO),
        AMSTA-MC, AMSTA-MV   1
      AMSTA-RGP (MR RAGGIO/
        MR McCARTNEY)   1
      AMSTA-MLF (MR KELLER)   1
WARREN MI 48397-5000

DIRECTOR
US ARMY AVIATION RESEARCH &
  TECHNOLOGY ACTIVITIES (AVSCOM)
ATTN: SAURT-R (MR ANDRE)   1
AMES RESEARCH CENTER
  (MAIL STOP 207-5)
MOFFETT FIELD CA 94035-1099

DIRECTOR
US ARMY MATERIEL SYSTEMS
  ANALYSIS ACTIVITY
ATTN: AMXSY-CM (MR NIEMEYER)   1
ABERDEEN PROVING GROUND MD
21005-5006

DIRECTOR
APPLIED TECHNOLOGY DIRECTORATE
U.S. ARMY R&T ACTIVITIES (AVSCOM)
ATTN: SAVDL-ATL-ATP (MR MORROW) 1
FORT EUSTIS VA 23604-5577

CDR
US READINESS COMMAND
ATTN: J4-E   1
MACDILL AIR FORCE BASE FL 33608

DIRECTOR
US ARMY MATERIEL CMD
MATERIEL SUPPORT ACTIVITY
ATTN: AMXTB-T (MR STOLARICK)   1
FORT LEWIS WA 98433

HQ, 172D INFANTRY BRIGADE (ALASKA)
ATTN: AFZT-DI-L   1
      AFZT-DI-M   1
DIRECTORATE OF INDUSTRIAL
  OPERATIONS
FORT RICHARDSON AK 99505

CDR
US ARMY GENERAL MATERIAL &
  PETROLEUM ACTIVITY
ATTN: STRGP-F (MR ASHBROOK)   1
    STRGP-FE, BLDG 85-3
      (MR GARY SMITH)   1
    STRGP-FT (MR FOSTER)   1
NEW CUMBERLAND PA 17070-5008

CDR
US ARMY LABORATORY COMMAND
ATTN: AMSLC-TP-PB (DR GONANO)   1
    AMSLC-TP-AL (LTC SCHRADER)1
ADELPHIA MD 20783-1145

CDR
US ARMY RES & STDZN GROUP
  (EUROPE)
ATTN: AMXSN-UK-RA (DR OERTEL)   1
BOX 65
FPO NEW YORK 09510

PROJECT MGR, M113 FAMILY OF
  VEHICLES
ATTN: AMCPM-M113-T   1
WARREN MI 48397

CDR, US ARMY AVIATION SYSTEMS
  CMD
ATTN: AMSAV-EP (MR EDWARDS)   1
    AMSAV-NS   1
4300 GOODFELLOW BLVD
ST LOUIS MO 63120-1798

CDR
US ARMY FORCES COMMAND
ATTN: AFLG-REG   1
    AFLG-POP   1
FORT MCPHERSON GA 30330

CDR
US CENTRAL COMMAND
ATTN: CINCCEN/CC J4-L   1
MACDILL AIR FORCE BASE FL 33608

CDR
US ARMY YUMA PROVING GROUND
ATTN: STEYP-MT-TL-M
    (MR DOEBBLER)   1
YUMA AZ 85364-9103

PROJ MGR, BRADLEY FIGHTING
  VEHICLE SYS
ATTN: AMCPM-FVS-M   1
WARREN MI 48397

CDR
US ARMY DEVELOPMENT AND
  EMPLOYMENT AGENCY
ATTN: MODE-FDD-CSSB
    (MAJ GROSSMAN)   1
FT LEWIS VA 98433-5000

PROJ MGR, MOBILE ELECTRIC POWER
ATTN: AMCPM-MEP-TM   1
7500 BACKLICK ROAD
SPRINGFIELD VA 22150

CDR
US ARMY EUROPE & SEVENTH ARMY
ATTN: AEAGG-FMD   1
    AEAGD-TE   1
APO NY 09403

CDR
THEATER ARMY MATERIAL MGMT
  CENTER (200TH)-DPGM
DIRECTORATE FOR PETROL MGMT
ATTN: AEAGD-MMC-PT-Q
    (MR CARLONE)   1
APO NY 09052

CDR
US ARMY RESEARCH OFC
ATTN: SLCRO-EG (DR MANN)   1
    SLCRO-CB   1
P O BOX 12211
RSCH TRIANGLE PARK NC 27709-2211

PROG MGR, TACTICAL VEHICLE
ATTN: AMCPM-TV   1
WARREN MI 48397

HQ, EUROPEAN COMMAND
ATTN: J4/7-LJPO (LTC McCURRY)   1
VAIHINGEN, GE
APO NY 09128

CDR
US ARMY GENERAL MATERIAL &
  PETROLEUM ACTIVITY
ATTN: STRGP-PW (MR PRICE)   1
BLDG 247, DEFENSE DEPOT TRACY
TRACY CA 95376-5051

PROJ MGR, LIGHT ARMORED VEHICLES
ATTN: AMCPM-LA-E   1
WARREN MI 48397

CDR
US ARMY ORDNANCE CENTER &
   SCHOOL
ATTN: ATSL-CD-CS   1
ABERDEEN PROVING GROUND MD
21005

CDR
US ARMY FOREIGN SCIENCE & TECH
   CENTER
ATTN: AIAST-RA-ST3 (MR BUSI)   1
        AIAST-MT-1   1
FEDERAL BLDG
CHARLOTTESVILLE VA 22901

PROJECT MANAGER, LIGHT COMBAT
   VEHICLES
ATTN: AMCPM-LCV-TC   1
WARREN, MI 48397

CDR, US ARMY TROOP SUPPORT
   COMMAND
ATTN: AMSTR-ME   1
       AMSTR-S   1
       AMSTR-E   1
       AMSTR-WL (MR BRADLEY)   1
4300 GOODFELLOW BLVD
ST LOUIS MO 63120-1798

TRADOC LIAISON OFFICE
ATTN: ATFE-LO-AV   1
4300 GOODFELLOW BLVD
ST LOUIS MO 63120-1798

CDR
US ARMY QUARTERMASTER SCHOOL
ATTN: ATSM-CD   1
       ATSM-TD   1
       ATSM-PFS (MR ELLIOTT)   1
FORT LEE VA 23801

HQ
US ARMY TRAINING & DOCTRINE CMD
ATTN: ATCD-SL-5   1
FORT MONROE VA 23651-5000

DIRECTOR
US ARMY RSCH & TECH ACTIVITIES
   (AVSCOM)
PROPULSION DIRECTORATE
ATTN: SAVDL-PL-D (MR ACURIO)   1
21000 BROOKPARK ROAD
CLEVELAND OH 44135-3127

CDR
US ARMY WESTERN COMMAND
ATTN: APLG-TR   1
FORT SCHAFTER HI 96858

HQ, US ARMY ARMOR CENTER AND
   FORT KNOX
ATTN: ATSB-CD   1
FORT KNOX KY 40121

CDR
US ARMY LOGISTICS CTR
ATTN: ATCL-MS (MR A MARSHALL) 1
       ATCL-C   1
FORT LEE VA 23801-6000

PROJECT MANAGER
PETROLEUM & WATER LOGISTICS
ATTN: AMCPM-PWL   1
4300 GOODFELLOW BLVD
ST LOUIS MO 63120-1798

PROG MGR, TANK SYSTEMS
ATTN: AMCPM-GCM-SM   1
       AMCPM-M60   1
WARREN MI 48397

CDR
6TH MATERIEL MANAGEMENT CENTER
19TH SUPPORT BRIGADE   1
APO SAN FRANCISCO 96212-0172

DEPARTMENT OF THE NAVY

CDR
NAVAL AIR PROPULSION CENTER
ATTN: PE-33 (MR D'ORAZIO)   1
P O BOX 7176
TRENTON NJ 06828

CDR
NAVAL SEA SYSTEMS CMD
ATTN: CODE 05M4 (MR R LAYNE)   1
WASHINGTON DC 20362-5101

CDR
DAVID TAYLOR NAVAL SHIP R&D CTR
ATTN: CODE 2759 (MR STRUCKO)   1
ANNAPOLIS MD 21402-5067

CG
FLEET MARINE FORCE ATLANTIC
ATTN: G4   1
NORFOLK VA 23511

CG
FLEET MARINE FORCE PACIFIC
ATTN: G4   1
CAMP H.M. SMITH HI 96861

CDR
NAVAL SHIP ENGINEERING CENTER
ATTN: CODE 6764   1
PHILADELPHIA PA 19112

PROJ MGR, M60 TANK DEVELOPMENT
ATTN: USMC-LNO   1
US ARMY TANK-AUTOMOTIVE
    COMMAND (TACOM)
WARREN MI 48397

DEPARTMENT OF THE NAVY
HQ, US MARINE CORPS
ATTN: LMM/2   1
WASHINGTON DC 20380

CDR
NAVAL AIR SYSTEMS CMD
ATTN: CODE 53645 (MR MEARNS)   1
WASHINGTON DC 20361

CDR
NAVAL RESEARCH LABORATORY
ATTN: CODE 6170   1
       CODE 6180   1
WASHINGTON DC 20375-5000

COMMANDING GENERAL
US MARINE CORPS DEVELOPMENT
    & EDUCATION COMMAND
ATTN: DO74   1
QUANTICO VA 22134

OFFICE OF THE CHIEF OF NAVAL
    RESEARCH
ATTN: OCNR-126   1
ARLINGTON, VA 22217-5000

CDR
NAVY PETROLEUM OFC
ATTN: CODE 43 (MR LONG)   1
CAMERON STATION
ALEXANDRIA VA 22304-6180

DEPARTMENT OF THE AIR FORCE

HQ, USAF
ATTN: LEYSF (COL LEE)   1
WASHINGTON DC 20330

HQ AIR FORCE SYSTEMS CMD
ATTN: AFSC/DLF   1
ANDREWS AFB MD 20334

CDR
US AIR FORCE WRIGHT AERONAUTICAL
    LAB
ATTN: AFWAL/POSF (MR CHURCHILL) 1
WRIGHT-PATTERSON AFB OH 45433-
6563

CDR
SAN ANTONIO AIR LOGISTICS
    CTR
ATTN: SAALC/SFT (MR MAKRIS)   1
        SAALC/MMPRR   1
KELLY AIR FORCE BASE TX 78241

OTHER GOVERNMENT AGENCIES

NATIONAL AERONAUTICS AND
    SPACE ADMINISTRATION   1
LEWIS RESEARCH CENTER
CLEVELAND OH 44135

US DEPARTMENT OF ENERGY
CE-151, ATTN:
    MR ECKLUND   1
FORRESTAL BLDG.
1000 INDEPENDENCE AVE, SW
WASHINGTON DC 20585

ENVIRONMENTAL PROTECTION
    AGENCY
AIR POLLUTION CONTROL   1
2565 PLYMOUTH ROAD
ANN ARBOR MI 48105

END

7-81

DTIC